Study on Motorcycle Dynamics at Low Speeds for Rider Support System

A thesis presented for the degree of
Doctor of Engineering

by

Sharad Singhania

Mechanical Engineering,
Graduate School of Industrial Technology,
Nihon University, Japan
25th August 2019

Contents

Study on Motorcycle Dynamics at Low Speeds for Rider Support System

by

Sharad Singhania

Abstract

Motorcycles, which are also known as powered two-wheeled vehicle, are a popular and preferred mode of daily transportation in many countries. The increased traffic congestion due to population and limitations in infrastructure in many of these countries limit the motorcycles to ride at low-speeds frequently. At these speeds, the motorcycles are unstable mainly due to reduced balancing forces because of lower gyroscopic forces from the rotating wheels. Thus, they require active input from the riders to balance the motorcycles, which cause fatigue to them. Therefore, improving low-speed stability becomes a key area of research. A system that improves this stability can support the rider by reducing fatigue and enhancing safety.

The present research aims to develop a rider support system that can balance and maneuver a motorcycle at low speeds, especially at 3-5 km/h. There are three stages of this research. In the first stage, the relationship between the input and output parameters of the motorcycle were studied using theoretical and experimental approach. A mathematical model for the motorcycle was derived, which was used to estimate the steering input from the output parameters required to balance it. Subsequently, experiments were performed on the motorcycle instrumented with required sensors to measure its various output parameters. The riders' steering inputs were also measured while they were riding on a straight path at different speeds. Statistical analysis between the input and output parameters was performed, and the relationship between them has been established, that also validated the theoretical results. The critical parameters have been selected using these relationships based on the literature. The analysis results show that the input estimated using the critical output parameters matches closely with the riders input.

In the second stage, the results of the previous analysis were used for developing a controller that can support the rider at low-speeds. The control algorithm was modeled in Simulink. Subsequently, a validated multi-body dynamics (MBD) model of the motorcycle is modeled using commercially available software VI-Motorcycle. The motorcycle model and the control algorithm were integrated to perform the co-simulation studies. The results of these studies show that the proposed control algorithm stabilizes the motorcycle at targeted speeds.

In the third stage, the directional stability using the discussed controller has been studied because riders maneuver the motorcycles in the desired direction apart from balancing it. A directional input has been added to the control algorithm. The final steering input to the motorcycle model is a superposition of the balancing and direction inputs. The results from this study showed that the motorcycle moves in the path corresponding to the direction input. It also proves the robustness of the controller for the low-speed stability.

Acknowledgment

I express my deep sense of gratitude to my thesis supervisor Professor Ichiro Kageyama at Nihon University for his encouragement and inspiring guidance during my doctoral degree. I express my deep sense of gratitude to my thesis co-supervisor Dr Venkata M Karanam in India at TVS Motor Company, for his motivation and mentoring during the research. Last three years has been a great learning experience under them. I express my special thanks to the reviewers and editors of my thesis, Professor Susumu Takahashi and Professor Hitoshi Tsunashima, for their critical and valuable feedback.

I thank my team members Ravi, Shruthi, Dinesh, KPC, Venkatesh, Barath, Goutham and Muthupudiavan; and seniors Dr V. Praveen, Dr H.B. Das and Mr V. Krishna for their support during my research. I would like to thank senior managers R Babu, R.V.N. Venkatesan, N. Jayaram and V. Harne at TVS for providing this opportunity and management of TVS for providing the financial support. I thank Ryoga, Meiko, Yuto, Satoru, Professor Y. Kuriyagawa and Mrs Yamamoto for their all kinds of supports, during my visit to the university.

I acknowledge my wife Pritha and daughter Pihu, who sacrificed their time with me and supported me during this research. Lastly, I express my sincere thanks to every person at TVSM and Nihon University, who have directly or indirectly helped me in reaching this milestone.

List of Figures

List of Tables

Chapter 1

Introduction

1.1 Introduction

Motorcycles are a preferred mode of daily transportation in many countries. The reasons for their popularity are traffic congestion caused by increased population and underdeveloped road infrastructure; and because they are the most economically viable option. The increased traffic and poor road infrastructure constrain them at extremely low speeds. The motorcycles are unstable at these speeds and require continuous inputs from the riders to attain stability. These inputs cause fatigue to them, and the low-speed instability is a safety concern for them. Therefore, this research presents a study on the low-speed stability of motorcycles.

This chapter has been broadly divided into four sections. Firstly, the background section presents the reasons for the reduced speeds of motorcycles and related concerns to the riders. This section shows that the increased traffic, poor economic condition and increased population result in increased motorcycles sales and traffic congestion. These situations reduce the average speeds of the motorcycles and their poor stability at low-speeds is physically tiring and a safety concern for riders. Secondly, a review of past studies on motorcycle dynamics presents brief details about their development from the stability point of view and parameters affecting it, in the literature review section. The past studies show the limitations in improving the low-speed stability using conventional methods and new area of research for improving it using controllers.

Thirdly, the scope and motivation of the research has been derived from the problems discussed in the background section and gaps found from the literature review section. It is found that there is a demand for dedicated research in the area of low-speed stability from increasing customers and traffic congestion. Therefore, there is a scope of studying the dynamics of the motorcycle to improve the low-speed weave and capsize mode instability, using an additional steering control system. Finally, the last section of this chapter presents a brief overview of each chapter of this thesis.

1.2   Background

The population of the world has been increased every year, especially in developing countries, as shown by the population reference bureau (PRB) [1]. The increased population increased the number of vehicles such as car, buses, trucks and taxis on the road, every year in different countries [2, 3]. Table 1.1 shows that the numbers of automobiles have been increasing in India. The number of motorcycles has increased from 14.8 million in 2013-14 to 21.1 million in 2018-19 [4, 5]. PRB also shows that the number of poor people earning less than $1.25 per day has been declined significantly over the years. It shows that their relative purchasing power has increased. These people are the main contributor to the increasing demand for the motorcycle as it is the most affordable motorized vehicle available.

Category	2013-14	2014-15	2015-16	2016-17	2017-18	2018-19
Passenger Vehicles	25,03,509	26,01,236	27,89,208	30,47,582	32,88,581	33,77,436
Commercial Vehicles	6,32,851	6,14,948	6,85,704	7,14,082	8,56,916	10,07,319
Three Wheelers	4,80,085	5,32,626	5,38,208	5,11,879	6,35,698	7,01,011
Two Wheelers	1,48,06,778	1,59,75,561	1,64,55,851	1,75,89,738	2,02,00,117	2,11,81,390
Quadricycle#			0	0	0	627
Grand Total	**1,84,23,223**	**1,97,24,371**	**2,04,68,971**	**2,18,63,281**	**2,49,81,312**	**2,62,67,783**

Table 1.1: Number of automobile sales in India over the past few years [5].

The increased number of vehicles causes traffic congestion. The reasons for these situations are insufficient infrastructure and lack of a balanced traffic system, as shown by Mahmud et al. in their research on the cause and effect of traffic jams in Dhaka [6]. Similar traffic conditions exist in many cities and developing countries that constrains the speeds of motorcycles. It becomes challenging for novice riders to stabilize them at these speeds; therefore, these riders need a motorcycle with enhanced stability. There are many research studies on high-speed stability [7, 8, 9]. Whereas, limited research studies available focused on low-speed stability of the motorcycles, as discussed in the next section.
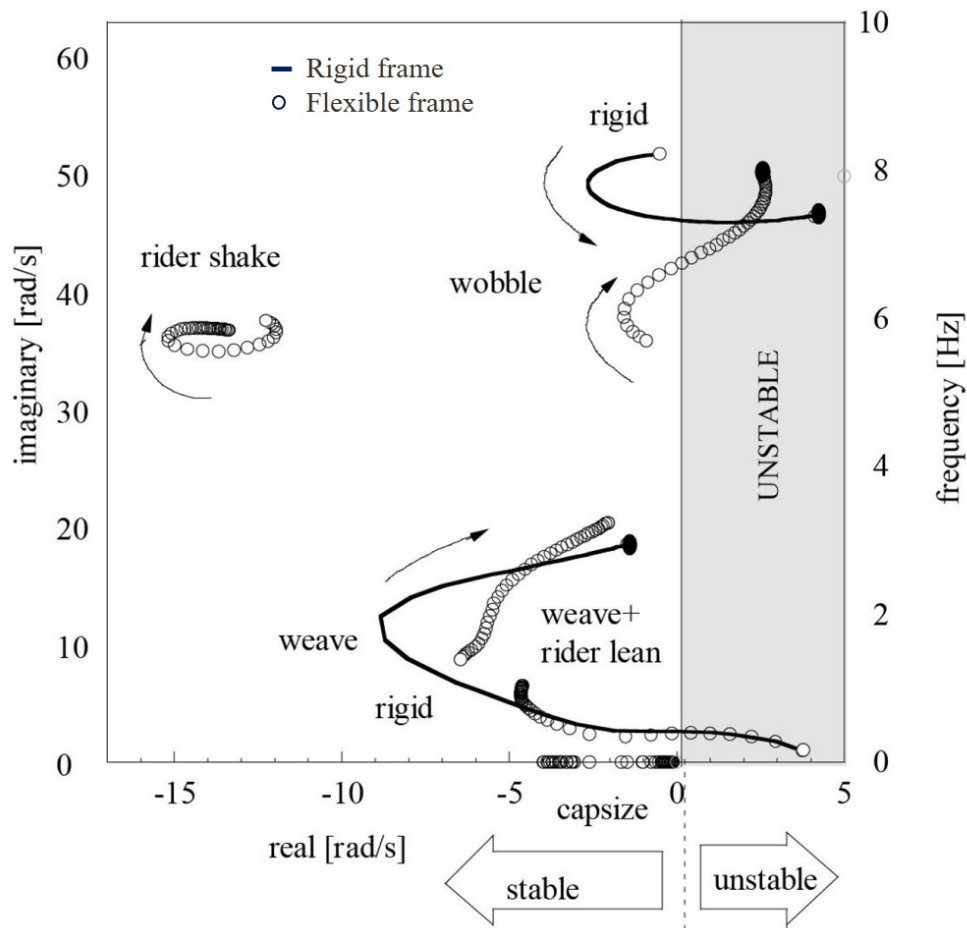
Figure 1.1: Root-locus plot for the stability of a motorcycle[10].

There are three major out-of-plane modes of the instability of motorcycles:

1. Capsize: it is a non-oscillating mode that is mainly controlled by the rider;

2. Weave: it is an oscillation of the entire motorcycle, but mainly the rear end;

3. Wobble: it is an oscillation of the front steering system including front wheel about the steering axis which does not involve the rear frame in any significant way.

Figure 1.1 shows the root locus for the lateral modes, including above mentioned three out-of-plane modes. The arrows show the direction of an increase in speed for the modes. The weave and capsizes modes are unstable at low speeds, as shown in the figure; therefore, this research focuses on improving them.

Many motorcycle manufacturers such as Piaggio [11], Honda [12] and BMW [13] proposed the concept of a three-wheeled motorcycle. The third wheel takes support from the ground to improves the low-speed capsize and weave stability. Although they designed these concepts for the dynamics similar to that of a motorcycle, they can not match it, especially the steering control and roll behavior. These concepts also confirm the saturation in improving the low-speed stability of conventional motorcycles. Popov et al. [7] have reviewed the literature on the motorcycle's control. It shows that limited research studies are available on low-speed stability. And, there is a scope to study and improve it using electronic control systems. Furthermore, this system can be useful to reduce the human hazard involved in some future development tests.

1.3 Literature review

This section presents a review of the research studies on the stability of the motorcycles. It includes the historical development of single-track vehicles, such as bicycles and motorcycles from the stability point of view. The research studies show that some design variables are crucial for motorcycles stability; however, they have limitations to improve it at low-speeds. The motorcycles are unstable at extremely low-speeds; but, additional inputs from rider can stabilize them [14]. Therefore, many authors presented advanced devices and methods, that increase low-speed stability such as steering actuator systems, gyroscopic moments and additional balancers.

Riders inputs are crucial for the motorcycles performances, which are from steering, body movements, thighs etc. They change with motorcycles speeds, types of maneuvers and rider experience levels; therefore, investigating them are also important for motorcycle stability. The effects of rider experience levels on the low-speeds stability of a motorcycle are discussed in this section to find the suitable rider model.

1.3.1   History of single-track vehicles

The evolutionary development of single-track vehicles took place during the 19$^{\text{th}}$ century. The first commercially successful two-wheeled, steerable and human-propelled machine was "Draisine walking machine," commonly called a "Velocipede," developed by *German Baron Karl Drais* in 1818. The development from the Draisine walking machine to the more stable "Safety bicycle" was the most important in the history of the bicycle [15]. *John Kemp Starley* developed the safety bicycle in 1885. It featured a steering system including front wheel, equally sized wheels and a chain drive to the rear wheel. It changed the perception of the single-track vehicles from a dangerous one to a daily mode of transportation for people. All the motorcycles of today have a similar layout as that of the safety bicycle. It shows that the domain of research for the layout and mass distribution optimization has been saturated for any significant gain in motorcycle stability. Although, minor improvements on them to improve maneuverability, riders efforts, speeds of the motorcycles etc. have been done.

Whipple was first to develop the theoretical model for a single-track vehicle to predict the instability modes [16]. This model has been a benchmark model and experimentally validated by many researchers. Sharp was first to develop the theoretical model for motorcycle stability, that includes a proper tire model [17]. Eaton [18] has validated this model experimentally on a motorcycle using the Weir's rider model [19]. Similarly, many authors investigated and presented a theoretical model for single-track vehicles.

1.3.2 Motorcycle stability

Motorcycles are unstable below the certain critical speed [17, 20]. Moreover, the required steering input or the gain value for the stability increases as speeds reduce [21]. Therefore, it is challenging to balance a motorcycle at low-speeds, especially for new riders. They become very cautious as it requires continuous input from them at such speeds [22]. It causes fatigue and a safety concern for them. Therefore, in this research, the focus is to improve the low-speed stability of the motorcycles.

The stability of a motorcycle is a function of its geometry and mass distribution. Cossalter has performed detailed studies on parameters such as caster angle, wheelbase, trail and mass-distribution for their effect on motorcycle stability [10]. The results of these studies determined the directional change in them. For example, changing the trail value from positive to negative makes a rideable bike un-rideable [23]. Doyle has conducted experiments on a bike, with zero trail values, zero caster angle and zero mass offset in the front steering system [24]. He found that it eliminates the roll angle of a bicycle to steer coupling; thus, no effect of steering input by the rider in such vehicles. In general, the center of gravity of a motorcycle lies longitudinally between the ground contact points of both front and rear wheels. The significant change in it towards the front of the ground contact point of the front wheel can stabilize a two-mass single-track vehicle having a negative trail [25]. It shows that the layout and mass inertia are inter-dependent for stability. However, the feasibility of such modifications is debatable.

The layout and mass distribution of the motorcycles can not be entirely modified for stability. They also influence other performance requirements, such as maneuverability, comfort, ergonomics, acceleration feel and braking. Although, all these changes can not self-stabilize the motorcycle at extremely low speeds below 7 km/h [25]. Therefore, it becomes necessary to explore other methods of improving them. Many research papers are available those discusses high-speed stability (weave and wobble) and handling characteristics of motorcycles [26, 27, 28] . Whereas, limited studies available on low-speed stability, those evaluate the rider inputs [7, 29, 30]. Therefore, it is the scope of the present research.

Motorcycles require precise control inputs from their riders for balancing below the critical speeds [20]. They balance it at low-speeds, even at 3 km/h [14], which shows that they provide additional stability to the motorcycles at low-speeds. Therefore, it is necessary to model an appropriate rider model for developing a system that can stabilize them at low-speeds. The riders models presented in the past are discussed next in this section.

1.3.3 Motorcycle rider modeling

The rider models can be developed specifically to the riding or test conditions. Many research studies show that the riders use different body inputs during different maneuvers such as steering input while riding on a straight path and their lean torque during cornering to achieve precise control of motorcycles. Some rider models for motorcycle control are as follows: a rigid body rider that is rigidly connected to the main rear frame for motorcycle stability [16]; two-piece body such that the lower part rigidly attached to the rear frame and the upper part behaves like an inverted pendulum on rear frame, with stiffness provided by spring and damper for bicycle stability and control [20]; upper body can steer, lean and move laterally; and more realistic multi-body riders, including full muscle-skeleton models for assessing the riders, accurately [31]. The present research also requires an accurate rider model. Therefore, this section presents the relevant studies that comment on rider actions at low-speeds.

Doria et al. [32] determined the degree of freedom required for a rider model that achieves similar motion and torque frequency responses to that during the experiments. They used a simulator that provided different frequency inputs to the bicycle mockup. The results showed that the phase of the rider motion response at low-frequency input was close to zero. Whereas, the roll displacements of the rider trunk was higher than that of a bicycle. Therefore, the rider can be a rigidly mounted with the frame, and the higher gain for the rider lean can be compensated in the vehicle roll angle gain. Kooijman et al. [33, 34, 35] conducted experiments on a large treadmill using an instrumented bicycle. The results showed that a very little rider upper-body lean occurs while balancing them. Whereas, it is achieved mainly by steering control actions only. They performed their experiments with two averagely skilled riders at

various speeds who adjusted to riding on treadmills. Cain et al. [36] show that the skilled and novice riders exhibit similar balancing performance using their lean at the low speeds. These research studies showed that the rider lean does not contribute significantly to the low-speed stability of bicycles. Moreover, the mass of motorcycles is much higher than that of bicycles; therefore, the influence of riders' lean on them will further reduce. It shows that a rigidly attached rider to the motorcycle frame can stabilize it through steering torque control.

Riders control motorcycles differently based on their experience. Prem et al. [37] found that the skilled rider provides a larger steering angle and have a shorter reaction time than a novice rider for a successful maneuver. Also, the novice riders showed more inter-rider variability than the experienced riders. Rice and Kunkel [38] and Prem and Good [37] found that the time-lag in the input is more important than its amplitude. They compared the magnitude of the steer or lean control for successful and unsuccessful runs for the same rider, during lane change experiments with both experienced and novice riders. Thus, this research presents the influence of different riders experiences on motorcycle control at low-speeds. The variations in gain values and response time were observed with their riding experience.

controllers for motorcycles: The past research studies divide the controllers used for motorcycles broadly into two categories: classic and modern control. In classical control approach, the system identification method is used to determine the gain values that includes time delays between input and output signals. In optimal control, the strategy is to minimize the cost function of the state or control variables using state-space techniques to achieve optimum performance [39]. Schwab et al. [33] found that the roll feedback gains become unrealistically large at low speeds for roll stability using the optimum controller (LQR). They found that the system has marginal stability and requires more realistic steer torque feedback gains for determining the feedback gains. The cost function optimization does not relate directly to the human-like controller. Hence, optimal control is unsuitable for developing a controller for the rider's feel. Also, there are some other control strategies for motorcycle control such as fuzzy logic, neural network, forward dynamics and inverse dynamics controllers. Although, the classic control strategies are better for studying rider actions, and developing controllers based

on that. Popov et al. [7] reviewed the modeling of the control of motorcycles. It showed that the classical control method is promising for determining the gain values based on actual rider control behavior. Therefore, the present research opted classic control approach for developing a controller for low-speed stability.

1.3.4 Improved stability from additional systems

Adding new systems to the motorcycles can improve their stability, especially at stationary and low-speeds. These systems include additional steering systems, gyroscopic systems and other balancing systems. This section presents brief about these systems.

Additional steering systems: In past research studies, the authors used two kinds of steering inputs for controllers: steering angle and steering torque. Weir [19] found that the rider uses steering torque associated with the rider lean to stabilize the motorcycles. He applies this input determined from the state parameters of the vehicle. The results of the study show that the amplitude of the rider input depends on the motorcycle state. It also has some delay due to human limitations. Eaton [18] used steering torque to investigate the stabilization of the motorcycle roll angle. He restricted the rider's body motion by a rigid brace during the experiments. However, there was a significant difference in his model from experimental results for speeds below 40 mph. In research studies on motorcycle maneuverability at medium speeds, [40, 41] found that the inputs to the motorcycle are mainly from the steering, more specifically steering torque. And, other rider inputs do not contribute to the motorcycle control and probably there for the rider's comfort. Rice [42] measured both the steering torque and steering angle with outputs such as rider lean, roll angle, yaw rate and lateral acceleration for motorcycles. Ruijs et al. [43] used steer torque control based on a Sharp [17] motorcycle model with tires and leaning rider to identify the controller gains for stability at speeds from 5 m/s to 60 m/s. However, in the above-mentioned research studies, the target speeds were relatively higher.

Many authors presented the concept of autonomous single-track vehicles based on added steering systems. A small humanoid robot can balance and steer a scaled-down bicycle by providing input to the handlebar using the lateral dynamics [44]. A mathematical model of the bicycle and motor with a controlled algorithm can reduce the effort of applying the steering angle for balancing it [45]. Tanaka et al. used steering control for balancing their bicycle robot, using the dynamic model derived from the equilibrium of gravity and centrifugal force [46]. Lenkeit [47] developed a motorcycle robot using steer angle control at a low speed below 30 km/h, and steer torque control at high speed above 30 km/h for path control. The results showed that the robot control was good at speeds below 20 km/h and above 35 km/h; whereas, it had low damped oscillations between these speeds. Many other authors examined the relations between input and output parameters of a motorcycle to construct a rider robot [48, 49, 50, 51, 52]. In these research studies, the target speeds were relatively higher. Also, these robots balanced the single-track vehicles using the controller input determined without assessing the actual rider inputs. Whereas, in the present research, the low-speed stability of the motorcycle is studied using an experimental approach with many riders.

Gyroscopic systems: Gyroscopic systems discussed in past studies provided two types of control using gyroscopic moments to balance the single-track vehicles: either the gyroscopic precession or the adjustment of the gyro speed [53, 54, 55]. These moments supported the single-track vehicles at low-speeds. Benzos et al. [53] used two identical gyroscopic rotors located between the bicycle wheels, sealed with the frame to pivot relative to the chassis. The pivot axis was perpendicular to the vehicle-plane of the bicycle. They assembled the rotors with a gear train to turn them by the same angle and speeds in the opposite direction. These ensured their vectors of kinetic momentum in opposite directions, which generated gyroscopic moments to balance the bicycle for any disturbance in the roll direction. Lot et al. [54] proposed that the most effective configuration for gyroscopic rotors are when they spin with respect to an axis parallel to the wheels' spin axis and swing with respect to the vehicle yaw axis. They also showed that the actively controlled gyroscopes are capable of stabilizing the vehicle in its whole range of operating speeds with negligible change in handling characteristics. Karnopp

[55] showed a relatively simple tilt control system using a gyroscope. This system was capable of stabilizing the vehicle at stationary, or on a low traction surface. Furthermore, the system could achieve a coordinated turn on high traction surfaces. However, the cost for this system was high; hence, it is questionable, whether they are reasonable. These systems also deteriorate the dynamics of the motorcycles by slowing them down. These systems do not provide balancing inputs similar to that of a rider, as the system behavior coupled with the steering input by them was not studied. Therefore, usage of such stability enhancement tool is questionable.

Other balancing systems: In research [56], the motorcycle achieved the low-speed stability by steering provided to both front and rear wheels, different from their typical design. However, these changes may not retain the conventional form and dynamics of the motorcycle. Yi et al. [57] designed a nonlinear controller to handle the vehicle balancing. The motorcycle balancing is guaranteed by the system internal equilibrium calculation and by the trajectory and system dynamics requirements. Kimura et al. [58] reduced the steering input required to improve the low-speed stability of motorcycles by adding an extra degree of freedom to them using a mechanism.

There are several other methods have been attempted to improve the stability of single-track vehicles at low-speeds using balancer systems. Keo et al. [59, 60] proposed a double inverted pendulum (roll and lean angle) stabilization model for the bicycle. They found that the stabilizing it using gyroscopic flywheel performed better than a balancer [59]. Whereas, the gyroscopic systems cannot control the roll angle to the desired value, unlike the balancer. Since the flywheel and the balancer have different advantages for stabilizing the bicycle, they used both; and validated using experiments. In another similar research, Keo et al. [60] presented a control strategy of an autonomous electric bicycle with both a steering handlebar and balancer. They showed that a steering handlebar and a balancer had better performance for balancing than with only a balancer using simulations studies. The balancer system worked under unexpected disturbances for stabilizing the bicycle but worked only at low speed. It behaved like a double pendulum due to its ability to steer at high speeds. However, stabilization and tracking control of the single-track vehicles has not implemented at a wide range of speeds by moving

mass control. Also, an inverted pendulum or laterally moving mass required higher gains than the steering control.

In summary, the past research studies showed that the improvements in low-speed stability in a conventional way by tuning the parameters such as layout and mass distribution has no significant improvements. Thus, the authors investigated other methods for improving it using controllers. They attempted rider models for motorcycle dynamics; however, their focus has been on tracking control (directional control) and stability control at higher speeds. Few of them developed new support systems such as gyroscopic, steering and balancer systems, to balance single-track vehicles at low-speeds. However, their approach was to attain the balancing from control engineering requirements. It showed that extensive study using different riders had not been performed to develop a controller that balance the motorcycles similar to the riders. Therefore, a gap is found to construct steering support systems using experimental study with different riders that improve the motorcycle's stability at extremely low-speeds ($\leq$ 5 km/h).

1.4 Scope and motivation of the thesis

The population, poor infrastructures and financial condition of people in many countries have increased the demand for motorcycles. Therefore, they become the most popular mode of transportation there in many countries. These situations cause traffic congestion and restrain them at low speeds. They have poor stability at these speeds and require active input from the riders. It causes fatigue to them, and it is a safety concern. These issues motivated us to do dedicated research to improve the low-speed stability of motorcycles.

The scope of the research has derived from the gaps identified in the literature review section. It is found that there is a scope of developing a steering support system by experiments with different riders that improve the stability of the motorcycle at extremely low speeds (≤ 5 km/h). Therefore, a theoretical, experimental and simulation methods have been presented in this research to develop and validate the same. The theory defined the stability regions for a motorcycle, which were validated by the preliminary experiments with expert riders. It provided conviction for performing an extensive experimental study. Then, detailed experiments with riders from various experience levels were conducted. The experimental results were analyzed using statistical methods to identify critical parameters for stability. These parameters were used to determine the gain values for a control algorithm to estimate the steering input to balance the motorcycle. The control algorithm was developed based on this steering estimation and modeled in Simulink. The Simulink control model was co-simulated with a validated motorcycle model in MBD software, VI-Motorcycle. In general, the default controller of the software can not balance any motorcycle model at speeds below 10 km/h. Whereas, the simulation results verified that the software could balance the MBD model at extremely low speeds using the control algorithm developed in this work.

1.5   Overview of each chapter

This thesis is broadly divided into three stages. Firstly, a theoretical model for the stability of the motorcycle is presented that determines the low-speed stability regions. These regions showed gain values required for the steering input and delay in it, with respect to the motorcycle state required for stability. Secondly, experiments have been performed that validated the theoretical model and identified the input and output parameters of the motorcycle critical for balancing it. A control algorithm developed based on these parameters is modeled in Simulink. It is integrated with a validated MBD model of the motorcycle prepared in commercially available software, VI-Motorcycle to perform simulation studies. These stages are described in the following chapters:

Chapter 2 presents a mathematical model for the low-speed stability of the motorcycle. It determines the stability regions that show the roll angle gains and corresponding lead time to stabilize them at low-speeds.

Chapter 3 presents the experiments details and method of analyzing them. At first, preliminary experiments with expert riders validated the theoretical results from Chapter 2 that provided assurance for further study. Then, detail experiments with riders from various experience levels were performed to identify critical parameters for low-speed stability. The chapter also presents a control algorithm based on these parameters.

Chapter 4 presents the co-simulation studies between the control algorithm modeled in Simulink and an MBD model of the motorcycle in VI-Motorcycle. The simulation results show that the control algorithm can balance the motorcycle model successfully.

Finally, Chapter 5 presents the conclusions and future scope of the research.

Chapter 2

Theoretical Model for Stability of a Motorcycle

2.1 Introduction

Various internal and external forces are applied to motorcycles when in motion, which influences their stability. This section presents a linear mathematical model for their low-speed stability using these forces. The model determines characteristic equations for the motorcycle stability in the roll direction for open and closed-loop systems. Stability regions for the motorcycle stability have determined from these equations. A motorcycle rider must apply steering inputs inside these regions to balance them. In this research, a scooter-type motorcycle has been selected for studying the low-speed stability. The brief details of the motorcycle layout, specifications and mass-distribution are provided in this chapter. The results of the theoretical analysis for the motorcycle are also discussed in this chapter.

2.2 Linear model for motorcycles

Figure 2.1 shows the schematic of a motorcycle and a rider system to achieve the low-speed stability. It shows that the rider estimates the required input to balance it using their state as feedback. The objective of the rider is to stabilize it by maintaining the reference values of the state parameters (i.e., roll rate $\dot{\phi} = 0$ and roll angle $\phi \approx 0$ in this case). The reference value for the roll rate is zero to achieve steady-state condition. Ideally, the reference values for the roll angle should also be zero for symmetric motorcycle moving in a straight path. Although, it can have a small offset due to the lateral center of gravity of motorcycles and while they take a turn. The disturbances presented in the model are due to the rider disruptions and road irregularities. These disturbances are a component of the input and the output parameters of the motorcycle respectively. The disturbances by the riders become an input to the motorcycle and influences the output parameters. Similarly, the road disturbance on the motorcycle changes the output parameters that influence the rider input. This relationship between the input and output parameters are studied to achieve the low-speed stability, as shown in the next section.
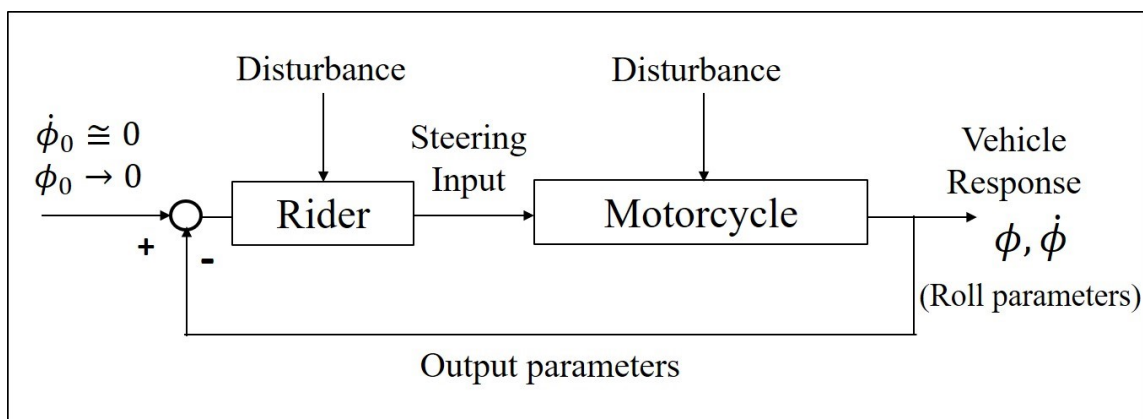
Figure 2.1: Block diagram for the low-speed stability of a motorcycle and rider system.

Figure 2.2 shows the schematic of a typical motorcycle. It shows the layout and mass-inertia parameters important for motorcycle stability. These parameters are listed in Table 2.1.

Table 2.1: Layout parameters of the motorcycle.

Parameters	Symbols
Fork offset	d_1
Wheelbase	l
Castor angle	ϵ
Radius of the front wheel	r_f
Radius of the rear wheel	r_r
Front wheel contact point with the ground	A
Rear wheel contact point with the ground	O
Point where the projection of steering axis intersects with the ground	B
Longitudinal center of gravity of the rider-motorcycle system from point O	l_r
Vertical center of gravity of the rider and motorcycle system from point O	h
Mass of the steering system including front wheel assembly	M_f
Front steering system inertia including wheel about the steering axis	I_f
Height of the center of gravity of the steering system from the ground	h_f
Roll inertia of the rider and motorcycle system about its center of gravity	I_g
Shortest distance between center of gravity of front steering system (including front wheel assembly) and steering axis	d
Roll axis of the motorcycle	x-axis
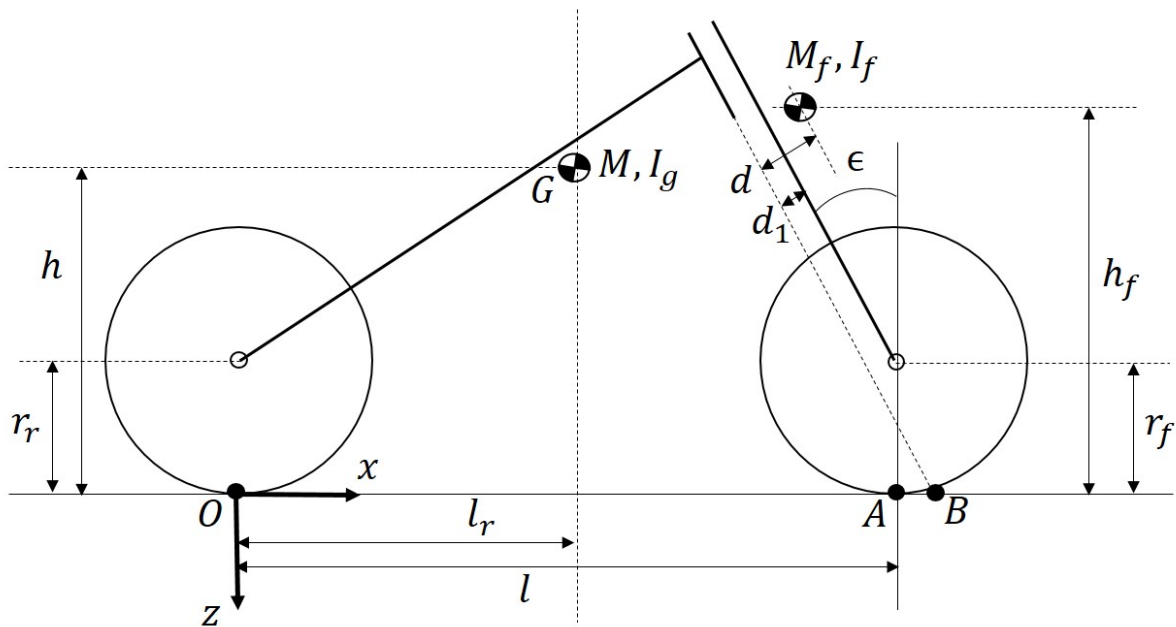
Figure 2.2: A typical layout of a motorcycle.

Table 2.2: Input and output parameters used in linear model.

Parameters	Symbols
Speed	v
Roll angle	ϕ
Yaw angle	ψ
Steering angle	δ
Kinematic steering angle	δ_R
Lateral displacement at O	y_o
Instantaneous turning circle radius	R

(a) Rear View   (b) Top View
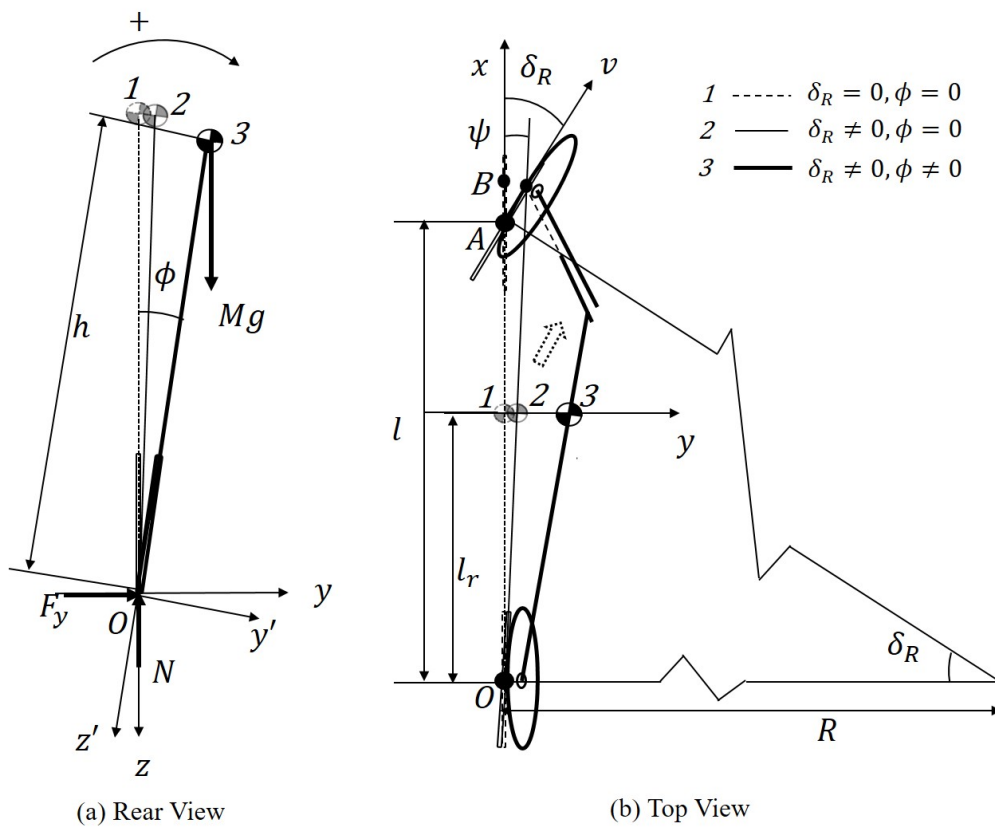
Figure 2.3: Schematic of linear model of motorcycle showing its different states.

Schematic Figure 2.3 depicts different states of the motorcycle while balancing. The symbols used in the figure are listed in Table 2.2. The figure shows that a motorcycle-rider system (mass M) at first steered by an angle (δ) and then rotated about roll axis (x-axis) by an angle (ϕ), as shown by Legend 2 and Legend 3, respectively. These angles are generated due to disturbances to the system and input by riders to balance it. Figures 2.3a and 2.3b show rear-view and top-view of the system respectively. Various forces acting on the motorcycle are due to weight

(Mg), normal reaction (N) and lateral force (F_y) as shown in Figure 2.3a. Figure 2.3b shows the effect of steering angle (δ) and roll angle (ϕ) on the motorcycle state. Marginal changes in δ and ϕ result in yaw angle (ψ), which makes the motorcycle to follow a circle of radius R. The significance of the steering mechanism on the stability of the motorcycle is described in this section.

Equation of motion

The equation of motion for the stability of the motorcycle in roll direction about the x-axis (the axis intersecting vehicle plane and ground plane at point O) is as follows:

$$I_o\ddot{\phi} + M\ddot{y}_oh = Mgh\phi + \boldsymbol{M_{gyro}} + \boldsymbol{M_{steering}} + \boldsymbol{M_{front\,normal\,reaction}}, \qquad (2.1)$$

where:

I_o is the roll inertia of the motorcycle with respect to point O, which is defined in terms of roll inertia about center of gravity I_g as follows:

$$I_o = I_g + Mh^2. \qquad (2.2)$$

The lateral acceleration of the motorcycle $\ddot{\boldsymbol{y}}$ about point O is a function of the centrifugal acceleration $\boldsymbol{a_c}$ and lateral velocity $\boldsymbol{v_y}$ as follows:

$$\ddot{\boldsymbol{y}}_{\boldsymbol{o}} = \boldsymbol{f}(\boldsymbol{a_c}) + \boldsymbol{f}(\boldsymbol{v_y})$$

These functions can be defined in terms of the forward velocity $\boldsymbol{v}$ and kinematic steering angle $\boldsymbol{\delta_R}$ as follows:

$$\ddot{\boldsymbol{y}}_{\boldsymbol{o}} = \boldsymbol{f}(\boldsymbol{v}, \boldsymbol{\delta_R}) + \boldsymbol{f}(\boldsymbol{v}, \dot{\boldsymbol{\delta}}_{\boldsymbol{R}})$$

$$\ddot{\boldsymbol{y}}_{\boldsymbol{o}} = \frac{\boldsymbol{v}^2}{l}\boldsymbol{\delta_R} + \boldsymbol{v}\frac{l_r}{l}\dot{\boldsymbol{\delta}}_{\boldsymbol{R}}. \qquad (2.3)$$

Gyroscopic moments on the motorcycle is a function of rotations of both front and rear wheels ($\boldsymbol{\omega_f}$ and $\boldsymbol{\omega_r}$ respectively). Additionally, it also depends on the steering rate $\dot{\boldsymbol{\delta}}_{\boldsymbol{R}}$ as follows:

$$M_{gyro} = f(\boldsymbol{\omega_f}, \boldsymbol{\omega_r}, \boldsymbol{\delta_R}) + f(\dot{\boldsymbol{\delta}}_{\boldsymbol{R}})$$

$$\boldsymbol{M_{gyro}} = -\frac{\boldsymbol{v}^2}{l}\left(\frac{I_{fw}}{r_f} + \frac{I_{rw}}{r_r}\right)\boldsymbol{\delta_R} - \frac{\boldsymbol{v}}{r_f}I_{fw}\dot{\boldsymbol{\delta}}_{\boldsymbol{R}} \tag{2.4}$$

Moment due to the front steering system vibration is defined as a function of steering acceleration $\ddot{\boldsymbol{\delta}}$ as follows:

$$\boldsymbol{M_{steering}} = f(\ddot{\boldsymbol{\delta}}) = -(I_f + M_f dh_f)\ddot{\boldsymbol{\delta}}. \tag{2.5}$$

Moment due to the front wheel normal reaction force is defined as a function of steering angle $\boldsymbol{\delta}$ as follows:

$$\boldsymbol{M_{front\,normal\,reaction}} = f(\boldsymbol{\delta}) = Mg\frac{l_r}{l}d_1\boldsymbol{\delta}. \tag{2.6}$$

The following equation is obtained by substituting the values from Equations (2.2)–(2.6) in Equation (2.1).

$$\begin{aligned}
&(I_g + Mh^2)\ddot{\boldsymbol{\phi}} + M\left(\frac{\boldsymbol{v}^2}{l}\boldsymbol{\delta_R} + \boldsymbol{v}\frac{l_r}{l}\dot{\boldsymbol{\delta}}_{\boldsymbol{R}}\right)h = \\
&Mgh\boldsymbol{\phi} - \frac{\boldsymbol{v}^2}{l}\left(\frac{I_{fw}}{r_f} + \frac{I_{rw}}{r_r}\right)\boldsymbol{\delta_R} - \frac{\boldsymbol{v}}{r_f}I_{fw}\dot{\boldsymbol{\delta}}_{\boldsymbol{R}} - (I_f + M_f dh_f)\ddot{\boldsymbol{\delta}} + Mg\frac{l_r}{l}d_1\boldsymbol{\delta}.
\end{aligned} \tag{2.7}$$

Further, the kinematic steering angle can be defined by the equation as follow:

$$\boldsymbol{\delta_R} = \tan^{-1}\left(\frac{\cos(\epsilon)\sin(\boldsymbol{\delta})}{\cos(\boldsymbol{\phi})\cos(\boldsymbol{\delta}) - \sin(\boldsymbol{\phi})\sin(\epsilon)\sin(\boldsymbol{\delta})}\right). \tag{2.8}$$

Equation (2.8) can be approximated in linear form for δ and $\phi \to 0$ as follows:

$$\boldsymbol{\delta_R} \approx \boldsymbol{\delta}\cos(\epsilon). \tag{2.9}$$

Substituting the value of kinematic steering angle from Equation (2.9) in Equation (2.7) gives the following equation:

$$(I_g + Mh^2)\ddot{\phi} - Mgh\phi =$$
$$-M\left(\frac{v^2}{l}\boldsymbol{\delta} + \boldsymbol{v}\frac{l_r}{l}\dot{\boldsymbol{\delta}}\right)\cos(\epsilon)h - \frac{v^2}{l}\left(\frac{I_{fw}}{r_f} + \frac{I_{rw}}{r_r}\right)\cos(\epsilon)\boldsymbol{\delta} - \frac{v}{r_f}I_{fw}\cos(\epsilon)\dot{\boldsymbol{\delta}} - (I_f + M_f dh_f)\ddot{\boldsymbol{\delta}} + Mg\frac{l_r}{l}d_1\boldsymbol{\delta}.$$
$$(2.10)$$

The open-loop transfer function for the low-speed stability of the motorcycle system can be defined from Equation (2.10) by the following expression:

$$G_o(s) =$$

$$\frac{\phi(s)}{\delta(s)} = \frac{-M\left(\frac{v^2}{l} + v\frac{l_r}{l}s\right)\cos(\epsilon)h - \frac{v^2}{l}\left(\frac{I_{fw}}{r_f} + \frac{I_{rw}}{r_r}\right)\cos(\epsilon) - \frac{v}{r_f}I_{fw}\cos(\epsilon)s - (I_f + M_f dh_f)s^2 + Mg\frac{l_r}{l}d_1}{(I_g + Mh^2)s^2 - Mgh}.$$
$$(2.11)$$

The transfer function defines the stability of the motorcycle at all the speeds. The poles of the open loop systems are as follows:

$$s = \pm\sqrt{\frac{Mgh}{I_g + Mh^2}} \qquad (2.12)$$

where,

$$\frac{Mgh}{I_g + Mh^2} > 0$$

Equation (2.12) shows that one of the open-loop poles of the system is always positive. Therefore, the system is unstable, and its low-speed stability cannot be achieved. It requires a control input to attain low speeds stability making the system a closed-loop system. This mathematical model presents the closed-loop system for the motorcycle, using the roll angle as the feedback parameter and steering angle as the control input to attain the stability.

The closed-loop feedback of the motorcycle can be defined using the following relationship between the steering angle ($\boldsymbol{\delta}$) and the roll angle ($\boldsymbol{\phi}$):

$$\boldsymbol{\delta}(t) = a.\boldsymbol{\phi}(t - \tau), \qquad (2.13)$$

where a is gain value and τ is lead time for the roll angle with respect to the steering angle. Equation (2.13) can be further simplified for $\tau < 1$ as follows:

$$\boldsymbol{\delta} = a.\boldsymbol{\phi} - a\tau\dot{\boldsymbol{\phi}}. \tag{2.14}$$

By substituting the value from Equation (2.14) in the Equation (2.10) following equation is obtained:

$$C_1\dddot{\boldsymbol{\phi}} + C_2\ddot{\boldsymbol{\phi}} + C_3\dot{\boldsymbol{\phi}} + C_4\boldsymbol{\phi} = 0, \tag{2.15}$$

where,

$$C_1 = -(I_f + M_f h_f)da\tau \tag{2.16}$$

$$C_2 = Mh^2 - \frac{Mhl_r\boldsymbol{v}\cos(\epsilon)a\tau}{l} + I_g + (I_f + M_f h_f)da - \frac{I_{fw}v\cos(\epsilon)a\tau}{r_f} \tag{2.17}$$

$$C_3 = Mh\boldsymbol{v}\cos(\epsilon)a\left(\frac{l_r}{l} - \frac{\boldsymbol{v}\tau}{l}\right) + \frac{I_{fw}\boldsymbol{v}\cos(\epsilon)a}{r_f} - \frac{\boldsymbol{v}^2\cos(\epsilon)a\tau}{l}\left(\frac{I_{fw}}{r_f} + \frac{I_{rw}}{r_r}\right) + \frac{Mgl_r d_1 a\tau}{l} \tag{2.18}$$

$$C_4 = \frac{\boldsymbol{v}^2\cos(\epsilon)a}{l}\left(\frac{I_f w}{r_f} + \frac{I_r w}{r_r}\right) - Mgh - Ma\left(\frac{gdl_r + h\boldsymbol{v}^2\cos(\epsilon)}{l}\right). \tag{2.19}$$

Equations (2.16)–(2.19) show constants C_1, C_2, C_3 and C_4 of closed-loop characteristic Equation (2.15). A motorcycle is stable when all the real-parts of Eigenvalues of the characteristic equation are negative, for different values of the roll angle gain a and it's lead time τ. The next section presents the stable zones for the motorcycle used for experiments. It also shows the results for their open and closed-loop stability.

2.3 Motorcycle specifications and theoretical results

2.3.1 Motorcycle specifications

The motorcycle chosen for the experiments is a small engine capacity scooter-type motorcycle. Table 2.3 provides its layout, mass and inertia. The same table also shows the symbols corresponding to the parameters used in this thesis.

Table 2.3: Layout, mass and inertia of the motorcycle including a rider weighing 65 kg.

Parameters	Symbols	Values	Unit
Total mass	M	165.70	kg
Wheelbase	l	1.236	m
Roll inertia at center of gravity	I_g	18.79	kgm^2
Height of center of gravity from ground	h	0.545	m
Horizontal distance of CG from rear axle	l_r	0.450	m
Caster angle	ϵ	25.8	degree
Fork offset	d_1	0.004	m
Front steering system mass	M_f	17.72	kg
Front steering system inertia	I_f	23.72	kgm^2
Height of front steering system CG from ground	h_f	0.540	m
Shortest distance: steering system CG and steering axis	d	0.005	m
Front wheel rolling radius	r_f	0.214	m
Front wheel spin inertia	I_{fw}	0.122	kgm^2
Rear wheel rolling radius	r_r	0.205	m
Rear wheel spin inertia	I_{rw}	0.112	kgm^2
Acceleration of gravity	g	9.81	m/s^2
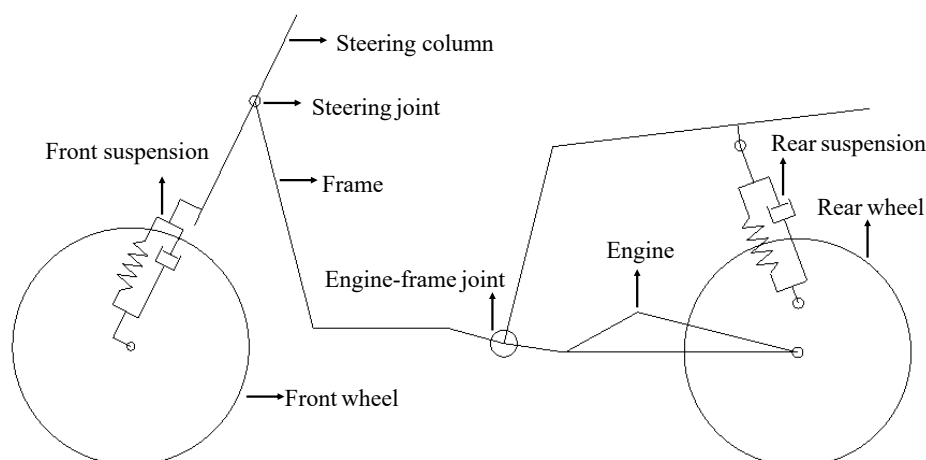
Figure 2.4: Skeleton of the scooter.

Figure 2.4 shows a skeleton of the scooter-type motorcycle. It depicts various subsystem of the motorcycle.

2.3.2 Theoretical results

The values of the variables from the Table 2.3 are substituted in Equations (2.17–2.19). The motorcycle is stable when all these coefficients are positive as per Routh-Hurwitz stability criteria. The results of a and τ for the positive coefficients of characteristic equation for the speeds range of 3 to 30 km/h are shown in Figures 2.5 and 2.6, respectively.

Figure 2.5 shows that the roll angle gain a is constant above 10 km/h; whereas, it increases sharply below 10 km/h. Figure2.6 shows that the lead time gradually increases as speed reduces, and it is always positive.
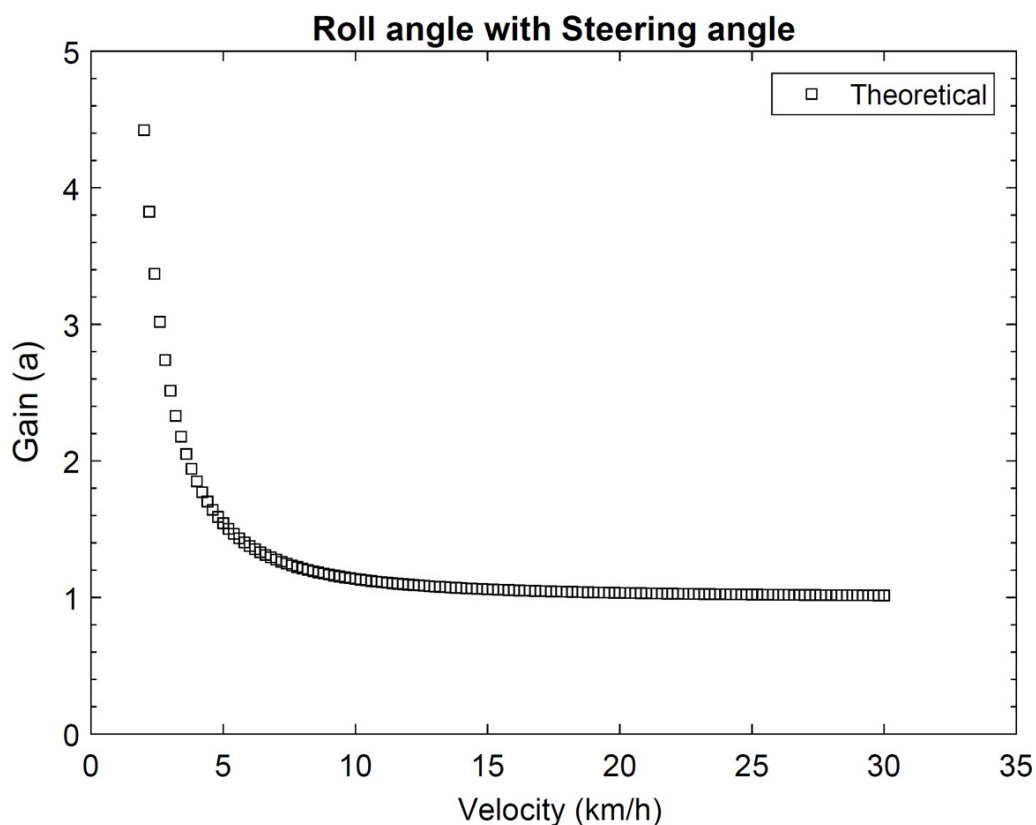
Figure 2.5: The theoretical gain for roll angle with steering angle
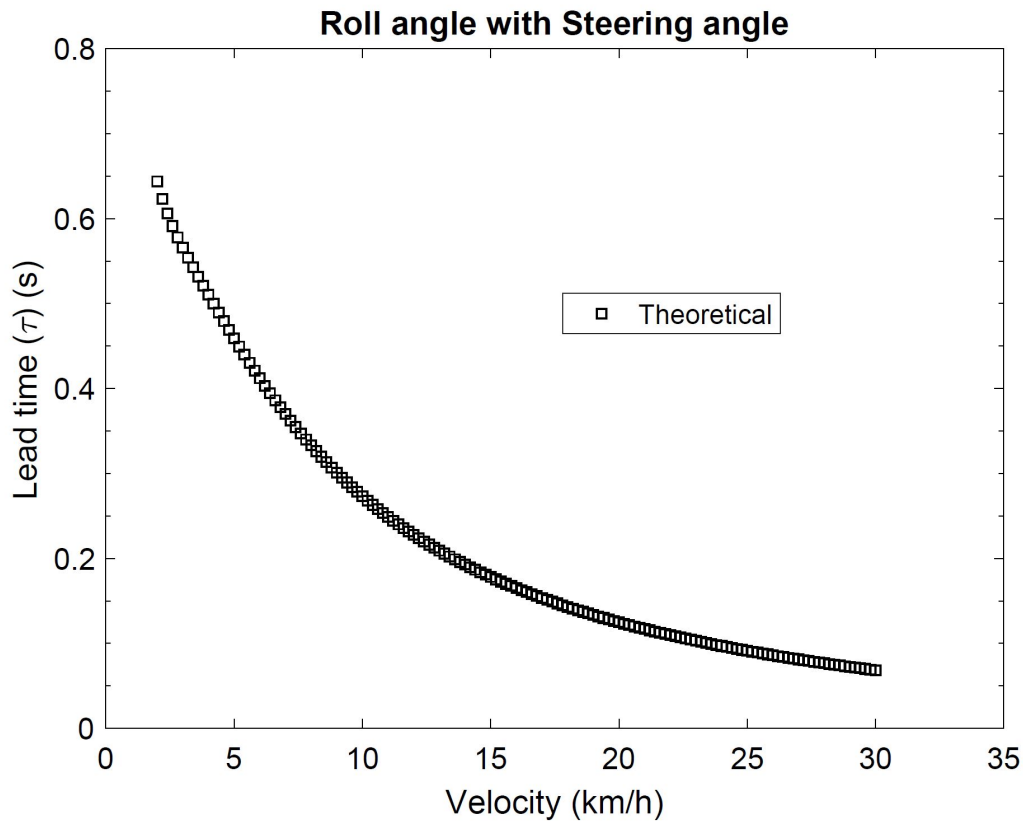
Figure 2.6: The theoretical delay time for roll angle with steering angle

Further, the poles of the open and closed-loop system are shown in this section. Root-locus plot for the open-loop system Equation (2.11) shows that one of the poles of the system is always positive at speeds 3, 5 and 10 km/h, as shown in Figure 2.7. Therefore, the low-speed stability for the open-loop system of the motorcycle cannot be achieved.

The closed-loop system discussed in the above section determines regions for the motorcycle stability at low-speeds. The motorcycle is stable for the values of a and τ, where all the real parts of the eigenvalues are negative. There were three eigenvalues of the closed-loop characteristic equation: λ_1, λ_2 and λ_3. The stability zones of the motorcycle were defined from the following criteria:

Stable zone: $\mathrm{Re}[\lambda_1] < 0$ & $\mathrm{Re}[\lambda_2] < 0$ & $\mathrm{Re}[\lambda_3] < 0$.

Unstable zone: $\mathrm{Re}[\lambda_1] > 0$ or $\mathrm{Re}[\lambda_2] > 0$ or $\mathrm{Re}[\lambda_3] > 0$.
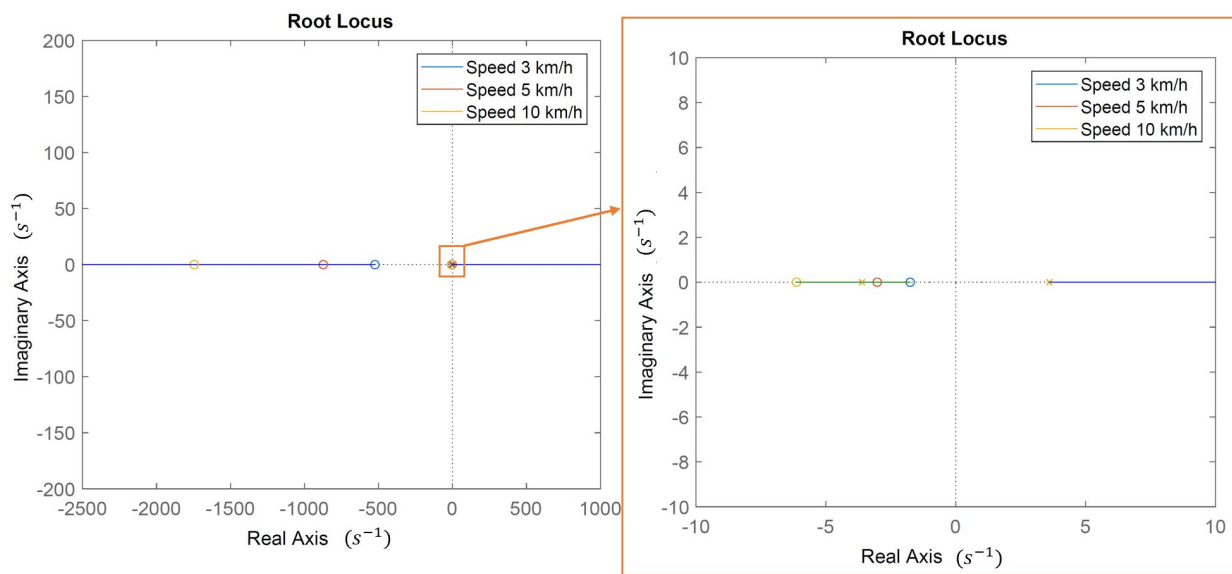
Figure 2.7: Root-locus plot for open-loop motorcycle system.

The shaded zones in Figures 2.8a and 2.8b show regions for the stable motorcycle corresponding to the roll angle gain a and roll angle lead time τ at speeds 3 and 5 km/h, respectively. The rider must be operating inside the shaded zone shown in Figure 2.8 to achieve the low-speed stability. In the next chapter, the theoretical results have been validated from the preliminary experiments results to get confidence for the detailed experimental study.
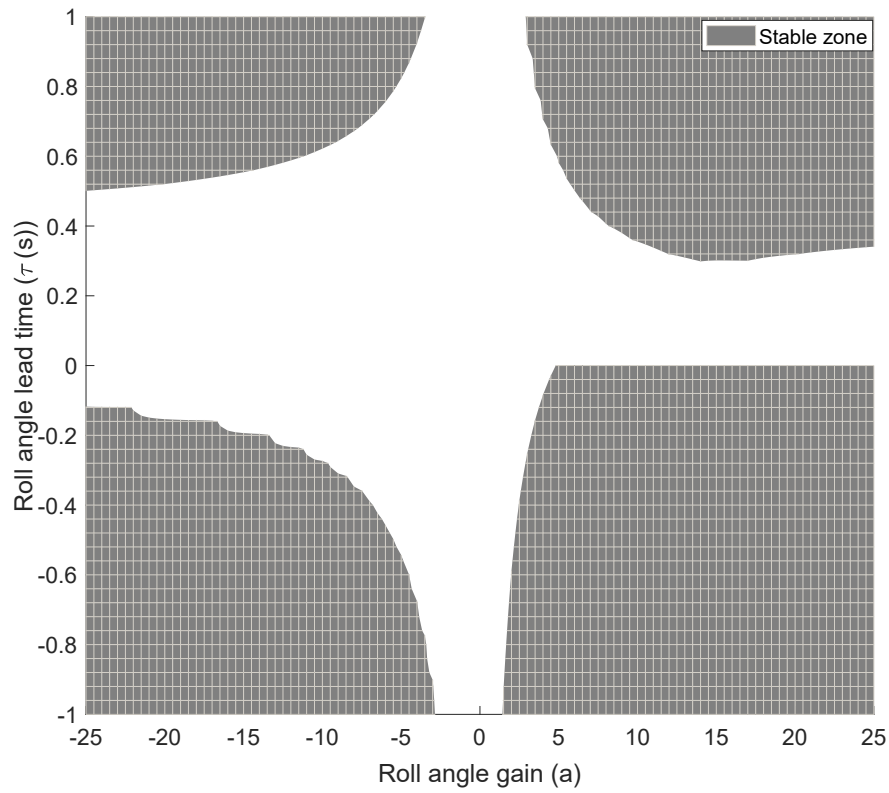
(a) At 3 km/h.
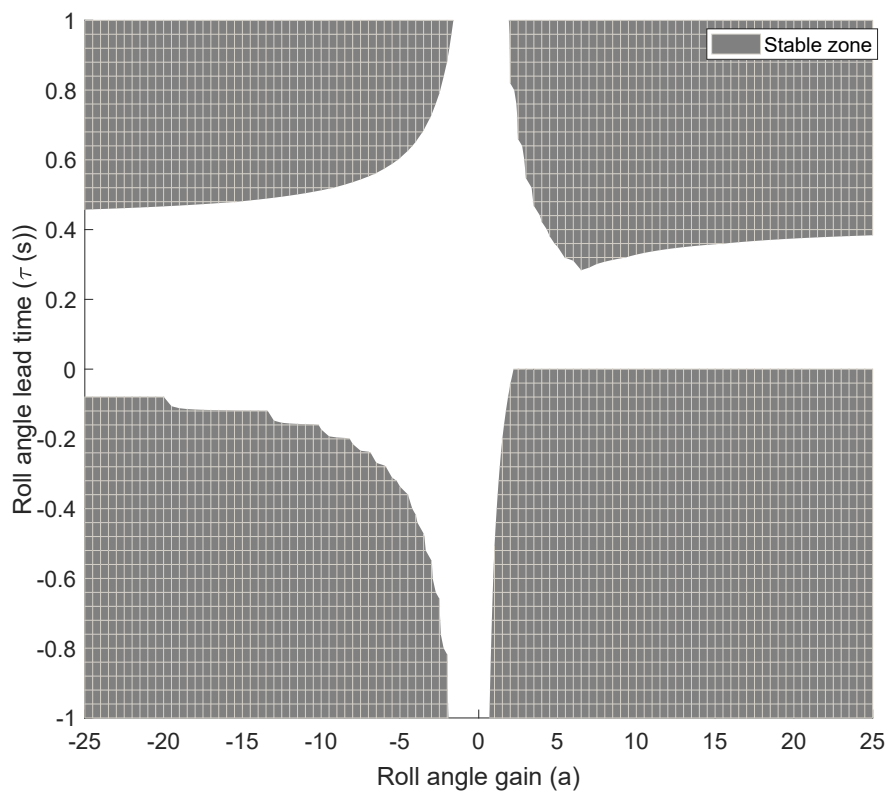
(b) At 5 km/h.

Figure 2.8: Regions of stability for different values of roll angle gain a and lead time τ for closed-loop system of the motorcycle.

Chapter 3

Experimental Details, Analysis and Results

3.1 Introduction

In this section, the stability of the motorcycle detailed in the previous chapter has been studied adopting an experimental approach. It was mounted with various sensors to measure the required dynamic parameters. First, preliminary experiments with three expert riders were conducted to validate the theoretical results at speeds 3 and 5 km/h. It also ensured that the method of analysis of the experimental data provides useful results, and provided certainty for further study. Next, detailed experiments with 19 more riders have been conducted for speeds ranging from 3 to 30 km/h. The wide speed range was chosen to observe its influence on the relationship between various input and output parameters of the motorcycle measured during the experiments. The same method of analysis has been performed for both the preliminary and detailed experiments. Different riders from a diverse background were participated to capture the maximum possible variations in the results. A statistical method has been used to analyze the experimental data to identify useful inputs and outputs parameters. An input estimation model was formulated from regression analysis using these parameters and validated. It was used for a controller for estimating input required for stability. This chapter presents, the

experiments, method of analyze them and results in detail.

3.2 Experimental preparations and methodology

3.2.1 Motorcycle instrumentation

The motorcycle shown in Figure 3.1 has been used for the experiments. Its specifications were given in Chapter 2. It was instrumented with two analogue sensors namely a potentiometer (range of linearity $\pm 50°$) and a piezoelectric sensor (range ± 200 Nm and sensitivity -175 pC/Nm); an inertia measurement unit (IMU) (angular rate range $\pm 400°$/s with an angle measurement accuracy of $0.2°$); a GPS antenna; and a data-logger which has a sample rate of 100 Hz . The brief details of the sensors mentioned above are shown in Table 3.1.

Figure 3.1: Instrumented motorcycle for the experiments
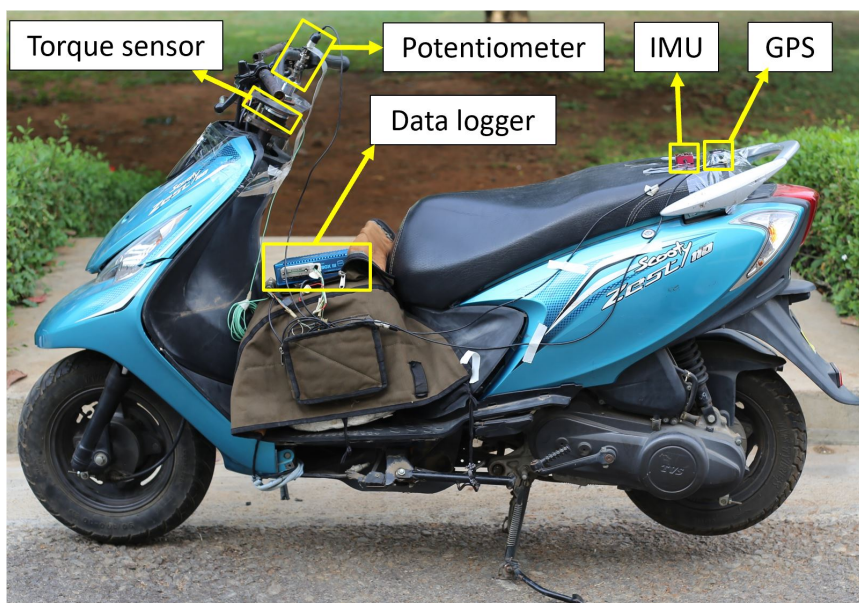
The torque sensor and potentiometer were connected to the data-logger using a de-connector to the analog port. The INS was connected to the data-logger using a serial cable. The GPS antenna was connected to the INS, which measures the speed, position and state of the motorcycle. These sensors were first calibrated for their accurate values and then used for experiments.

Table 3.1: Details of the sensors used in experiments.

Sensors	Descriptions
Torque Sensor	The sensor used to measure the steering torque was from KISTLER that can measure up to $\pm$ 200 Nm about an axis perpendicular to flanges used to mount it [62]. It was a Quartz sensor for measuring quasi-static or dynamic torque acting around its axis. It had several shear-sensitive quartz plates inside, which is kept between the two steel disks. Quartz exhibits the piezoelectric effect. The strain given onto the crystal produces an electro-motive torque which was a measure of steering torque.
Potentiometer	The potentiometer (sometimes called a pot) was used to measure the steering angle in terms of the voltage difference. It was from 2D [63]. In a linear potentiometer, change in angle result in a linear change in voltage. A variable resistor inside it changes the resultant resistance of the potentiometer with the angle of rotation. Hence for the same current supply, the voltage changes and gave a measure of the change in the angle.
Inertia Navigation System (INS)	The INS system used for measurement of the roll, pitch and yaw angles and its corresponding velocities was Ellipse2-N from SBG system. It was a small-sized high-performance sensor with integrated L1 global navigation satellite system (GNSS) receiver [64]. It had low noise gyroscopes and efficient vibrations handling. Its accuracy was 0.1^o for roll and pitch angles and 0.5^o for heading.
Global Positioning System (GPS) Antenna	A magnetic patch antenna was used to obtain vehicle velocity and & position through GPS tracking. It was directly connected to the INS sensor to measure velocity. The antenna used for the experiments was RLACS156 from VBOX [65].
Data-logger	Above mentioned sensors were connected to a data-logger known as VBOX 3i [66]. It used a powerful GPS/GLONASS receiver logging data 100 times a second (100 Hz) to achieve high-level accuracy.

These sensors were mounted on the motorcycle for the experiments. The rotating shaft of the potentiometer was mounted on top of the handlebar, and its non-rotating body was fixed to the frame. The handlebar and front steering system were disassembled to mount the piezoelectric sensor. Two flanges were fixed to them such that the faces of the flanges were perpendicular to the steering axis. The sensor was mounted between these flanges under high preload. The IMU was mounted on top of the pillion seat, and the GPS antenna was kept on a metal plate fixed to the rear frame of the motorcycle at the highest point on the motorcycle. The experiments were conducted using this instrumented motorcycle.

3.2.2 Experimental details and method of analysis

Experimental procedures

Experiments were conducted on a proving ground using the motorcycle instrumented with aforementioned sensors at speeds 3 – 30 km/h. The motorcycle was ridden on the same dry asphalt road to inhibit the road variations in the results. The riders were instructed to follow a straight line marked on the proving ground, and not keep their foot down in order not to take any support from the ground. The experiments were conducted mainly to focus on balancing the motorcycle. Twenty-two riders those belong to a different age, gender, height, weight and experience, participated in the experiments as shown in Appendix-5. Different riders are chosen to capture the maximum variations possible in the results.

Method of analysis

The experimental data were divided into the sample size of 300 (i.e., 3 s) to examine the instantaneous input and output parameters while balancing the motorcycle at low speeds. The maximum correlation coefficient (MCC) and the lead time between these parameters were calculated. Steering angle and steering torque were selected as the input parameters; roll and yaw angles and their corresponding velocities were selected as the output parameters for the analysis. The MCC defined herein as a cost function to determine the maximum possible correlation between the input and the output parameters by shifting the output parameter over the input parameter. The time step at which the cost function became maximum was defined as the lead time. The MCC is a measure of the dependency of the input parameter on the output parameter, and the lead time indicates the usability of the output parameter by the rider for predicting the steering control.
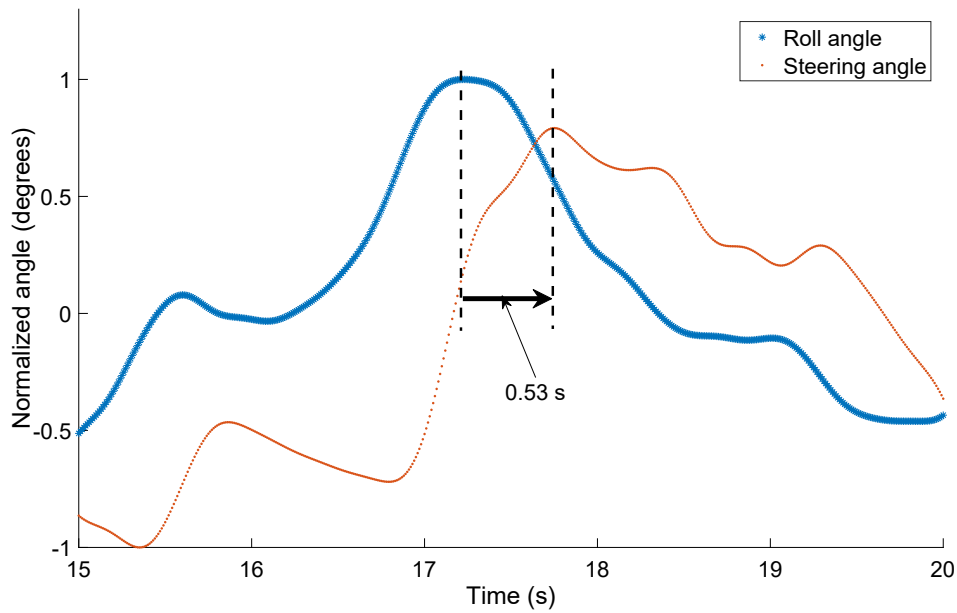
Figure 3.2: Steering angle and roll angle curve of a rider normalized in $[-1,1]$ range at 3.1 km/h.

For example, Figure 3.2 shows time series data for roll angle and steering angle of a professional rider, normalized in $[-1,1]$ range. The correlations between these parameters were calculated while shifting the roll angle curve in the time domain at a step size of 0.01 s in the direction shown by the arrow in the figure. The maximum correlation was observed after shifting it by 0.53 s. This correlation is named as the MCC, and the time by which it was shifted is the lead time (i.e., 0.53 s). The MCC and the lead time were determined from the experimental data for all the riders. The validation of theoretical data and analysis of experiments are done using the same method of analysis.

The experiments were conducted in two stages. Firstly, it was performed with three expert riders those had certified professional training. It validated the theoretical results and assured to start detailed experiments with many riders. Secondly, the detailed experimental studies with different riders categories were performed, to examine their control inputs and outputs to attain stability. These experiments are described in this chapter.

3.3 Preliminary experiments and analysis

These experiments were performed to validate the theoretical results. It ensured the correctness of the analysis methods and provided conviction for further studies using it. They were done in three stages. Firstly, the expert riders have ridden the instrumented motorcycle. They are selected because a low experience rider may provide unstable input to the motorcycle, which differs from the theoretical results. The experimental data were analyzed using the methods discussed in the previous section. Secondly, the repeatability and reliability of the experiments were determined for the validity of the results. Thirdly, the theoretical results were validated with the experimental results using the relationship between the steering angle and the roll parameters in Equations (2.13) and (2.14). The MCC and the lead time were also calculated for the roll angle with the steering angle to validate the stability regions from theoretical results.

3.3.1 Repeatability and reliability of experiments

The average (avg) and standard deviation (SD) from the experimental data were calculated and compared to ensure their repeatability and reliability. Table 3.2 shows the avg and SD for both the motorcycle speed (v) and the positive values of the roll angle gain (a) for each experiment. They were calculated for three professional riders, who have ridden the motorcycle at target speeds of 3, 5 and 10 km/h. Each rider repeated the experiments two times (named as 'set' in the table). Each parameter in the set is divided into the sample size of 300 (i.e., 3 s) as described earlier. The table shows that the values of avg and SD for the motorcycle speeds and the roll angle gains match closely when the same rider repeats the experiment. It ensures the repeatability of the experiments.

The avg and SD of the RA gain increased sharply when the target speed reduced from 5 to 3 km/h than the same from 10 to 5 km/h; although, the SD of the speeds were similar. It was because of the increasing effort and correction in steering input required to attain the low-speed stability as speed reduces. The avg and SD in the RA gains were similar for all the rider at the

particular target speed, which ensured the reliability of the experiments.

Table 3.2: Averages and standard deviations of motorcycle speed (v) and roll angle gain (a).

Target Speed		3 km/h				5 km/h				10 km/h			
		Speed		RA Gain		Speed		RA Gain		Speed		RA Gain	
Rider	Set	avg	SD	avg	SD	avg	SD	avg	SD	avg	SD	avg	SD
1	1	2.46	0.32	14.49	4.26	5.54	0.44	6.21	1.34	10.16	0.34	2.59	0.67
1	2	2.56	0.48	14.18	4.20	5.49	0.63	6.55	1.72	10.32	0.35	2.42	0.66
2	1	3.12	0.34	16.31	4.11	5.69	0.71	7.00	1.73	10.62	0.52	2.22	0.50
2	2	2.95	0.40	17.42	5.31	5.81	0.36	7.52	1.44	10.48	0.40	2.63	0.54
3	1	3.12	0.46	9.20	3.92	5.27	0.79	6.46	1.58	11.07	0.59	1.88	0.66
3	2	3.02	0.38	10.78	4.02	5.60	0.57	5.22	1.10	10.36	0.35	2.22	0.51

3.3.2   Validation of theoretical results

The values of roll angle gain and lead time calculated with the steering angle from the experimental data were compared with the theoretical results, as shown in Figures 3.3 and 3.4, respectively. These figures also show the error bars for the standard deviation of uncertainty in them by the different riders. Experiments results were compared with the theoretical results from chapter 2. The results show that they correspond to each other and validate the theory.

The Figure 3.3 shows that the theoretical and experimental results match closely at speeds above 7 km/h. Whereas, their match is poor below 7 km/h as the correlation coefficients (CC) between the steering angle and roll angle is low at these speeds, as shown in Figure 3.5. The CC was calculated for the time domain data of the input and output without shifting them, unlike MCC, to observe the direct relationship between them. The figure also shows the CCs between the steering torque and roll angle, which was significantly weak compared to the correlation between the steering angle and roll angle, above 7 km/h. It shows that the roll angle can estimate steering angle more accurately than the steering torque at these speeds. Whereas, these correlations reduce at speeds below 7 km/h. It can also be attributed to the contribution of other dynamic parameters to the stability at low-speeds. The detailed analysis for other parameters influencing steering input is shown in the next section.
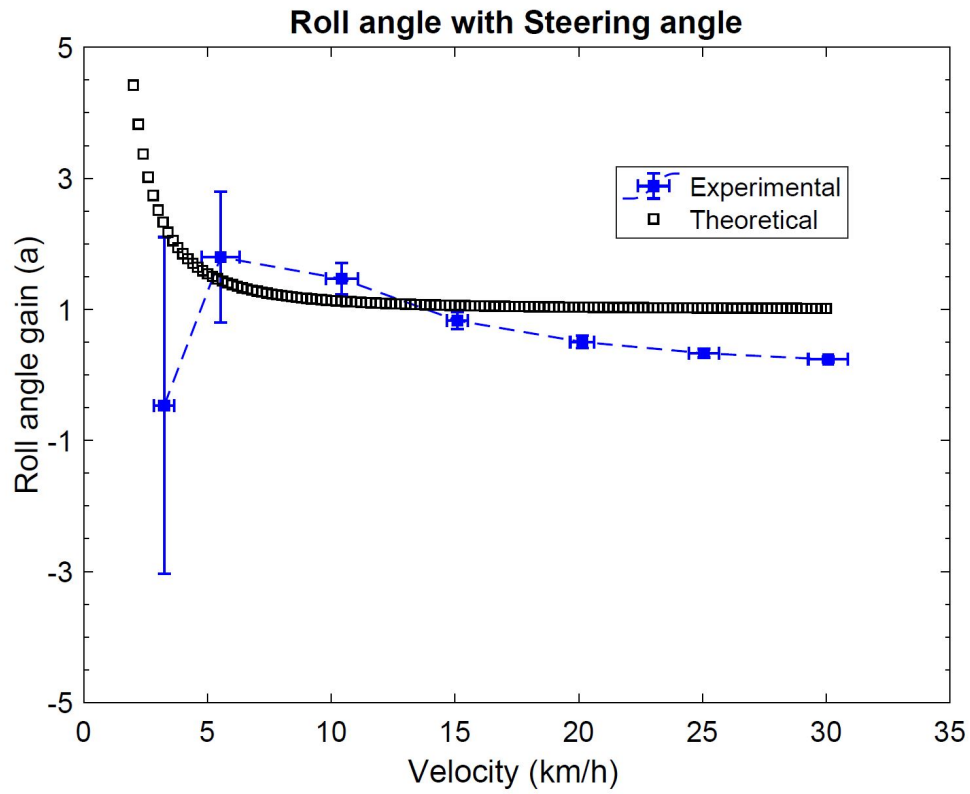
Figure 3.3: Validation of theoretical gain
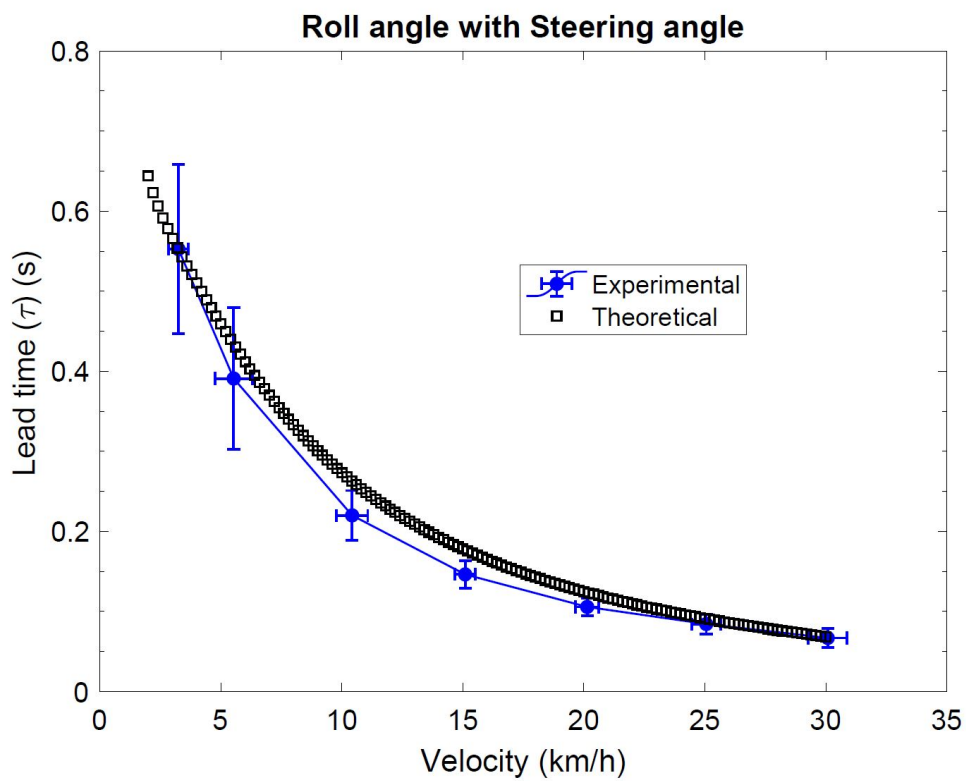
Figure 3.4: Validation of theoretical delay time
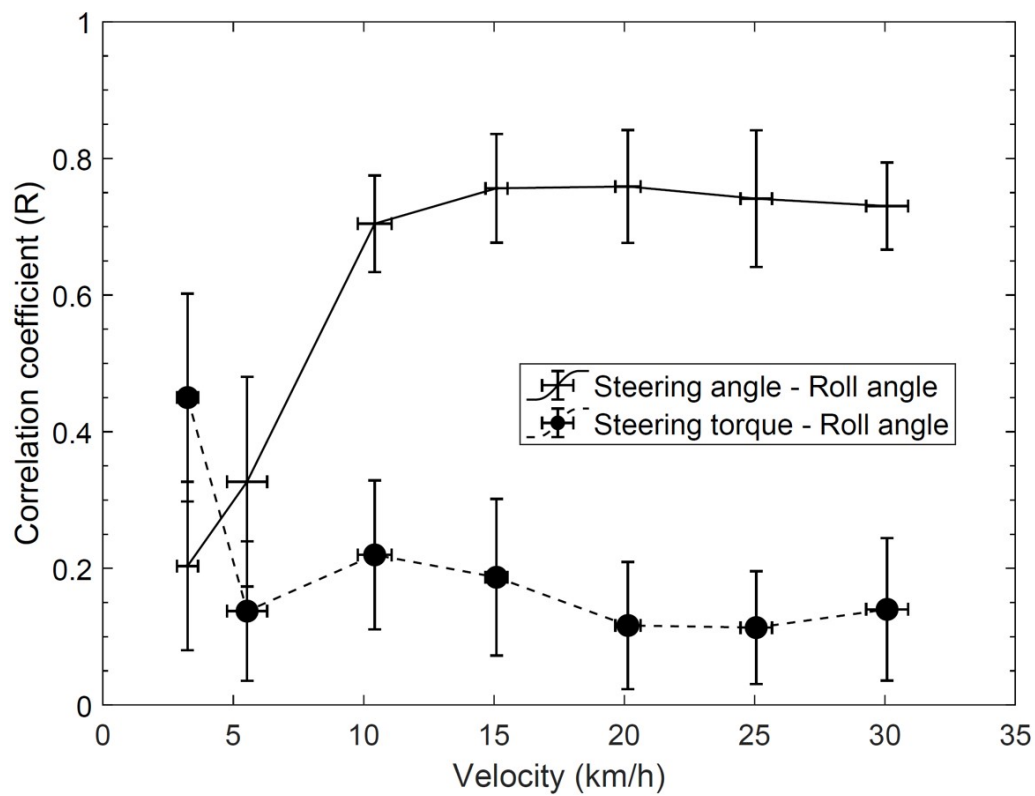
Figure 3.5: Steering angle and steering torque correlation with roll angle

Further, the roll angle gains a and the lead time τ were calculated from the experimental data using the Equation (2.13). These results were compared with the theoretical results at speeds 3 and 5 km/h from Chapter 2, as shown in Figures 3.6a and 3.6b, respectively. The MCCs were strong and were more than 0.8 for all the data-points in the figures. The figures show that the values of a and τ are in the stable regions; thereby, validating the theoretical model. It also confirms that the model can be used to predict the stable zone for a motorcycle at low-speeds.
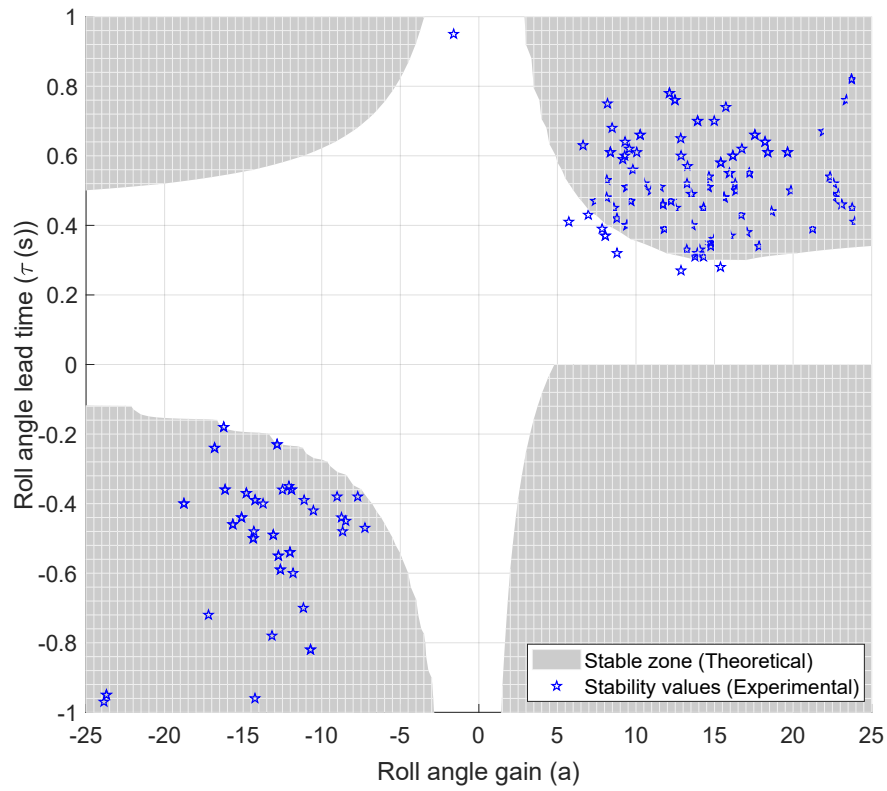
(**a**) Results for 3 km/h for expert riders.
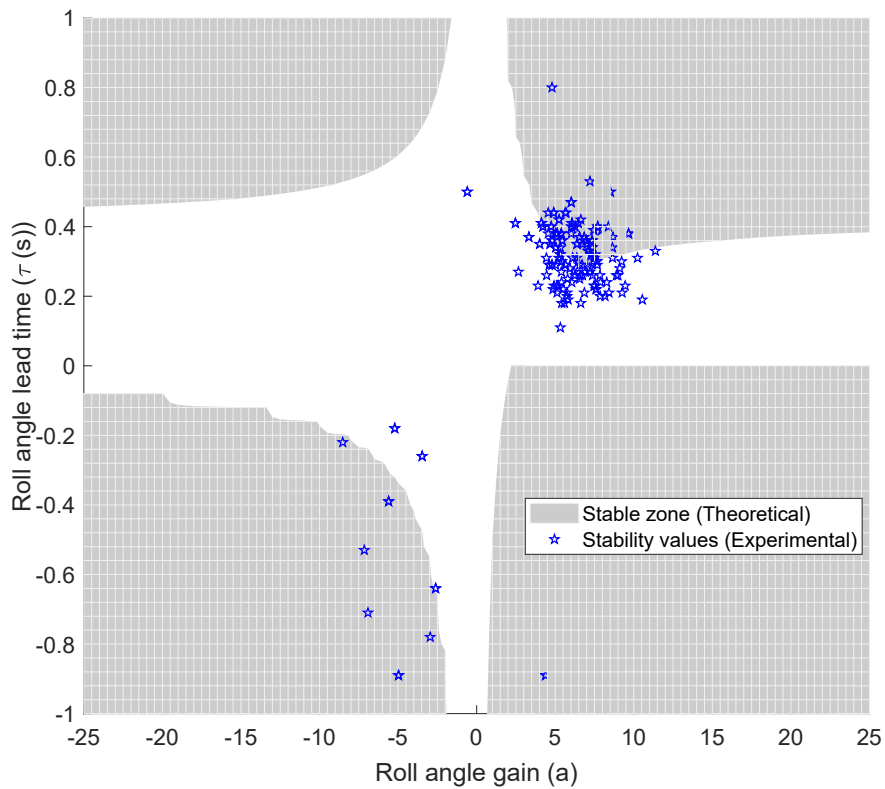
(**b**) Results for 5 km/h for expert riders

Figure 3.6: Validation of theoretical results from experiments for expert riders.

Linear multiple regression analysis (MRA) between the steering angle as a dependent variable; and the roll angle and the roll rate as independent variables, was performed from the experimental data using the following equation:

$$\delta = a_1 \phi + a_2 \dot{\phi}, \qquad (3.1)$$

where, a_1 and a_2 are the regression coefficients of the roll angle and the roll rate, respectively. The regression coefficient a_2 is compared with the corresponding coefficient $(-a\tau)$ from theory, as per the Equation (2.14) in the Section 2. These both coefficients were determined from the experimental data. The correlation coefficients between them were strong and more than 0.7. Figure 3.7 shows that both the coefficients match closely, which shows the strong relationship between the theoretical model and experimental results.
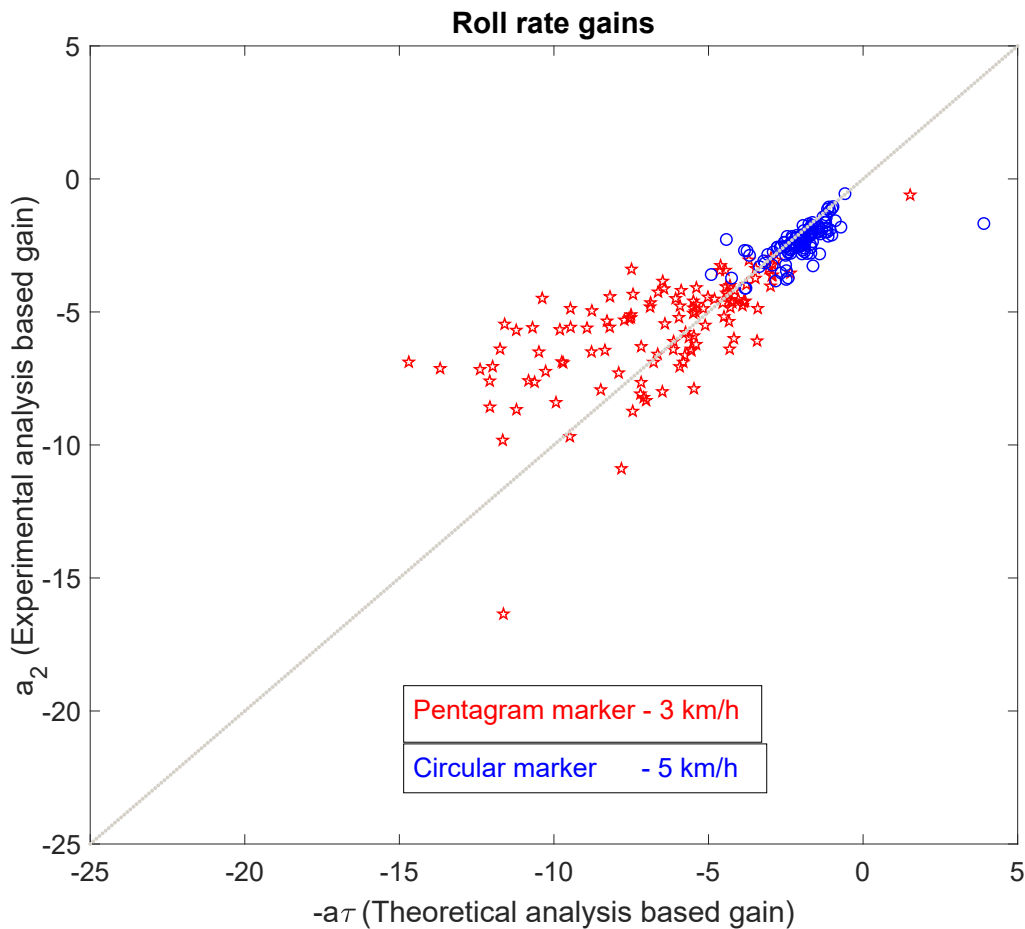
Figure 3.7: Validation of roll rate gain values based on theory and experiments.

The experimental results from this section validated the theoretical results, which assured that they provide useful results. Therefore, detailed experiments with the different categories of riders were conducted and presented in the next section.

3.4 Detailed experiments and analysis

3.4.1 Introduction

The detailed experiments were conducted with twenty-two riders, including three expert riders from preliminary experiments section. The objective was to identify the essential input and output parameters for the low-speed stability of the motorcycle. The experiments and method of analysis were the same, which were described in the preliminary analysis section. This section can be divided into four stages. Firstly, the roll angle gain a and the lead time τ were calculated for all the riders as per Equation (2.13) and compared with the theoretical results. This comparison showed the variations in inputs of different riders with their riding experience. Secondly, parametric analysis between the input and output parameters was performed to identify the useful parameters for the low-speed stability. Thirdly, steering estimation model was constructed using these parameters to be used in a controller for developing a steering support system. This estimation model was also validated with the experimental results. Lastly, the importance of this estimation model was assessed by comparing the gain values of identified output parameters for different riders.

3.4.2 Riders details

The riders were selected from diverse backgrounds that included different age groups, genders, weights, riding experience, training, etc. Twenty-two riders, including the expert riders, participated in preliminary experiments, were selected to accommodate all the possible variations in the experimental results. It also ensured the validity and statistical significance of the results. They were categorized into three levels: beginner riders, who had riding experience of less than 2 years or 1000 km/year; intermediate riders, who had riding experience of more than 2

years and 1000 km/year (without professional training); and expert riders, who were certified professional riders with riding experience of more than 2 years and 1000 km/year. The detail of the riders is given in Appendix-5.

Figure 3.8 shows body-mass-index (BMI) versus age plot for the riders, which shows that their age ranges from 20 to 60 years, and their BMI ranges from 18 to 30. It also shows that the variations in BMI were maintained for each rider experience level to ensure the validity of the results, shown in Figure 3.9.
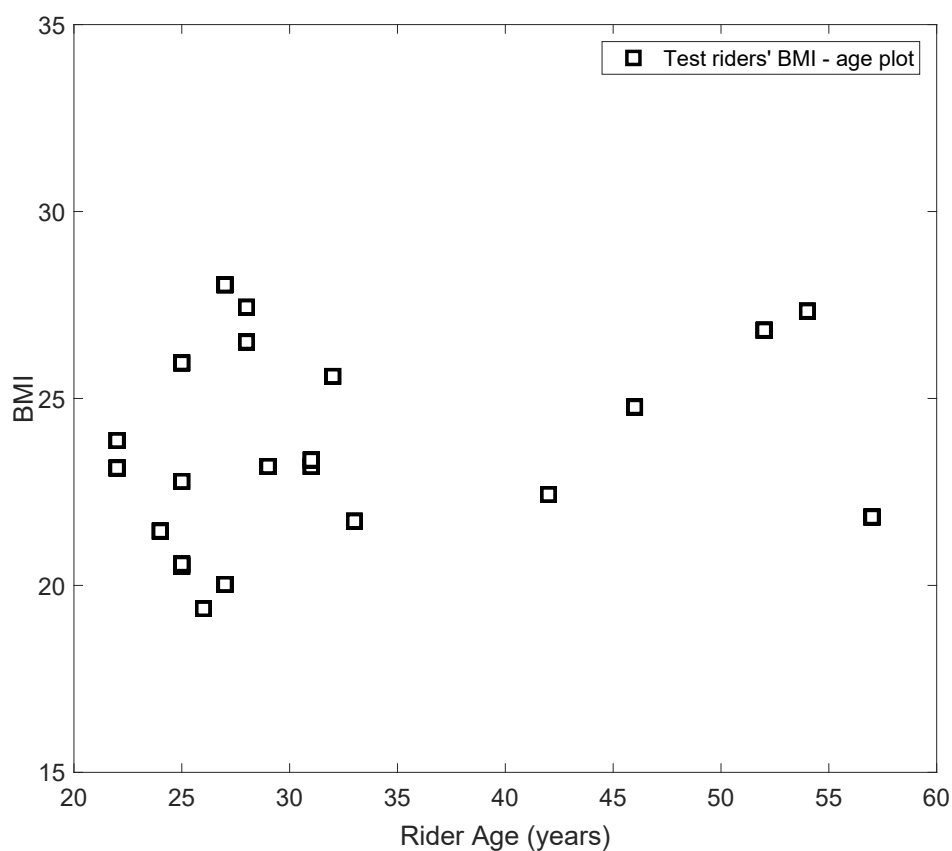
Figure 3.8: Riders BMI versus their age.
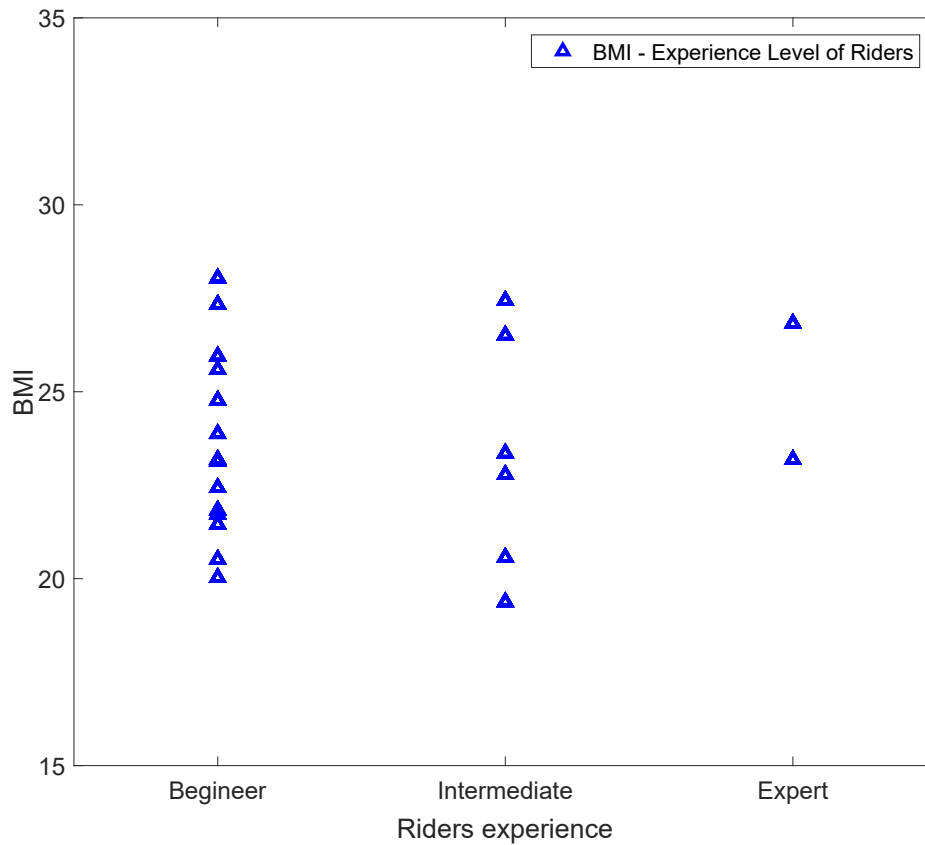
Figure 3.9: Riders BMI versus their riding experience level.

3.4.3 Experimental and theoretical results comparison

The experimental data were analyzed similarly to the analysis of preliminary experiments. The roll angle gains a and lead time τ were compared with the theoretical results at speeds 3 and 5 km/h, as shown in Figures 3.10a and 3.10b, respectively. The MCCs were strong and above 0.7 for the analysis. The figures show that some data-points of a and τ spread outside the stability regions. It can be attributed to the contribution of other dynamic parameters to the stability at low-speeds. Therefore, detailed experiments with all these parameters are presented in this section.
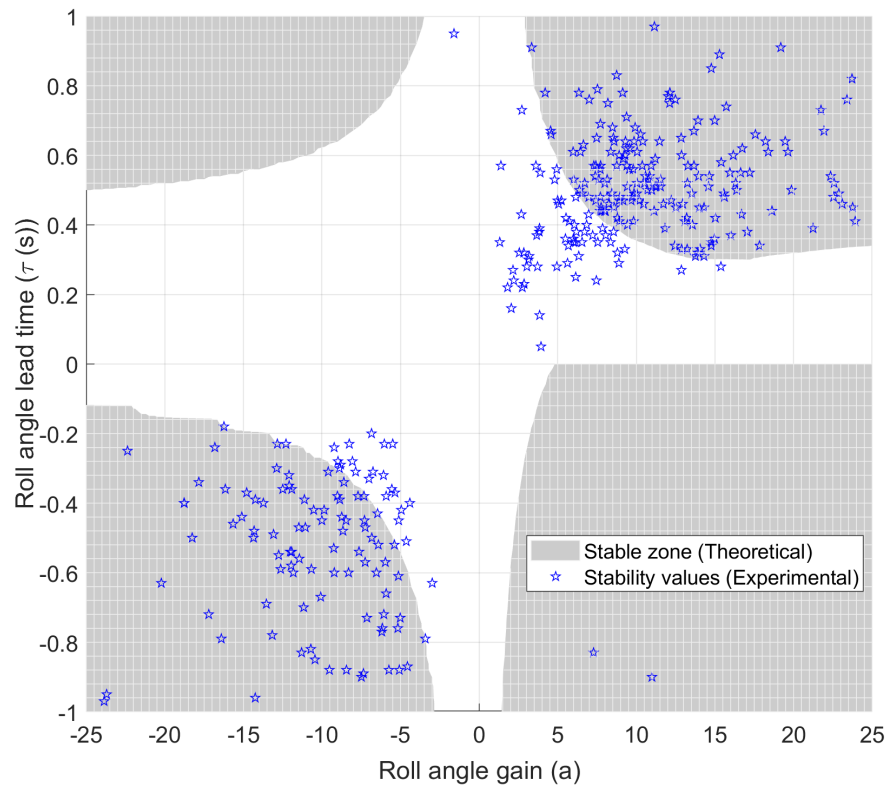
(a) Results for 3 km/h for all riders.
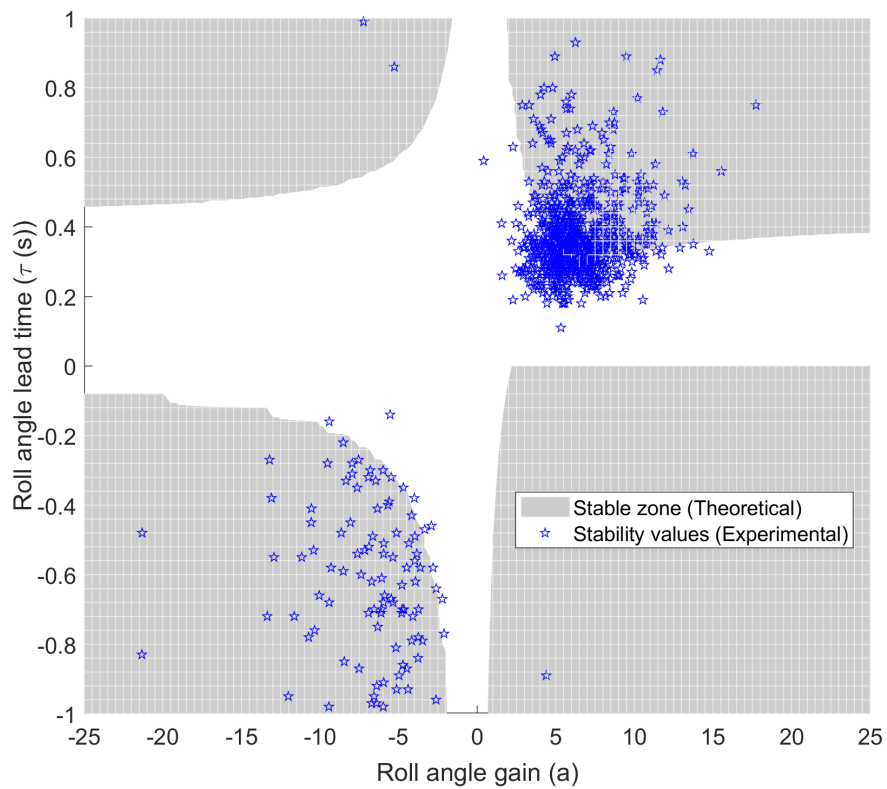
(b) Results for 5 km/h for all riders.

Figure 3.10: Validation of theoretical results from experiments for all riders.

3.4.4 Experimental analysis

The statistical analysis between the input and output parameters were performed to identify useful input and output parameters contributing to low-speed stability. Steering angle and steering torque were the input parameters; roll and yaw angles and their corresponding velocities were the output parameters selected for the analysis. The analysis of experiments was done in two stages. Firstly, the MCC and lead time between the input and output parameters were calculated to identify useful output parameters for the low-speed stability. Secondly, multiple regression analysis was performed between the corresponding identified output parameters with the steering torque and the steering angle. The results helped in identifying the suitable input parameter for low-speed stability. Then, multiple regression analysis between identified input and output parameters was performed to predict the steering input requirements.

Output parameter evaluation

The MCC and lead time for different output parameters with the steering angle are shown in Figures 3.11 – 3.14. These figures include error bar plots for the standard deviation of uncertainty in the calculated MCC and lead time. The MCC was calculated for the leading side of the output parameters as it would only be used by the riders for the steering control. The analysis of the experimental results was done using the following two steps. First, the MCCs between the input and output parameters were compared to identify whether there was any relationship between them to estimate the input parameter. Second, the lead time values were compared to examine the output parameter for their usability by riders for estimating steering inputs for low-speed stability.

Figure 3.11 shows that the MCC between the roll angle and steering angle was strong and above 0.7. It shows that the roll angle could be a useful parameter for estimating steering angle. The lead time for the roll angle ranged 0.3 – 0.6 s at speeds below 10 km/h, and less than 0.2 s above this speed. It shows that the riders had sufficient time to estimate the steering angle using the roll angle at speeds below 10 km/h as it was within the limit of human reaction time. Whereas, the lead time was small and beyond the human limit above these speeds. These results show

that the roll angle was a useful parameter for estimating steering angle, especially at speeds below 10 km/h.

Figure 3.11: Maximum correlation (R) and lead time for roll angle with steering angle

Figure 3.12: Maximum correlation (R) and lead time for roll rate with steering angle

Figure 3.12 shows that the MCC between the roll rate and steering angle was close to 0.6. The lead time for roll rate varied from 0.3 to 0.6 s at all speeds range, which was within the human limit to use it for estimating the steering angle to stabilize the motorcycle. Therefore, the roll rate was also a useful parameter for estimating the steering angle.

Figure 3.13 shows that the MCC between the yaw angle and steering angle was weak, $0.2 - 0.6$. It shows that the yaw angle was not used by riders for estimating steering angle for low-speed stability. The lead time was also relatively higher, 0.5 - 0.8 s for yaw angle with the steering angle, and had higher standard deviations. The weak MCC, more lead time and their higher standard deviations show that it was not used by the riders; therefore, it was not a useful parameter for estimating steering angle.

Figure 3.13: Maximum correlation (R) and lead time for yaw angle with steering angle

Figure 3.14: Maximum correlation (R) and lead time for yaw rate with steering angle

Figure 3.14 shows that the MCC between the yaw rate and steering angle was below 0.3 for speeds above 10 km/h. Therefore, it cannot be used for estimating steering angle at these speeds. Whereas, the MCC was significantly strong and close to 1 below this speed; but, the lead time was very low and close to zero. This low lead time is beyond the human limits to use the yaw rate; therefore, it was not a useful parameter to estimate the steering angle for low-speed stability.

A similar analysis was performed between the various output parameters and steering torque. Figures 3.15 – 3.18 show the MCC, lead time and their error bar plots representing their standard deviation for output parameters with steering torque.

Figure 3.15 shows that the MCC between the roll angle and steering torque was strong and close to 0.6 at speeds below 15 km/h. It reduced from 0.6 to 0.2 above this speed. The lead time for the roll angle ranged 0.4 – 0.7 s at all the speeds, which was sufficient to be used by the riders to use it for stabilizing the motorcycle. Therefore, the roll angle was a useful parameter for steering torque estimation at speeds below 15 km/h.
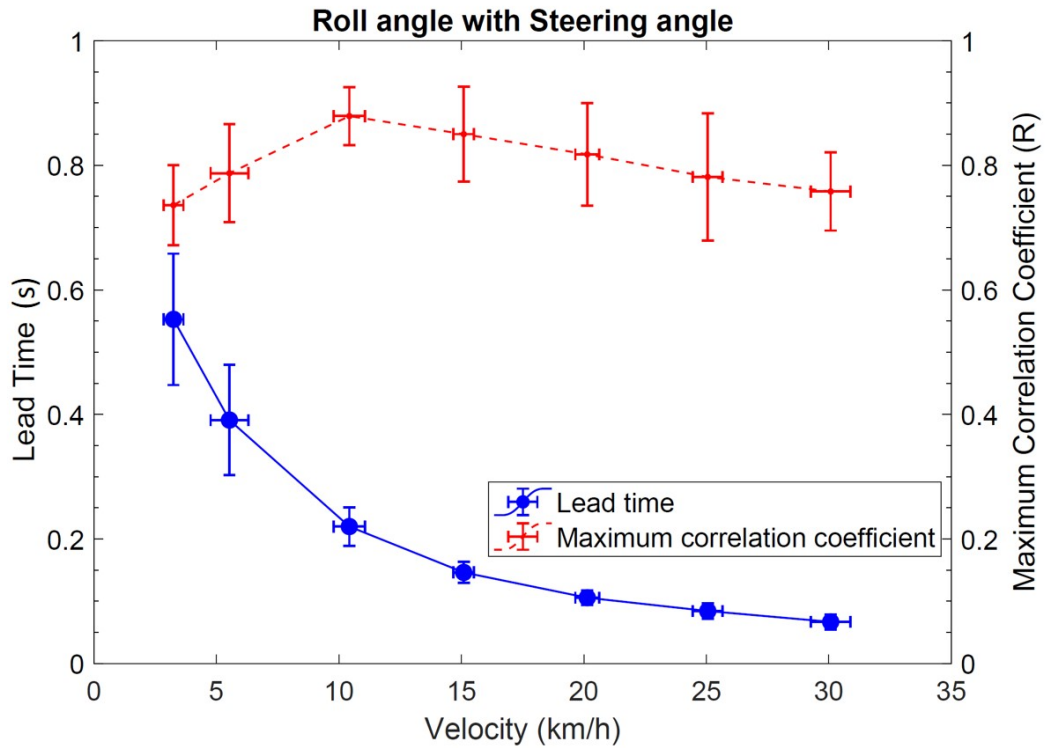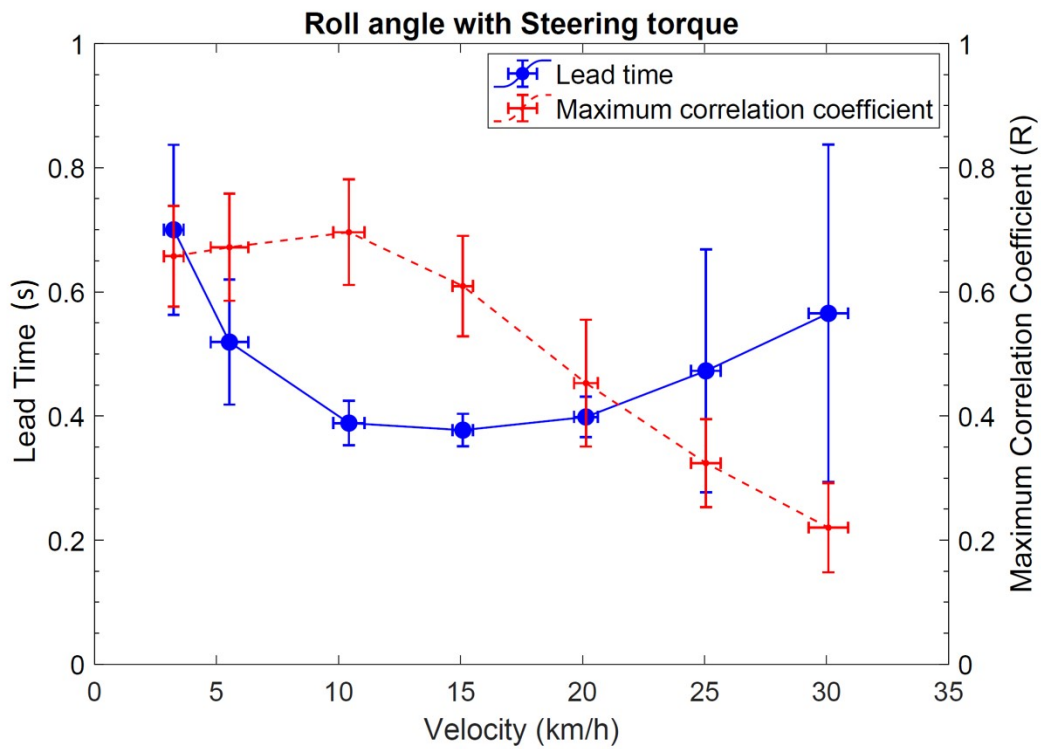
Figure 3.15: Maximum correlation(R) and lead time for roll angle with steering torque
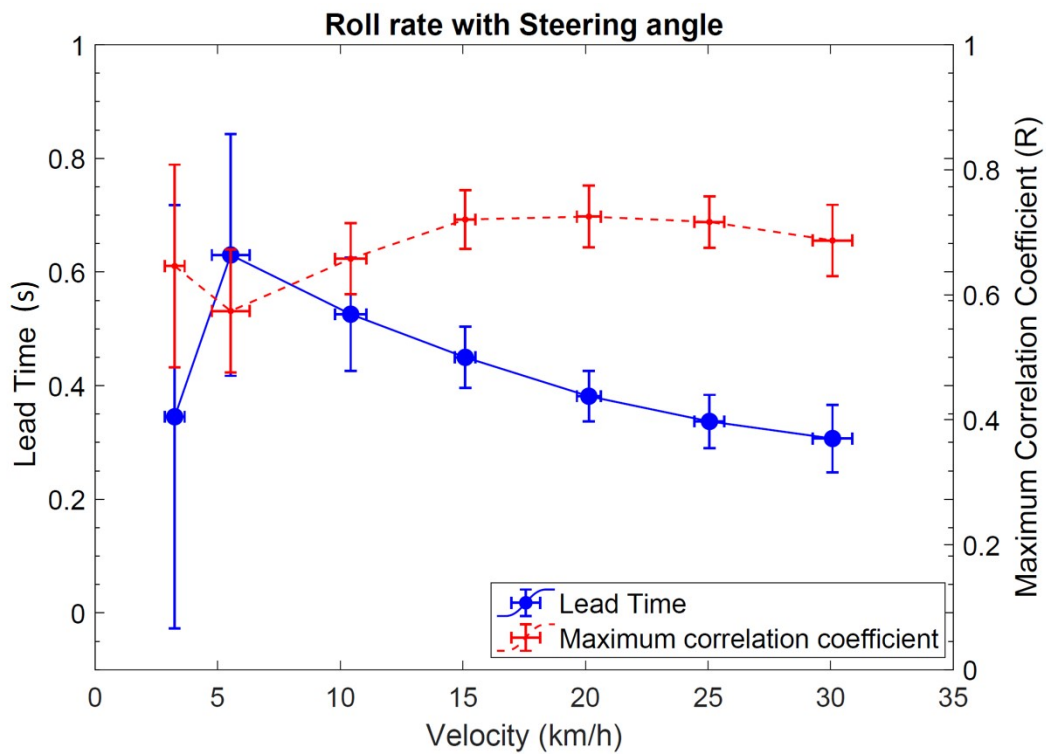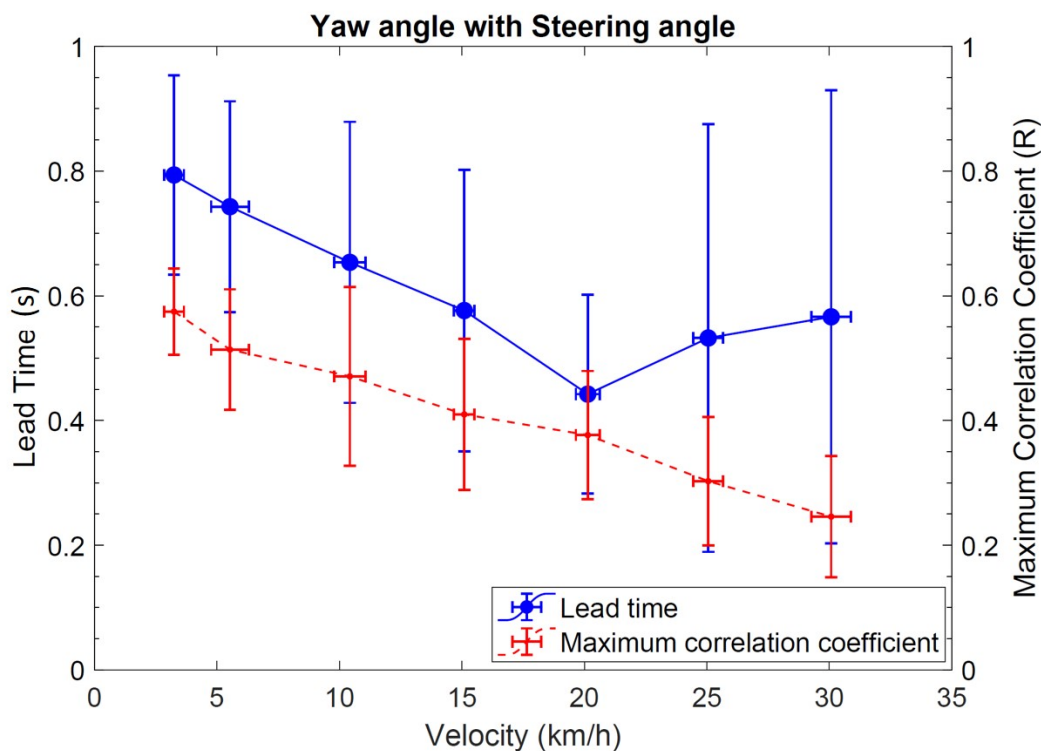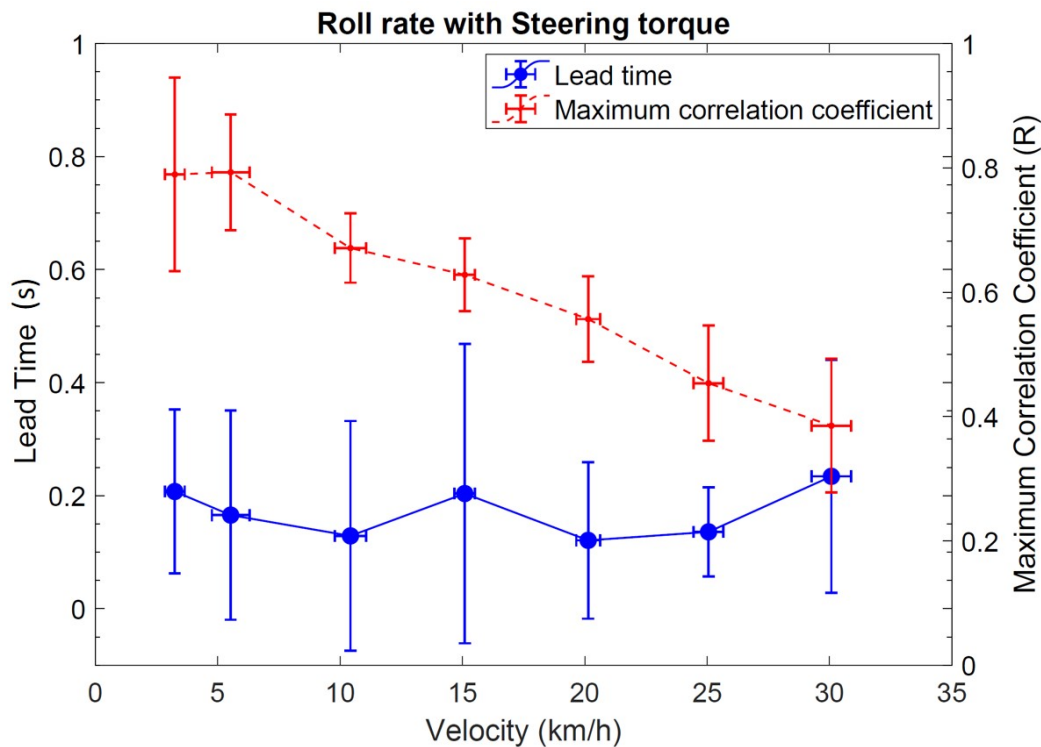

Figure 3.16: Maximum correlation(R) and lead time for roll rate with steering torque

Figure 3.16 shows that the MCC between the roll rate and steering torque ranged $0.4 - 0.8$, and gradually reduces as speed increases. It shows that the relationship between them was good at speeds below 20 km/h. The average lead time for roll rate was more than 0.2 s at all the speeds and their standard deviations were high. It showed that the riders used it for stabilizing the motorcycle and it was a useful parameter for estimating steering torque at speeds below 20 km/h.

Figure 3.17 shows that the MCC between the yaw angle and steering torque is weak, below 0.4. The lead time for the yaw angle was high and close to 0.8 s at all the speeds, which was high for not to balance the motorcycle. Therefore, it was not a useful parameter for estimating steering torque.
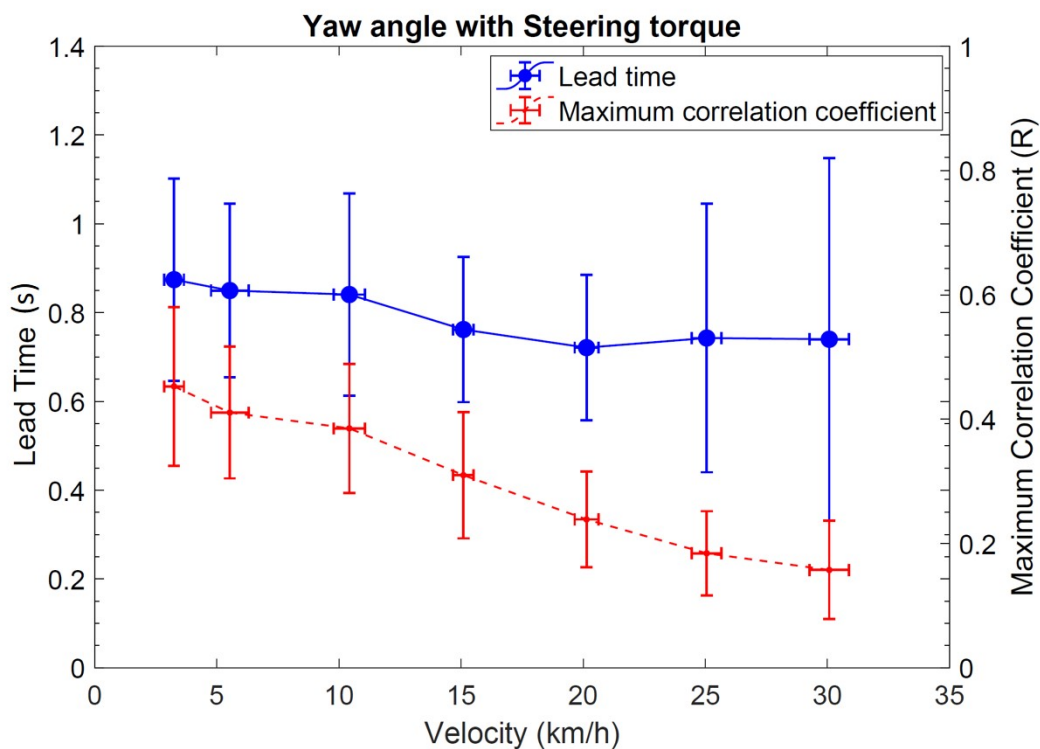
Figure 3.17: Maximum correlation(R) and lead time for yaw angle with steering torque
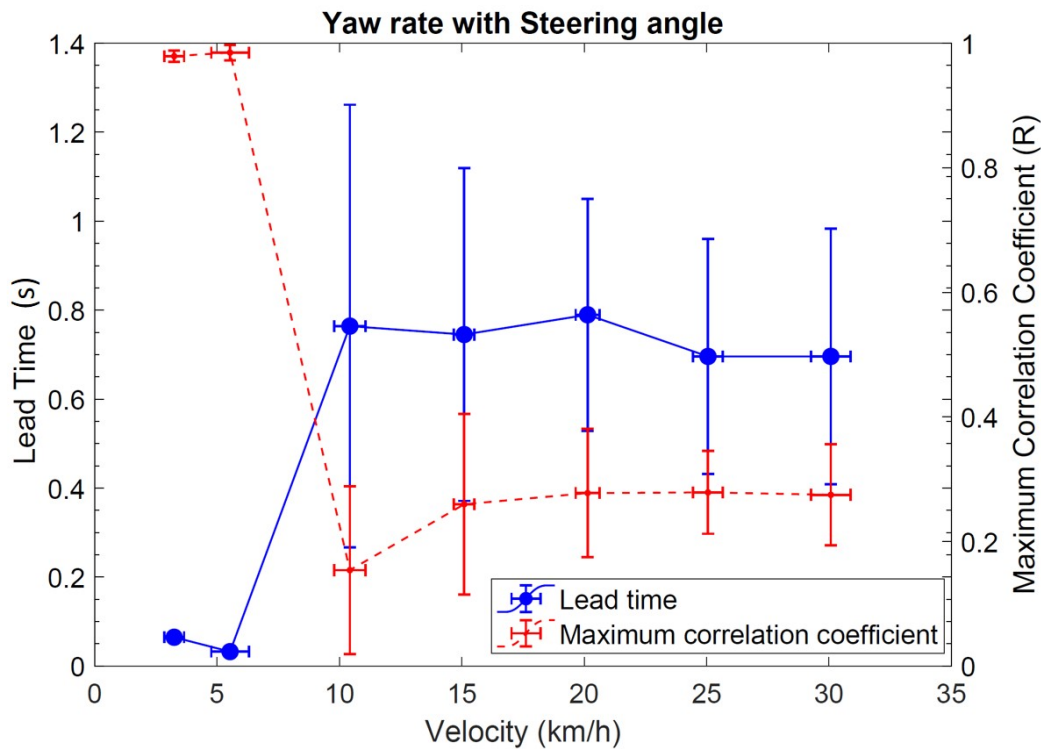
Figure 3.18 shows the MCCs between the yaw rate and steering torque were ranging from $0.3 - 0.9$; gradually reducing as speed increases. The MCCs were strong, above 0.6 below 20 km/h. The lead time for yaw rate is 0.2 s and below with negligible standard deviation in it below 20

km/h. It shows that the yaw rate was not a useful parameter for estimating steering torque by the riders.
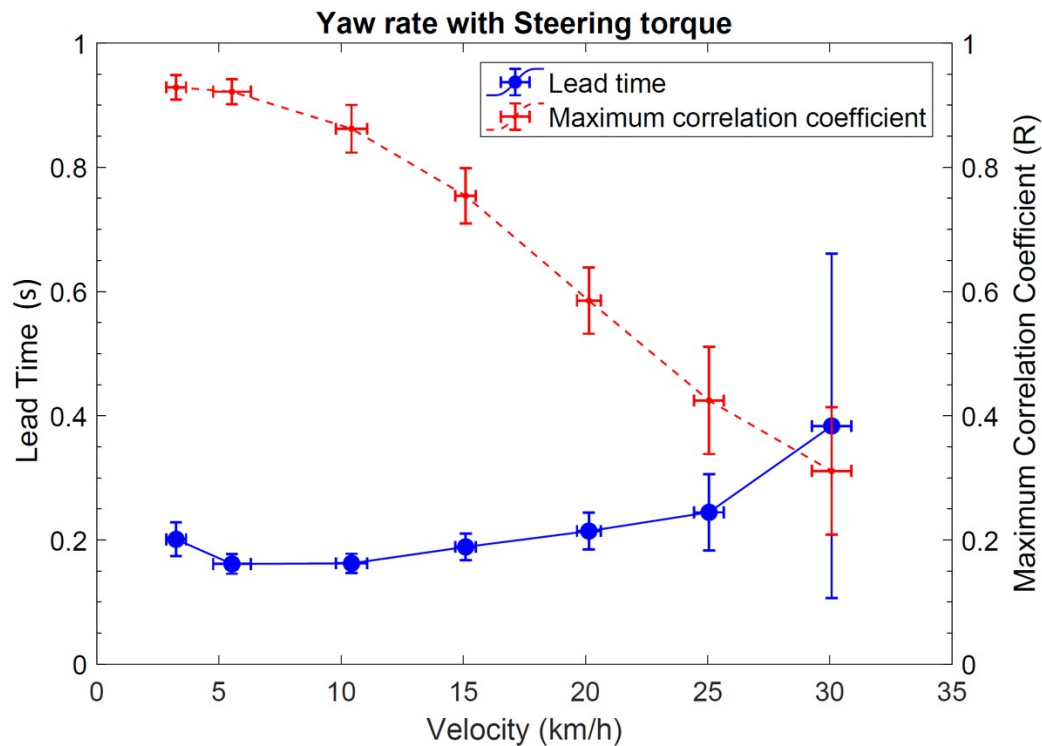
Figure 3.18: Maximum correlation(R) and lead time for yaw rate with steering torque

The above analysis results showed that that roll angle and roll rate are the useful output parameters have been used by riders for estimating the steering inputs to stabilize the motorcycle at speeds below 10 km/h. In the next section, the analysis to identify the appropriate input parameter between the steering angle and steering torque is discussed.

Input parameter evaluation

The input parameter between the steering angle and steering torque were selected based on two requirements for further studies. Firstly, it should be able to be estimated accurately from the useful output parameters. Secondly, it should be applied as late as possible to accommodate the delay in the system. A multiple regression analysis (MRA) between the useful output parameters as independent variables and the input parameters as dependent variables was performed, to estimate and identify the input parameter that can be estimated accurately between the steering angle and the steering torque.

A linear MRA was performed using the roll angle and roll rate to estimate the steering angle and steering torque from the equation as follows:

$$Steering\,Input\,(\delta\,or\,T) = a_1\phi + a_2\dot{\phi} \tag{3.2}$$
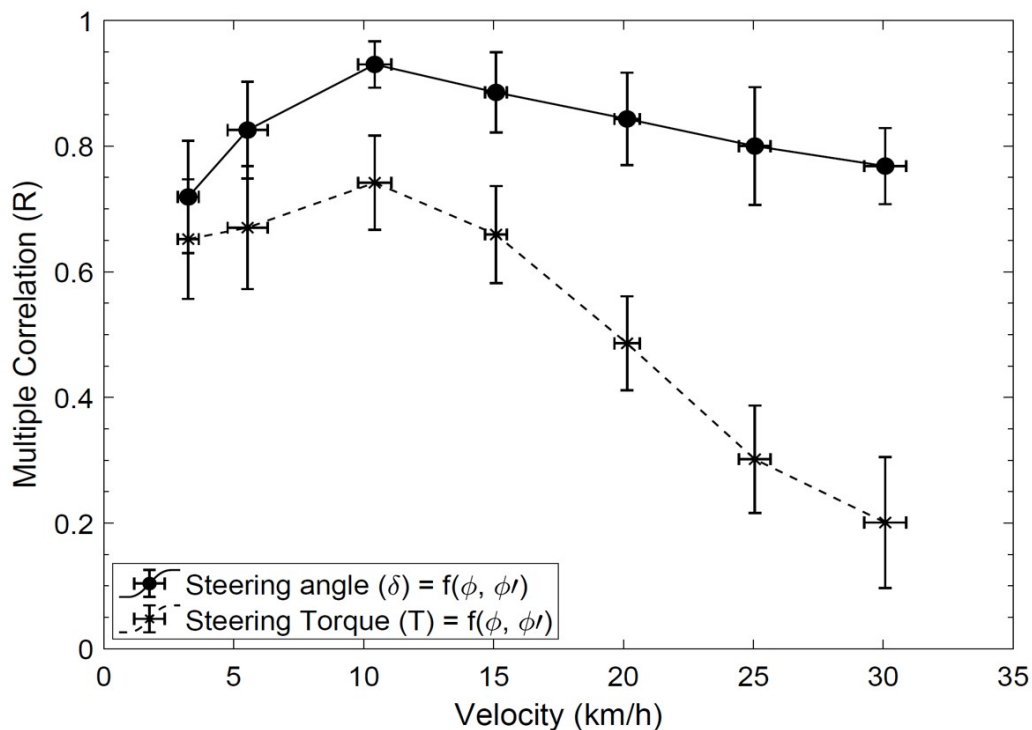
Figure 3.19: Multiple correlation of roll angle and roll rate with steering angle and steering torque

The results from the MRA show that the steering angle had higher regression correlation (RC)

of more than 0.7; whereas, it ranged from 0.2 to 0.7 for steering torque, as shown in Figure 3.19. It shows that the steering angle can be estimated more accurately than steering torque using the output parameters. Further, the MCC and lead time were calculated for the steering torque with the steering angle as shown in Figure 3.20. The CC ranges from 0.5 to 0.9. This strong correlation showed that the lead time calculation was accurate. The figure shows that the steering angle was leading the steering torque at speeds below 20 km/h; whereas, it had delay above this speed. The value of steering angle lead time was low (below 0.2 s), and RC for steering angle was significantly higher in comparison to that of steering torque. Therefore, the steering angle was selected as an appropriate input parameter and used in further studies.
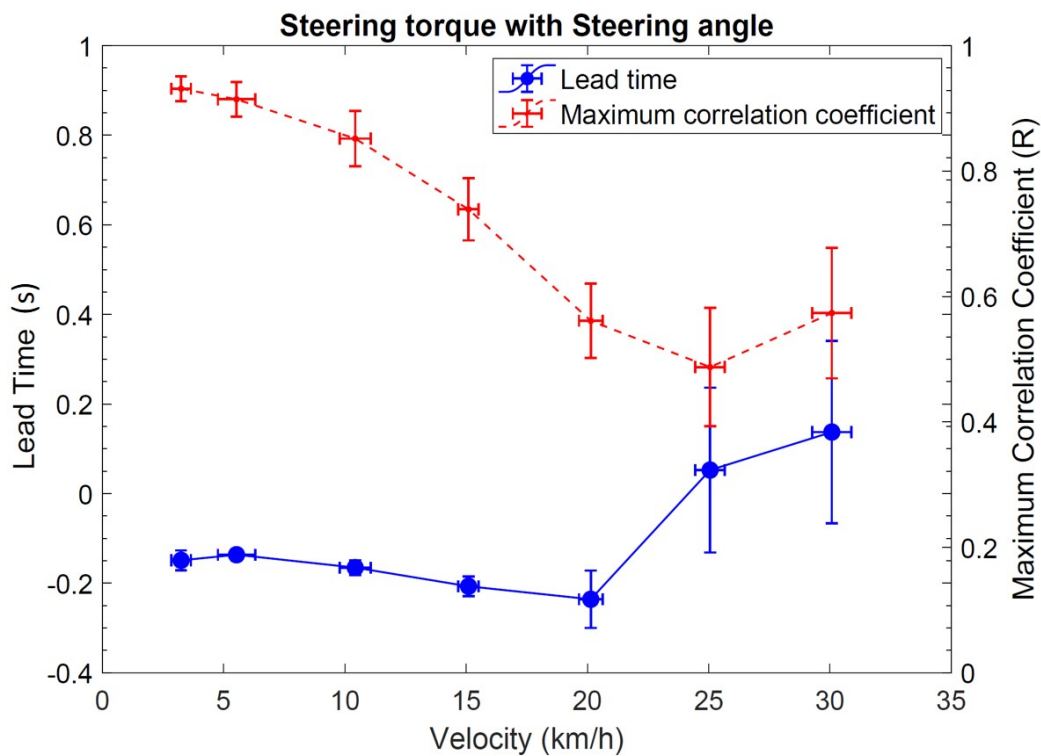
Figure 3.20: Lead time and multiple correlation(R) for steering torque with steering angle

3.4.5 Estimation and validation of the control input

Steering angle estimation

An MRA was performed using the steering angle as a dependent parameter; and, the roll angle and roll rate as independent parameters. Gain values (Regression coefficients) for the roll angle (a_1) and roll rate (a_2) were calculated using the Equation 3.2 and shown in Figure 3.21. The figure shows that the values of a_1 and a_2 increased as the speed reduced, which shows the inputs requirements for stability at low speeds were more. Also, the larger SD for these coefficients indicated that the rider inputs to achieve the stability were different at these speeds.
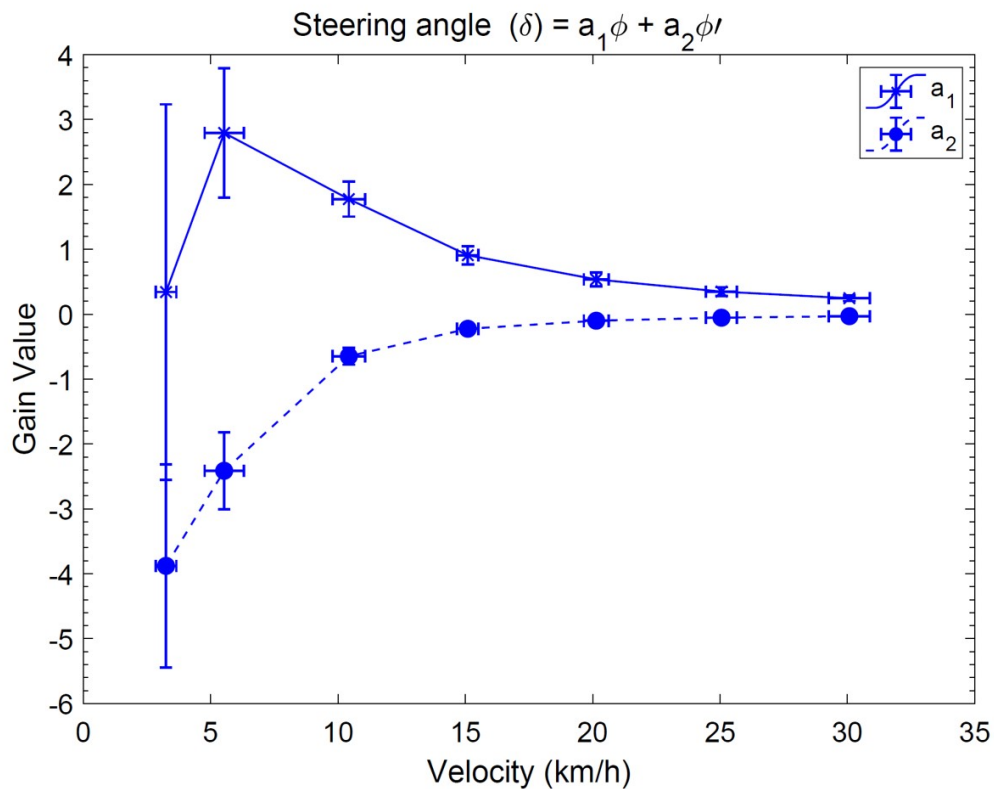
Figure 3.21: Multiple regression coefficients for roll angle and roll rate with steering angle

The values of the roll angle gain (a_1) and roll rate gain (a_2) can be calculated from the following equations:

$$a_1 = 0.011v^3 - 0.27v^2 + 2.5v - 5 \tag{3.3}$$

$$a_2 = -0.044v^2 + 0.92v - 6.4 \tag{3.4}$$

where v is the longitudinal velocity of the motorcycle in km/h.

Further, the roll angle, roll rate and steering angle were normalized, and the gain values for the roll angle and roll rate were calculated again. The percentage contribution of these gains values for estimating the normalize steering angle are shown in Figure 3.22. The figure shows the contribution of the roll rate was significantly more at low speeds than that of the roll angle, and vise versa. It shows that the roll rate was a useful parameter at low-speeds below 5 km/h; whereas, the roll angle became important above this speed for the steering angle estimation for motorcycle stability. In the next section, the validation of this steering angle estimation model is presented by comparing the same with corresponding measured data.
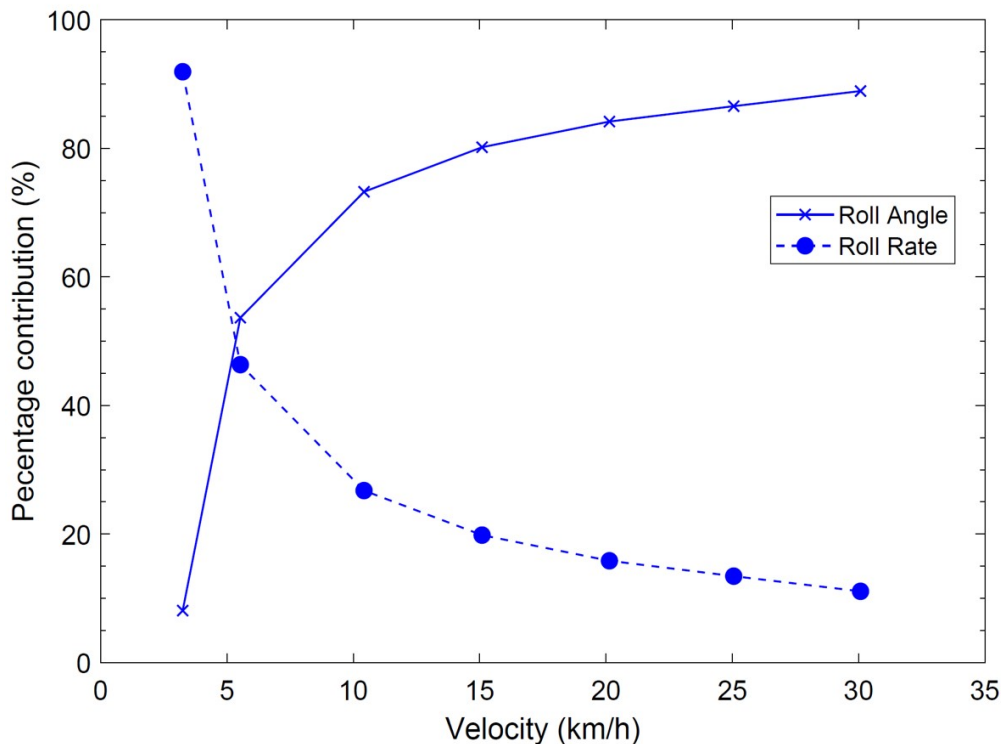
Figure 3.22: Multiple regression coefficients for roll angle and roll rate with steering angle

Validation of steering angle estimation

The steering angle estimated using the MRA was compared with its experimental measurements. Figures 3.23 and 3.24 show the results of the comparison at speeds 3.1 and 5.8 km/h, respectively. They show that the steering angle estimation matches reasonably with the same applied by the rider to stabilize the motorcycle at these speeds.
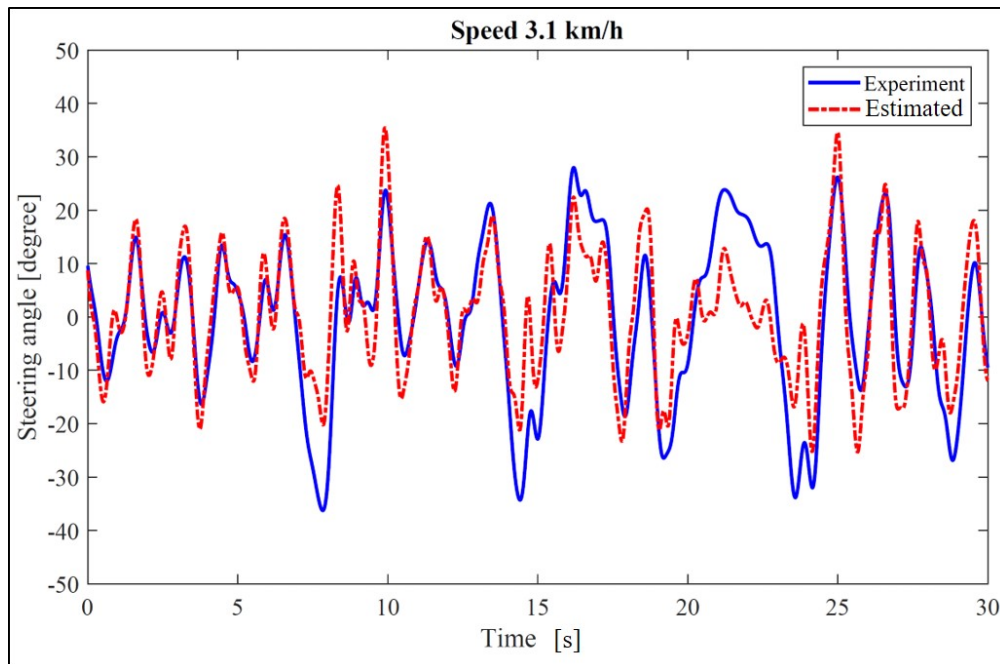
Figure 3.23: Steering angle prediction validation at 3.1 km/h
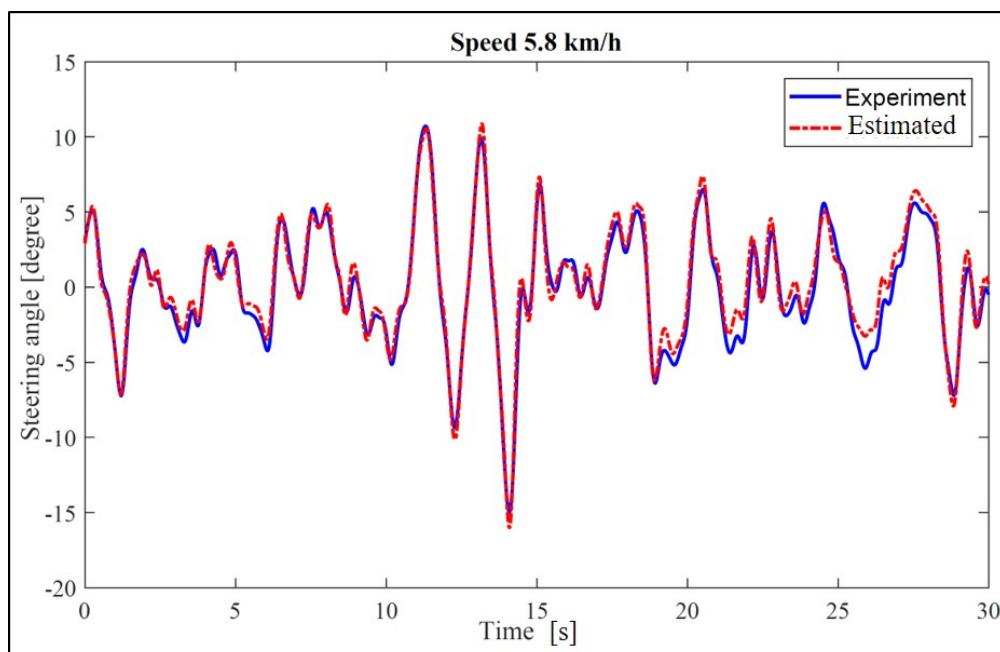
Figure 3.24: Steering angle prediction validation at 5.8 km/h

3.4.6   Steering estimation by different riders

The roll angle gain a_1 and roll rate gain a_2 were calculated individually for different experience levels of riders to observe the difference in their control inputs. They were categorized into three experience levels: beginner, intermediate and expert as discussed in section 3.4.2. The regression Equation 3.2 was used to calculate the gain values from the experimental data. Figures 3.25 and 3.26 show the gain values for roll angle and roll rate, respectively, with the riders' experience levels and motorcycle speeds. The gain values were found to be higher for the expert riders in compared with the beginner riders. The RC showed in Figure 3.27 also has a similar trend. It shows that the expert riders were able to use the roll angle and the roll rate parameters as the feedback more accurately than the beginner riders to estimate the required steering angle control.
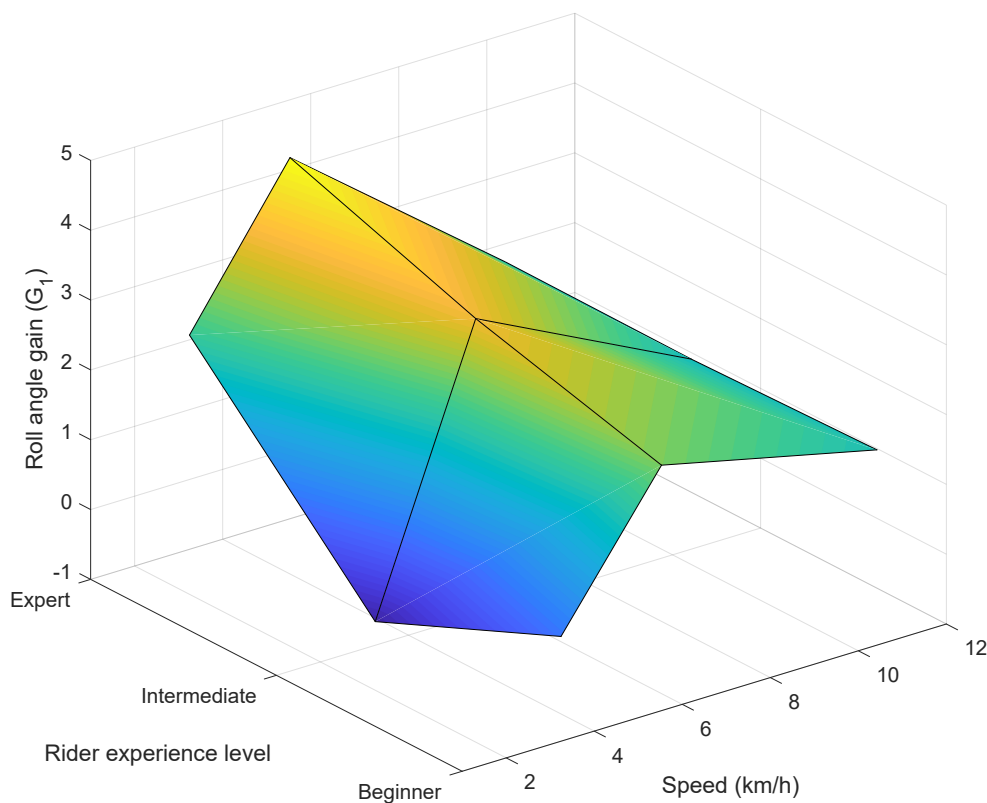
Figure 3.25: Gain values of the roll angle for various riders experience levels at different speeds.
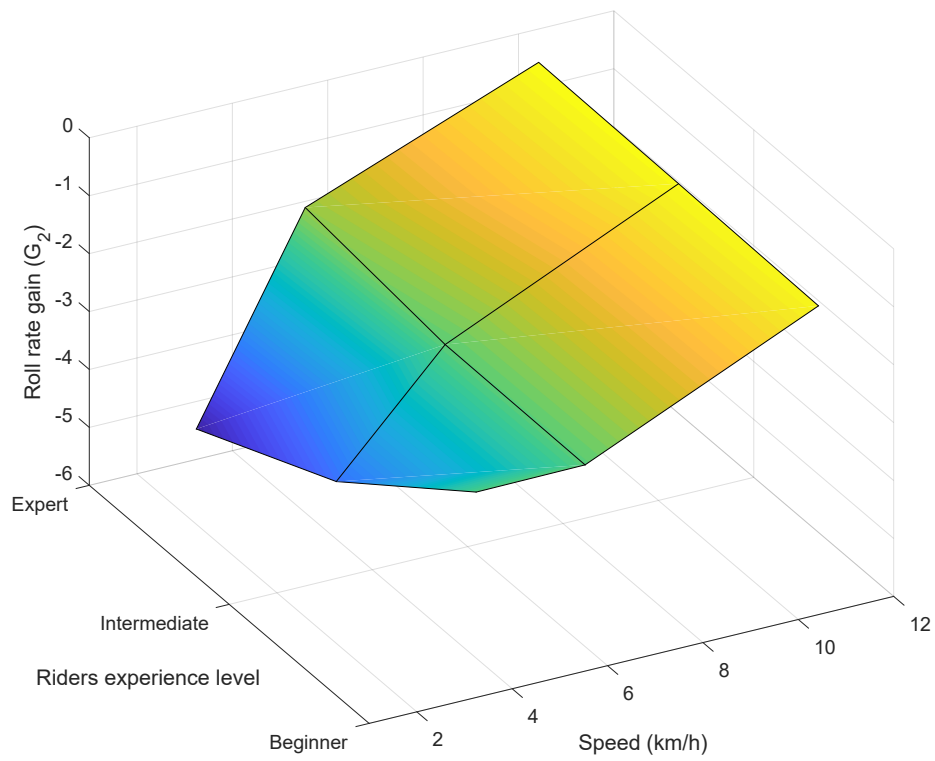
Figure 3.26: Gain values of the roll rate for various riders experience levels at different speeds.
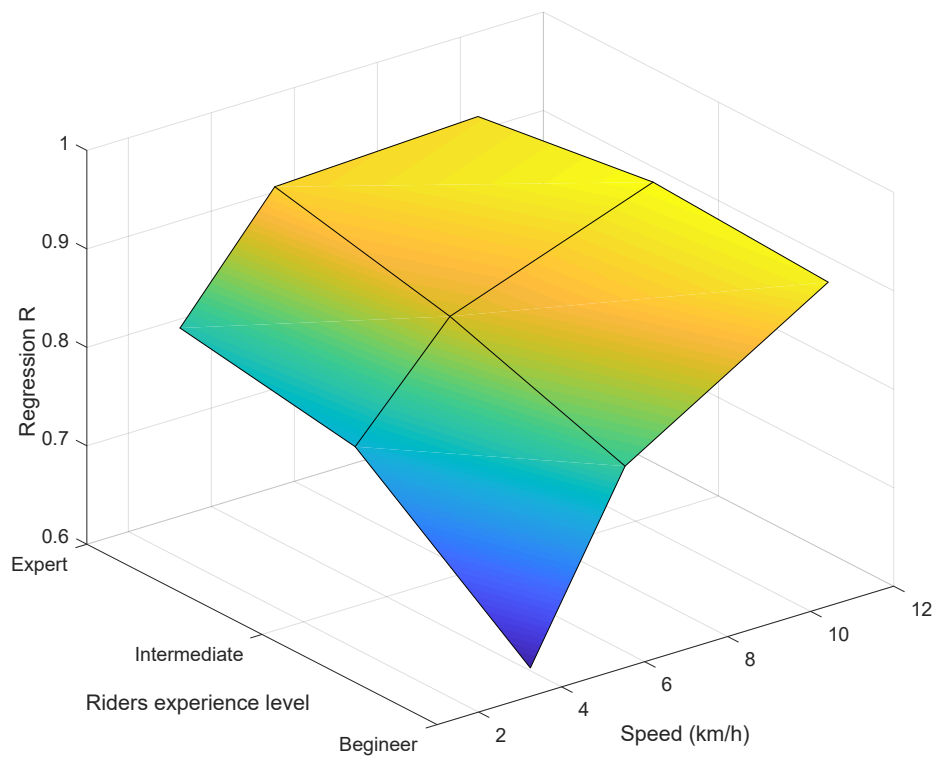
Figure 3.27: Regression correlations for various riders experience levels at different speeds.

The low gain values for the beginner riders can also be attributed to their slow response time to use these parameters to estimate the steering angle. It also reduces their comfort and confidence in stabilizing the motorcycle at low-speeds; although, they improve their response time with their riding experience. Therefore, a control system that accurately determines these steering inputs can support the riders. Furthermore, developing a controller that provides steering input similar to a human can also be studied and improved for other riding maneuvers such that it will not interfere with the intent of the riders.

Chapter 4

Modeling and Validation of Control Algorithm Using MBD Simulation

4.1   Introduction

A control algorithm was developed to stabilize the motorcycle at low speeds, based on the steering estimation model discussed in Chapter 3. The Simulink model of the control algorithm was integrated with a validated multi-body dynamics (MBD) model of the motorcycle used for experiments. The motorcycle was modeled in an MBD software, VI-motorcycle. Co-simulation studies have been performed between the Simulink and MBD software. The results of these studies validated the control algorithm. In this chapter, the control algorithm model, MBD model of the motorcycle, co-simulation studies and their results are discussed.

4.2 Control algorithm

The control algorithm developed for balancing the motorcycle is shown in Figure 4.1. Wherein, a_1 and a_2 are the gain values for the roll angle and the roll rate, respectively. They were determined using the MRA by Equations (3.3) and (3.4), as discussed in the previous section. They were keyed in the regression Equation 3.1 for estimating steering angle (δ).The reference values for roll angle and roll rate are zero since the objective of the research is to achieve the low-speed stability.
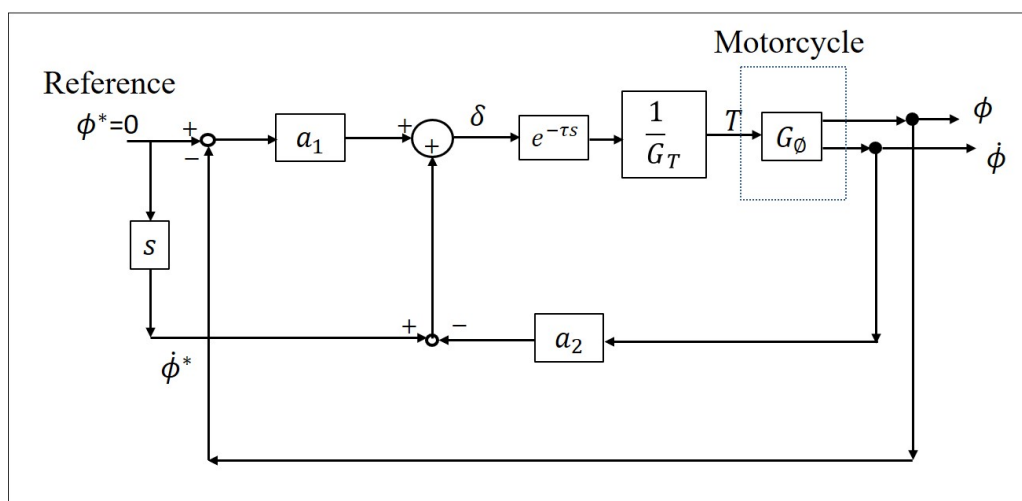
Figure 4.1: Control algorithm to balance the motorcycle.

4.2.1 Control model in Simulink

The Simulink model of the control algorithm is shown in Figure 4.2. It has a plant, which was imported from the MBD software, and contains the details of the MBD model and simulation conditions. In the plant, output signals are the roll angle and roll rate; the input signal is steering torque as it is the only input provided for the steering control in the software. In the control model, both the roll angle and roll rate have delay blocks to simulate the actual riding controls and to tune the controller. They were multiplied with the proportional and derivative gains (K_p and K_d), respectively, which are the roll angle gain a_1 and roll rate gain a_2 derived from the experimental analysis. These values were then added to estimate the steering angle, which was multiplied with a gain value to determine the steering torque.
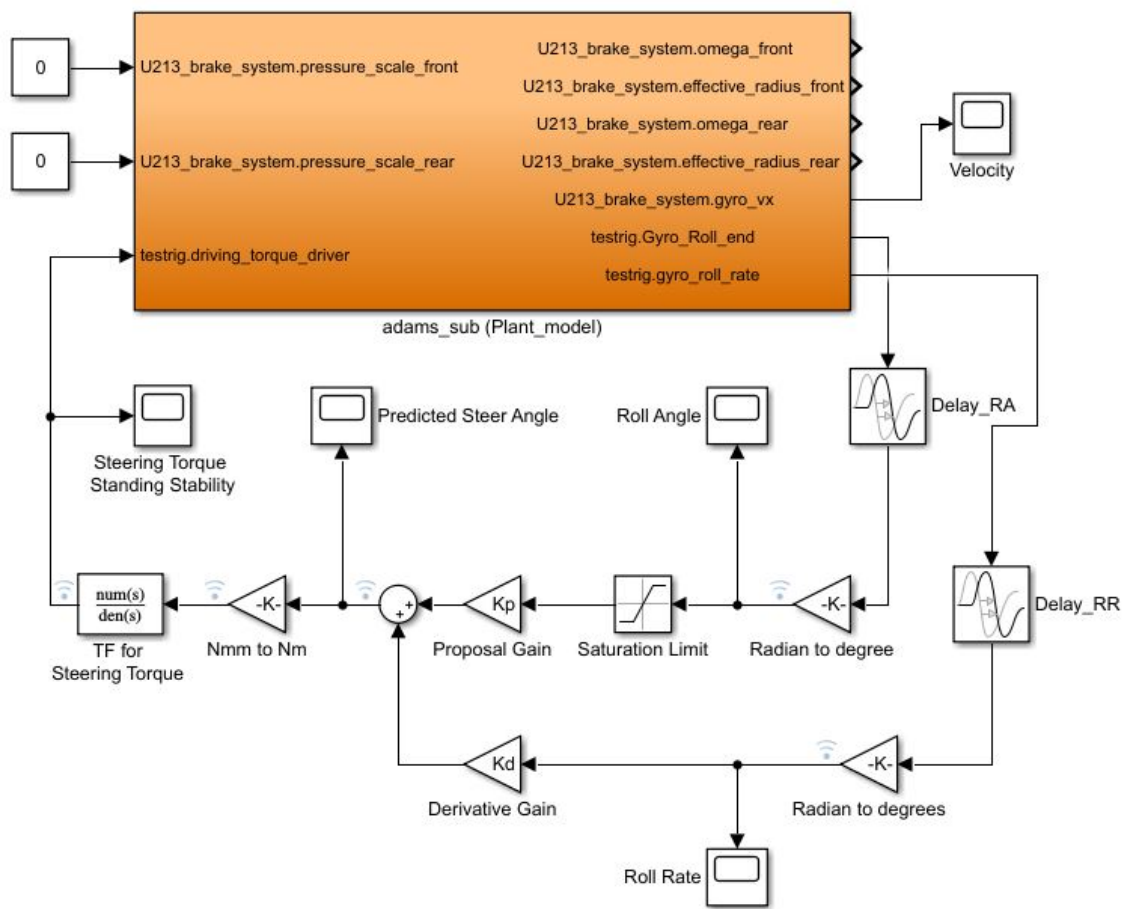
Figure 4.2: Stability Control of the motorcycle

4.2.2 Steering torque estimation for co-simulation

MBD model of the motorcycle required steering torque as the input. Thus, estimating it accurately from the experimental data was essential. In general, steering torque T is a function of steering angle (δ), steering rate ($\dot{\delta}$) and steering acceleration ($\ddot{\delta}$). Although, a linear relationship between the steering angle and steering torque was defined as the CC between the steering torque and steering angle were found to be high (more than 0.9 at speeds 3 and 5 km/h), as shown in Figure 4.3.
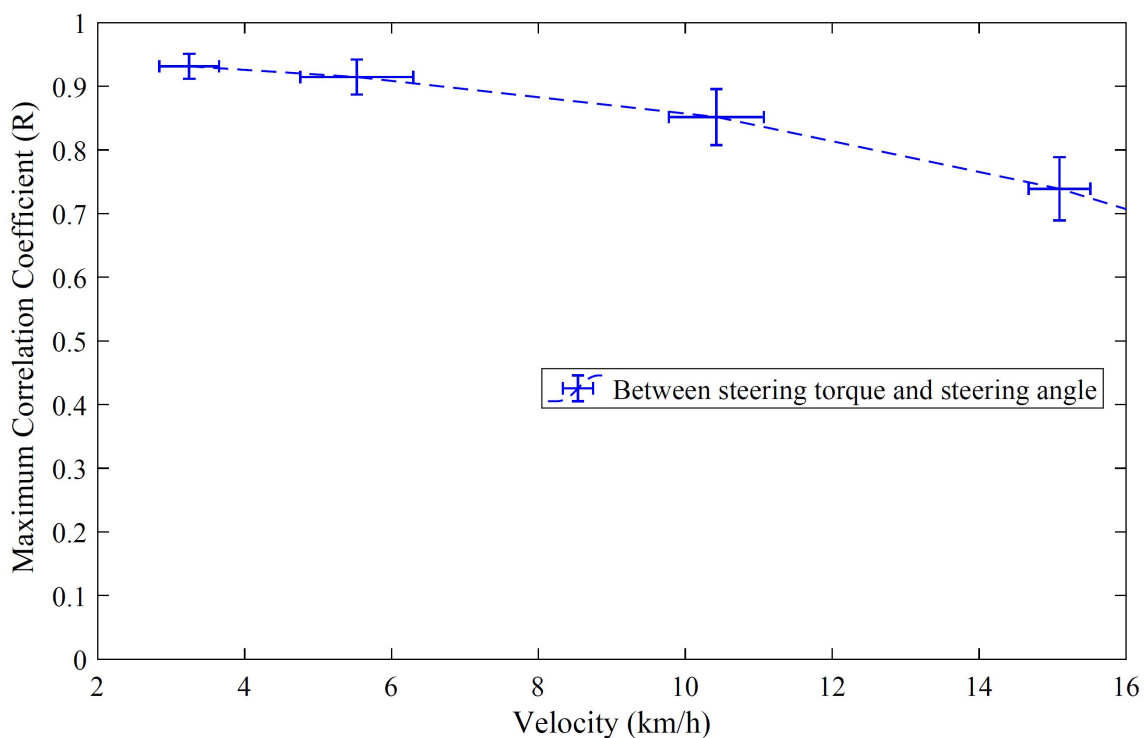
Figure 4.3: Maximum correlation coefficient between the steering angle and the steering torque.

The relation between the steering angle and the steering torque is defined using the following equation:

$$T = \delta/G_T \tag{4.1}$$

where, $1/G_T$ is gain value for the steering angle to determine the steering torque. Its value can be calculated from the experimental data using the following equation:

$$G_T = -0.069v + 1.8 \tag{4.2}$$

The value of G_T is calculated at the MCC point, where the steering torque has a lead time of τ with the steering angle. These values of G_T and τ are shown in Figures 4.4 and 4.5, respectively. The lead time can be defined by the following equation:

$$\tau = -0.0061v - 0.11 \tag{4.3}$$
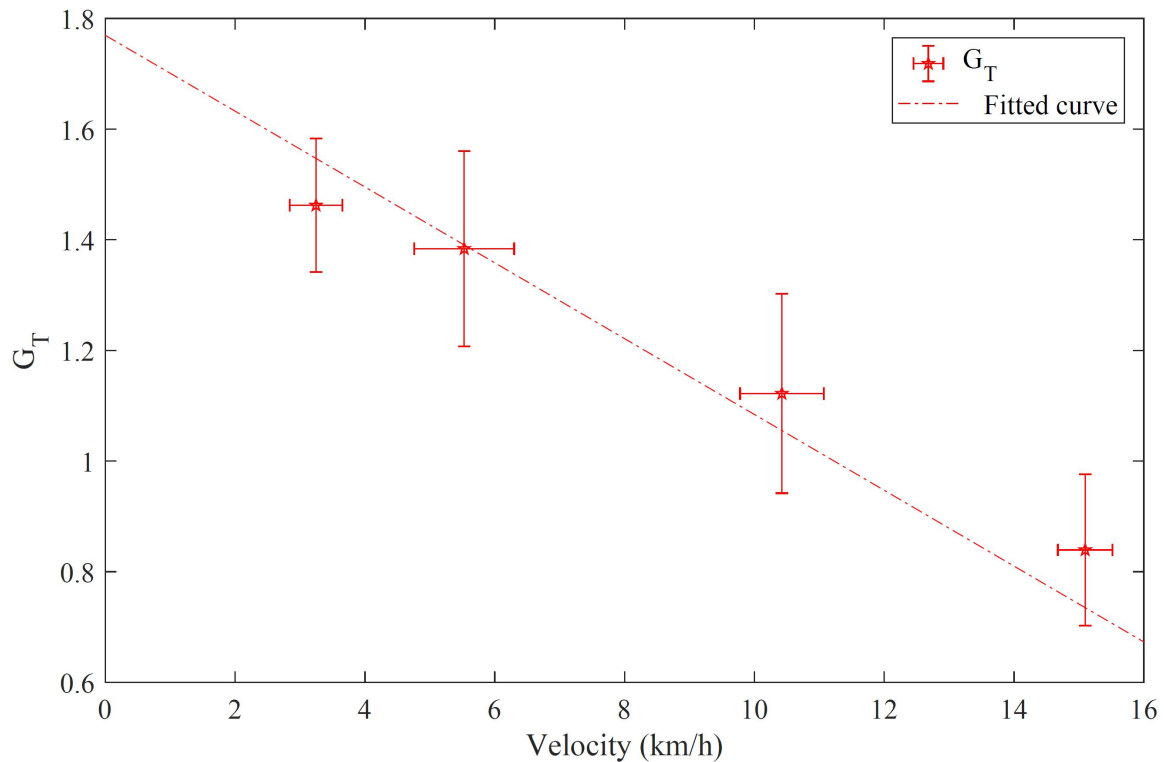
Figure 4.4: Values of the G_T for estimating steering torque from steering angle

The magnitude and point of application of the steering torque were determined from the gain value $(1/G_T)$ and the lead time (τ), respectively. It was applied to the motorcycle G_ϕ in the control algorithm, shown in Figure 4.2. The results of this section were used in the Simulink model of the control algorithm. Further, it was verified by co-simulating it with MBD model of the motorcycle, as described in the next section.
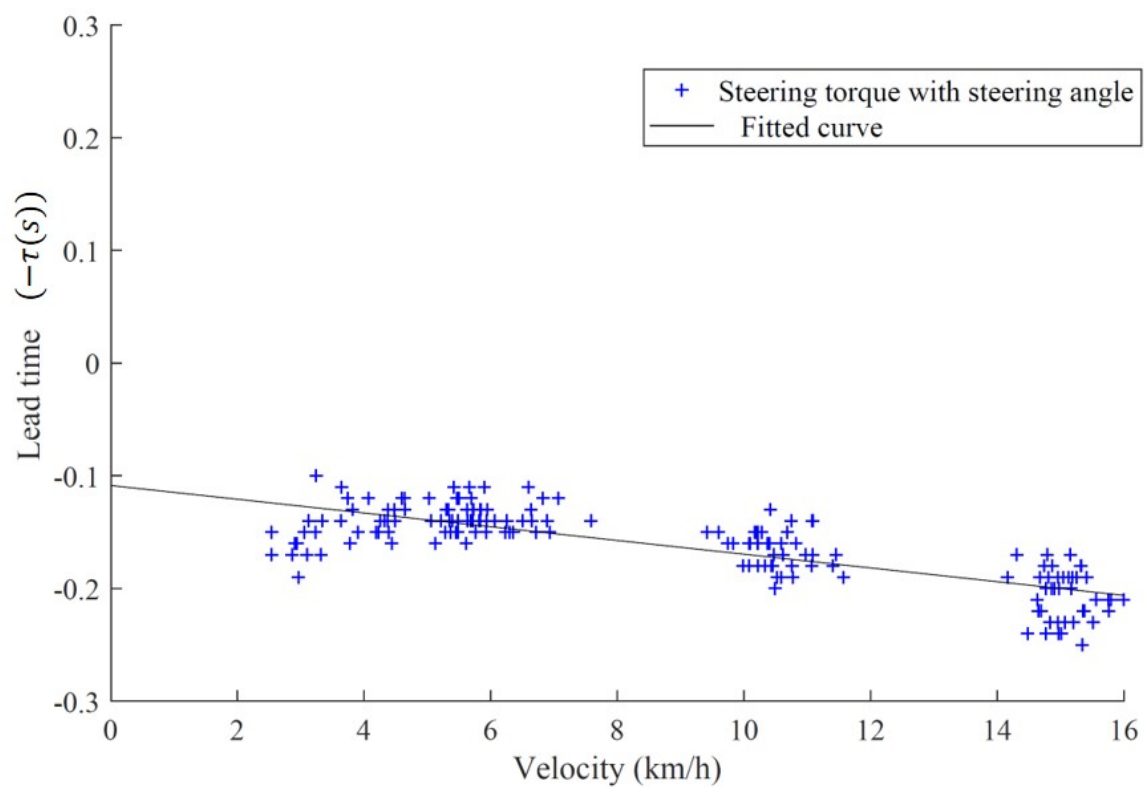
Figure 4.5: Lead time values for the steering torque with the steering angle.

4.3 Multi-body dynamics Model

An MBD model of the motorcycle is modeled using commercially available software VI-Motorcycle, as shown in Figure 4.6. The model consists of the various subsystem as per the kinematics and dynamics requirements of the motorcycle. It had ten subsystem assemblies: front fork, rear suspensions, front wheel, rear wheel, engine, driveline, brakes, frame, toggle-link and rider. The subsystems were selected as rigid bodies as the dynamic loading was significantly low for the low-speed stability simulations. The tire model by Pacejka is used in the MBD model. The detailed construction of the model for a motorcycle using the MBD software can be referred from the research paper by Karanam et al. [67]. The details of the spring-damper properties of the suspension systems, mass-inertia of the motorcycle subsystems and tire properties are given in Appendixes 1, 2 and 3, respectively. The details of the layout of the motorcycle model in MBD software was the same as that for the experimental motorcycle described in Chapter 2.
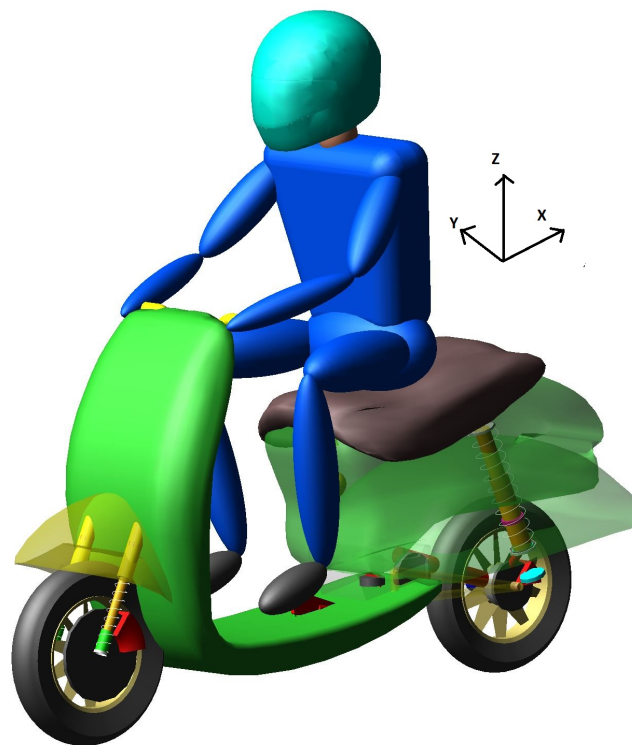
Figure 4.6: MBD Model of the motorcycle

The MBD model has twelve degrees of freedom (DOF), which are associated with the following motions of the vehicle:

- Steering rotation,

- Front fork translation,

- Rear shock-absorber translation,

- Toggle-link rotation,

- Forward motion of the motorcycle,

- Roll motion of the motorcycle,

- Longitudinal slippage of the front tire,

- Longitudinal slippage of the rear tire,

- Lateral slippage of the front tire,

- Lateral slippage of the rear tire,

- Vertical motion of the front tire,

- Vertical motion of the rear tire,

The frequencies of the steering angle and the roll angle at 3 km/h were below 1 Hz, as shown in Figure 4.7. As discussed in the introduction section of this paper, the riders lean does not contribute significantly to the low-speed stability at these speeds and frequencies [32]. Therefore, the rider in the MBD model is fixed to the frame as a rigid body in this research. Further, the MBD model of the motorcycle is validated by experiments for the dynamic behavior before conducting simulation studies [68, 69].
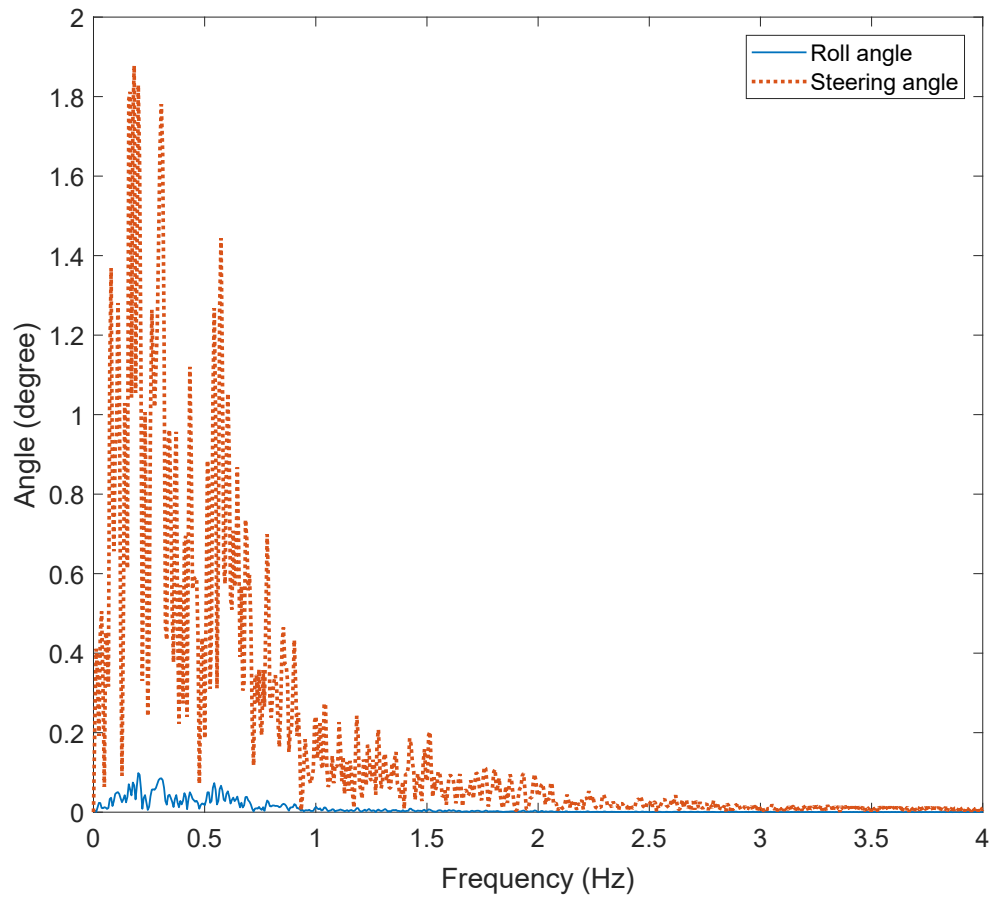
Figure 4.7: Fast Fourier transform of the steering angle and the roll angle @ 3km/h.

4.4 Co-simulation procedure

The MBD model of the motorcycle and the control algorithm developed to achieve standing stability are integrated using some procedures, which are discussed in this section. It includes steps that need to be followed in both the software, VI-MotorCycle and MATLAB/Simulink. At first, the control plug-in switched ON in VI-MotorCycle, and the MBD model of the motorcycle was opened. The state variables of the motorcycle model which in this case is steering torque modified to zero. Whereas, the steering angle was a consequence of the effect of the applied steering torque on the motorcycle. The modification in the steering torque broken the connection of the default controller of the software such that the steering actions can be defined using the Simulink model of the control algorithm [70]. Then, the plant model for the Simulink control model was exported using the tab shown in Figure 4.8.
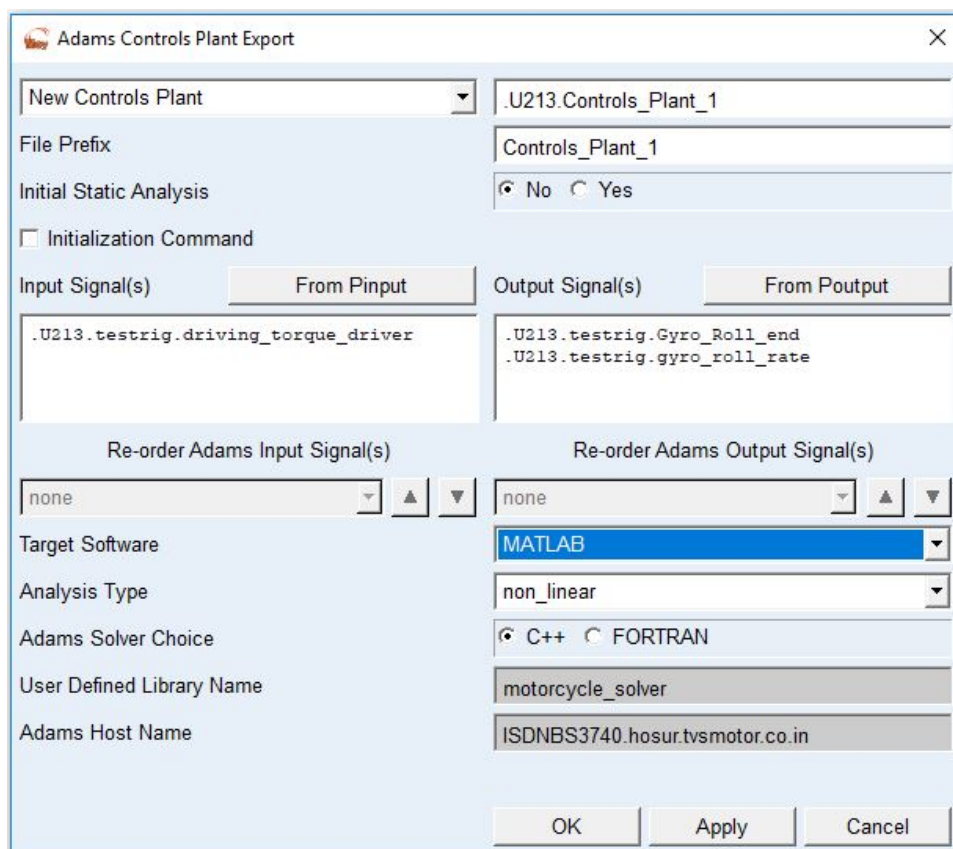
Figure 4.8: Plant Export for ADAMS Control

Once the model interface has been defined, a straight line analysis was submitted in order to generate all the files required for the co-simulation analysis. The simulation is carried out while keeping the lateral controller switched OFF. Whereas, the longitudinal controller is switched ON to maintain the desired speed of the motorcycle during co-simulation. The MBD software supports the files_only analysis mode for the co-simulation. This procedure created a set of standard solver files such as adm, acf, nam, vdf, etc. in the working folder. In addition to these standard files, a .m file was also created which was required for the Simulink model. Next, in the MATLAB environment, the working directory of the MATLAB is changed to the same folder in which the MBD solver files have been created. From the working directory, loading and executing the interface script (.m file) by entering its name in the MATLAB command prompt appeared the following information:

%%% INFO : ADAMS plant actuators names :

1 brake_system_3D.pressure_scale_front

2 brake_system_3D.pressure_scale_rear

3 testrig.driving_torque_driver

%%% INFO : ADAMS plant sensors names :

1 brake_system_3D.omega_front

2 brake_system_3D.effective_radius_front

3 brake_system_3D.omega_rear

4 brake_system_3D.effective_radius_rear

5 brake_system_3D.gyro_vx

6 testrig.Gyro_Roll_end

7 testrig.gyro_roll_rate

The information shows other exported variables, which were the default ones related to the ABS system. In this simulation, other state variables can be neglected as these were not set to be used by the Simulink. The execution of MATLAB interface file (.m file) also generated a Simulink file named as adams_sys, which contains the Simulink plant model named as adams_sub. The plant model had the MBD model information such as the motorcycle layout, mass-inertia details, test

conditions. The plant model is set for the communication interval of 0.01 in accordance with the sampling rate of 100 Hz of the measured experimental data. It has been used for building the architecture of the control algorithm is shown in the next section.

4.5   Co-simulation studies and results

The co-simulation was run in the Simulink, which run the MBD model in the background. The default controller of the MBD software was unable to balance the motorcycle model at speeds below 10 km/h. On the contrary, the motorcycle model is balanced at 3 km/h during the co-simulation using the developed control algorithm, as shown in Figure 4.9. Figure 4.10 shows that the steering angle determined from the regression analysis matches the steering angle from the co-simulation. It confirms that the control algorithm estimates the steering angle required to achieve low-speed stability accurately during the co-simulation. The steering input to the motorcycle model provided in terms of steering torque shown in Figure 4.11.
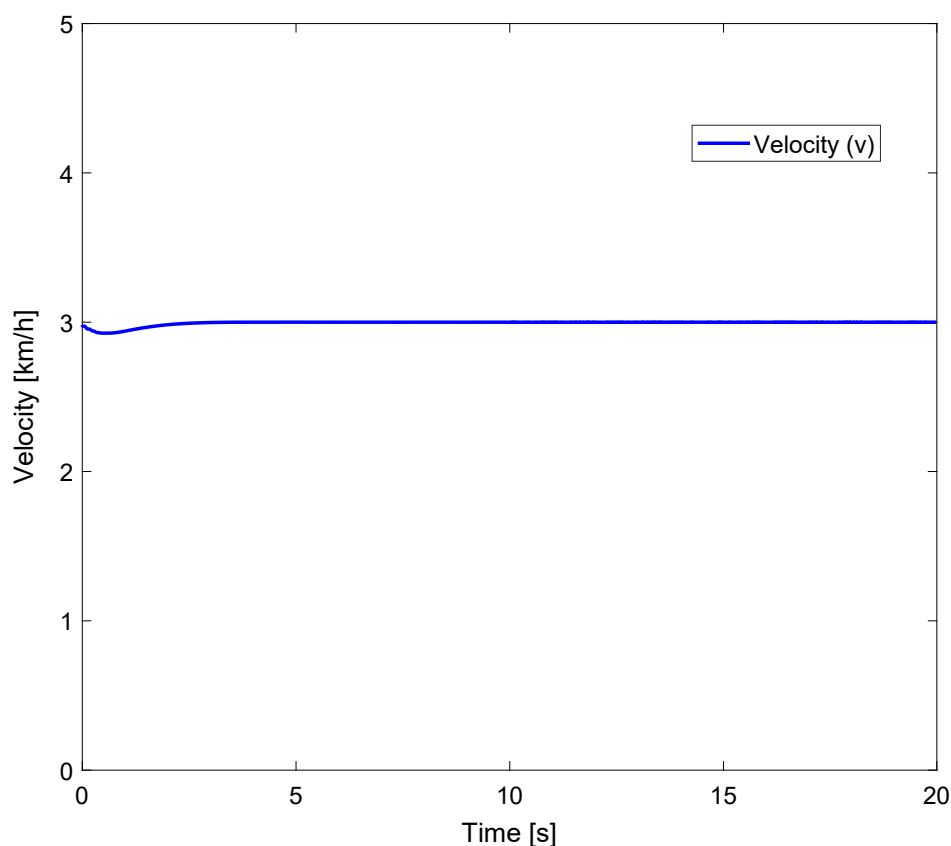
Figure 4.9: Motorcycle speed during the co-simulation.
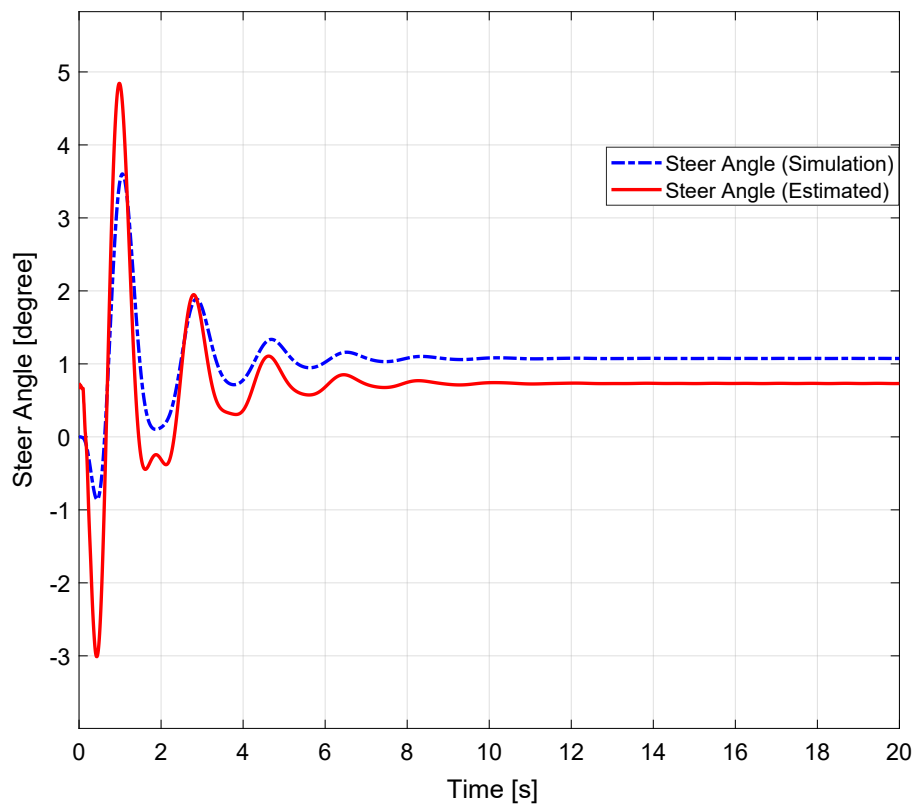
Figure 4.10: Comparison of actual and estimated steering angle in simulation.
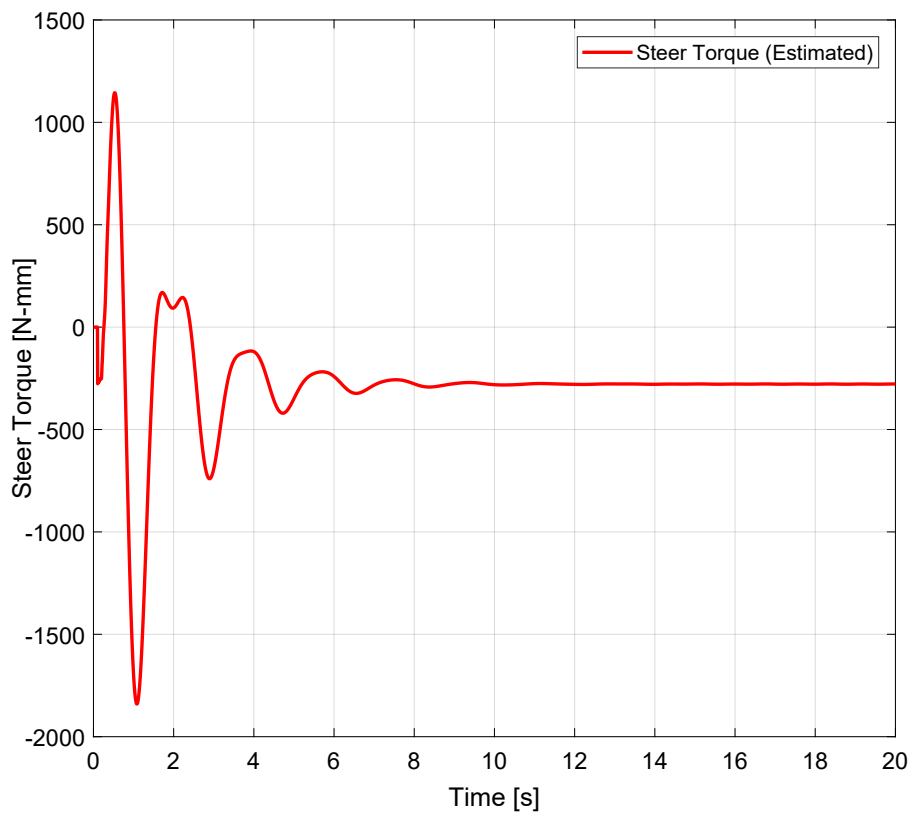
Figure 4.11: The steering torque estimated from the analysis applied to the motorcycle model.

Figures 4.12 and 4.13 show the output parameters from the simulation results. The roll rate in the simulation is zero after the initial oscillations, as shown in Figure 4.13. It shows that the motorcycle reaches the steady-state low-speed stability at 3 km/h. Also, the motorcycle model is moving almost in a straight path as the roll angle is close to zero, shown in Figure 4.12. The constant non-zero values of the roll angle and the yaw rate are due to two reasons: Firstly, the lateral center of gravity of the motorcycle due to its non-symmetrical subsystems about the motorcycle plane, including the one-sided engine; Secondly, absence of directional control that results in it to move in a circle of small radius. Also, there is a constant difference in the steady-state values of the steering angle between the simulation and estimation, as shown in Figure 4.10. This variation due to modeling limitations, also causes the motorcycle model to move in a different direction. However, a control algorithm with directional control will resolve this limitation by introducing some other feedback parameters such as yaw angle or yaw rate.
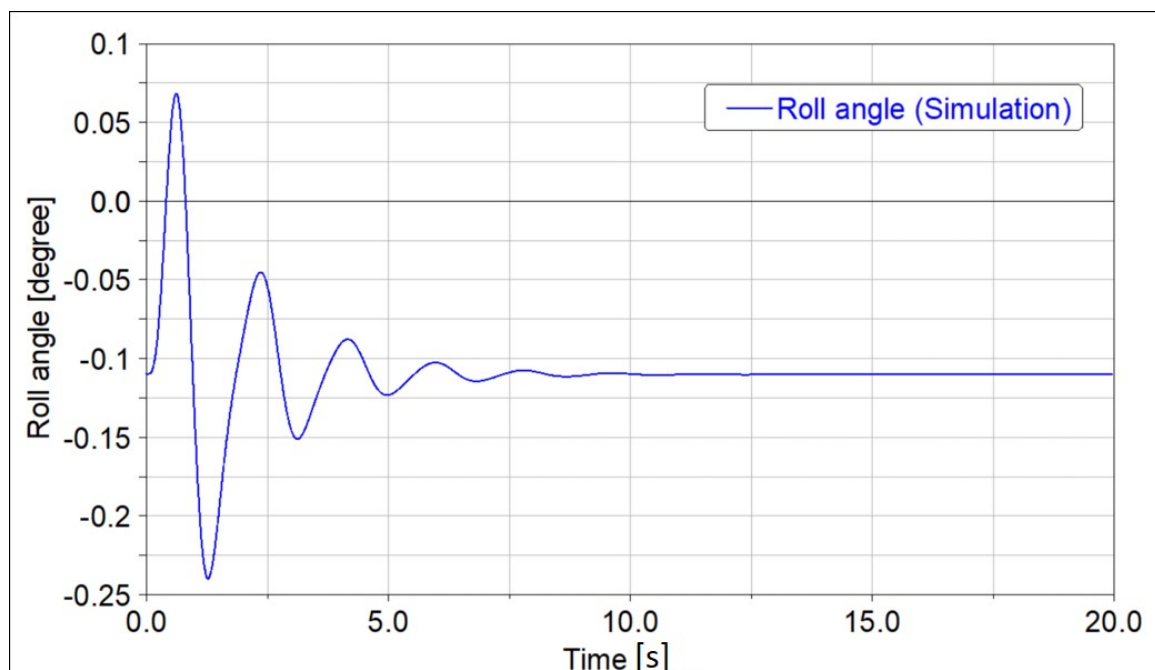
Figure 4.12: Roll angle result from the simulation.
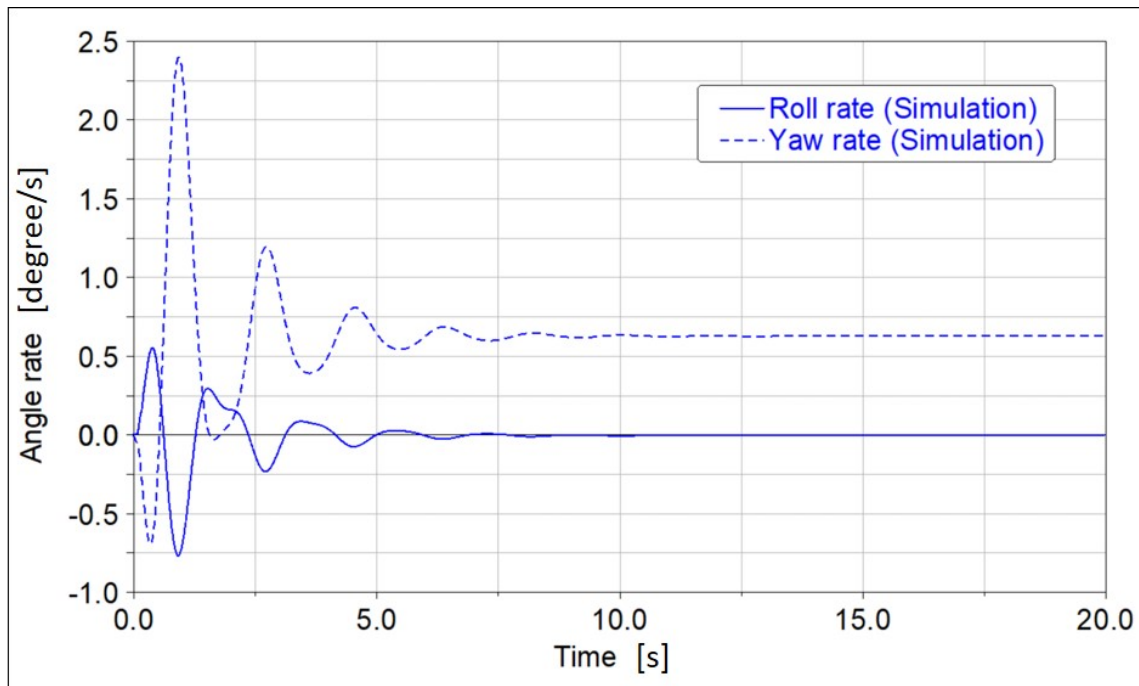
Figure 4.13: Yaw and roll rate results from the simulation.

The co-simulation results verify that the new control algorithm balances the motorcycle using the gain values determined from the analysis of the experimental data. The objective of the research is restricted to the stability at extremely low speeds; therefore, the direction is not controlled in the MBD software. The directional control for maneuvering it in the desired path and studies on rider body's degree of freedom at low-speeds are the future scope of the research.

4.6   Simulation studies for directional stability

The riders provide both stability and directional inputs to the motorcycles. Besides, they also apply additional input for any disturbances due to the road irregularities. Hence, the robustness of the controller has to be assured while balancing the motorcycle. Therefore, the studies on motorcycle stability in the straight path were extended for directional stability. The input to the steering is a superposition of both the stability and direction inputs. Thus, an additional constant steering torque was applied as the directional input. The Simulink model for it is shown in Figure 4.14. It shows that constant value is added to the final steering torque, which was estimated in the previous stability analysis.
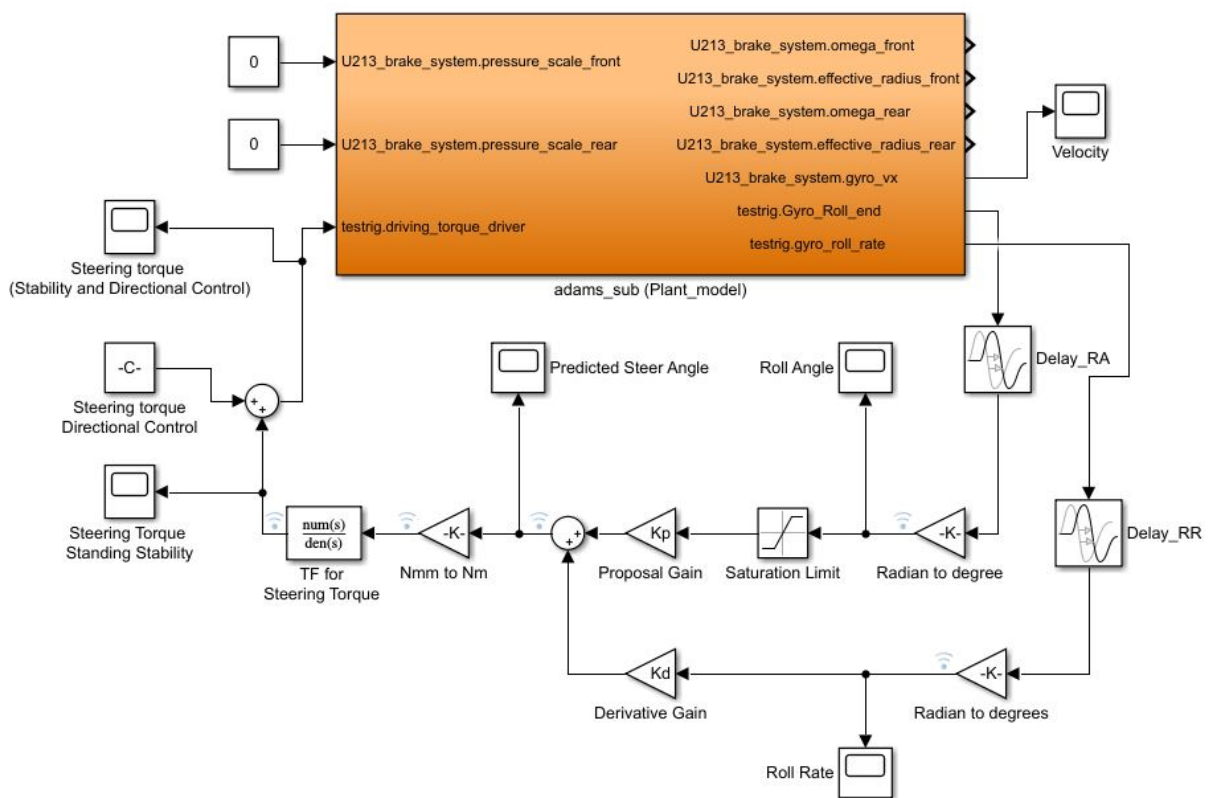
Figure 4.14: Directional control model for the motorcycle

The objective of this simulation studies was to evaluate the stability of the motorcycle, for additional steering input. Constant steering torque values of -5 Nm and 5 Nm were applied in addition to the steering torque estimated from the control model for stability. Figure 4.15 shows that in both cases, the motorcycle achieved the target speed of 3 km/h.
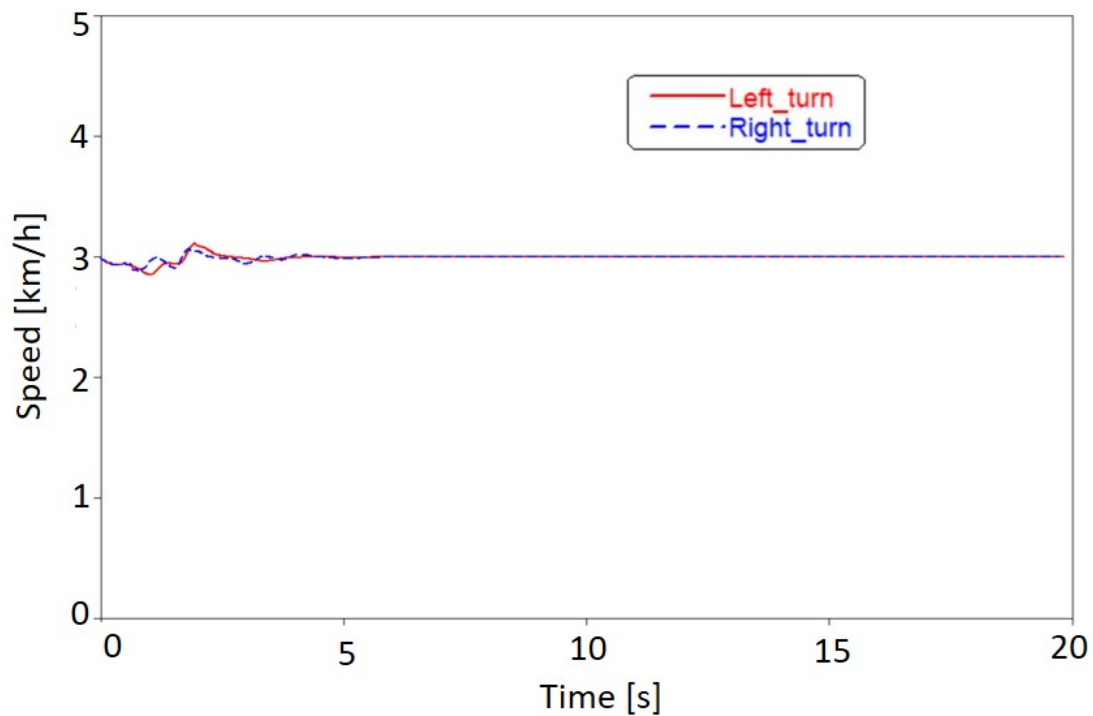
Figure 4.15: Speed of the motorcycle while taking a turn

Figure 4.16 shows that the initial oscillations in steering angle and steering torque are different for the left and right turn; however, the motorcycle is stable in both cases. It was confirmed from the roll angle curve as its values are constant and close to zero after the initial oscillation, as shown in Figure 4.17. Figures 4.17 and 4.19 show the gradually increasing yaw angle and constant yaw rate curves, respectively. They indicated that the motorcycle is traveling in opposite lateral directions, as shown in Figure 4.18. The roll rate is zero after the initial oscillation, which indicates that it has reached the steady-state stable condition, as shown by Figure 4.19. These results validate that the developed control algorithm is robust.
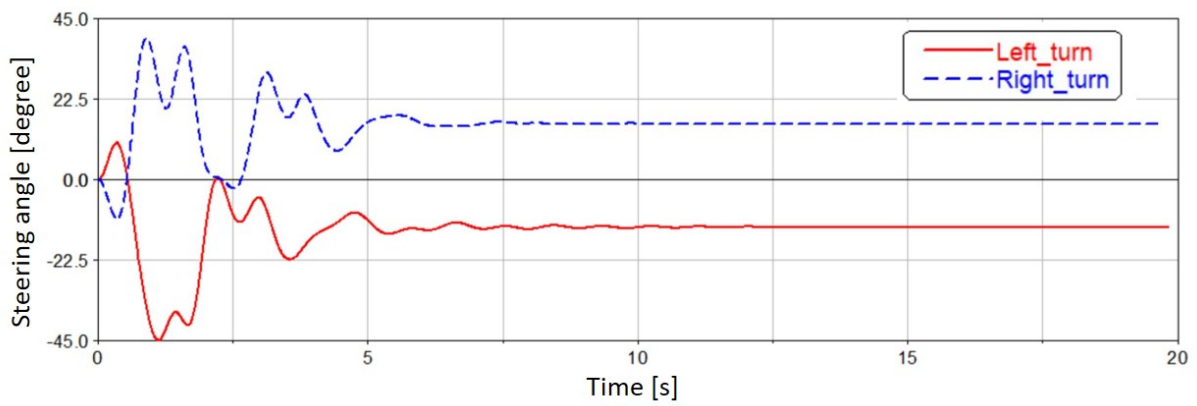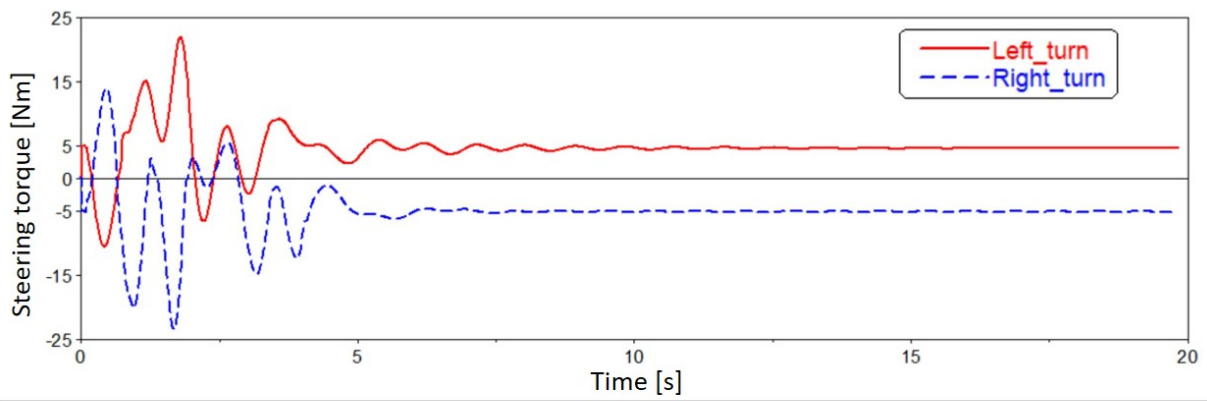
Figure 4.16: Steering torque and steering angle while taking a turn.
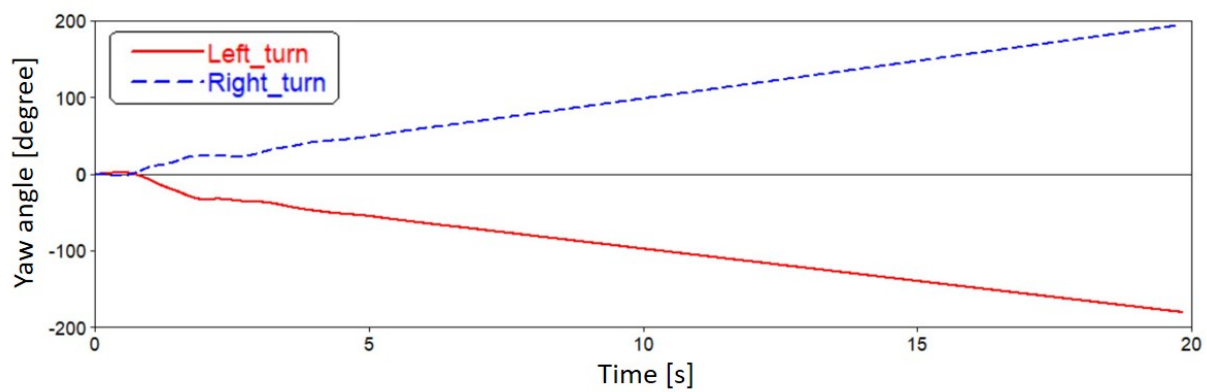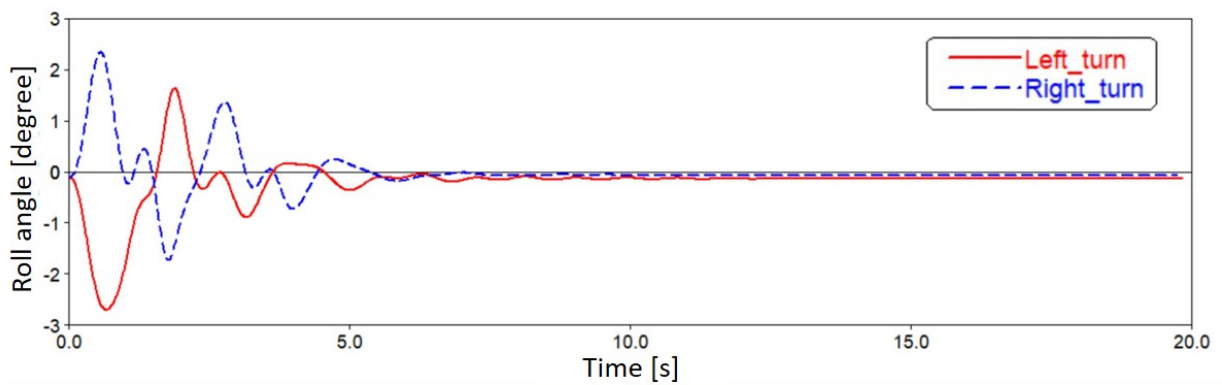
Figure 4.17: Roll angle and yaw angle while taking a turn.
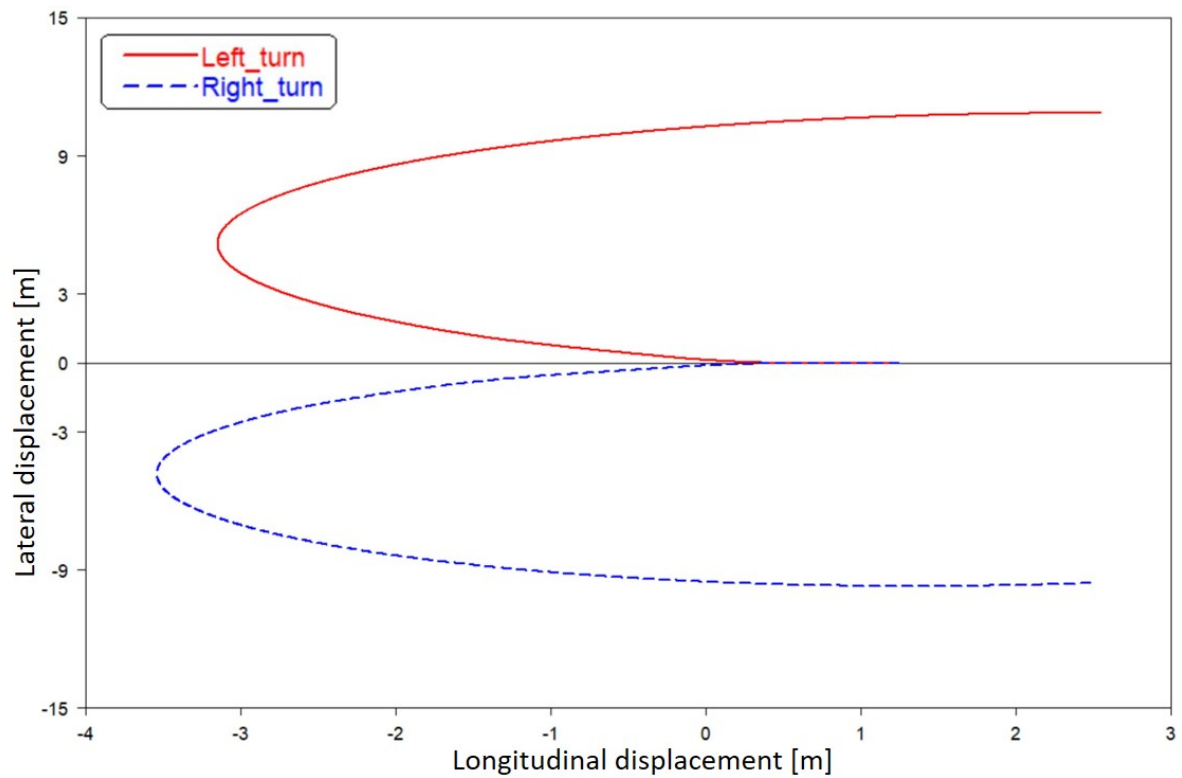
Figure 4.18: Lateral displacement versus longitudinal displacement while taking a turn.
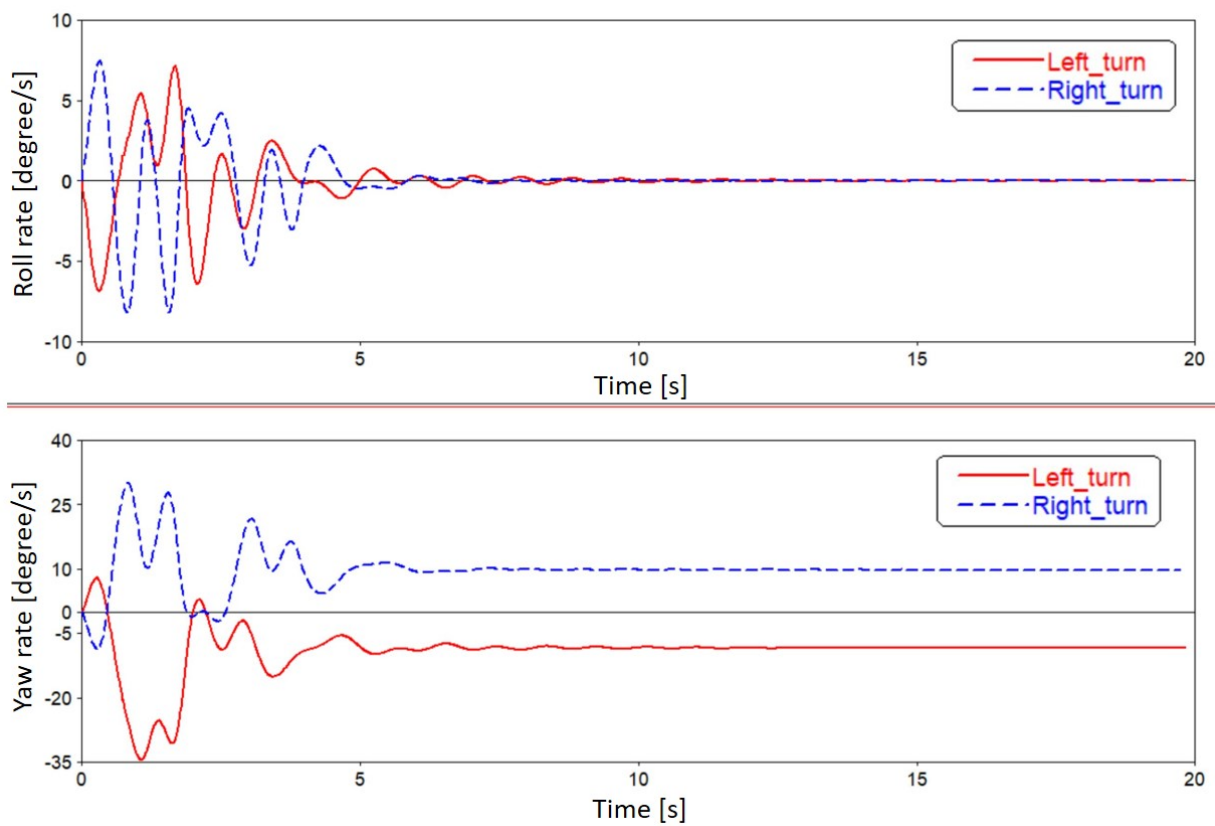
Figure 4.19: Roll rate and yaw rate while taking a turn.

Chapter 5

Conclusions and Future Scope

5.1   Conclusions

In this research, the low-speed stability of a motorcycle in the roll direction is studied using theoretical and experimental methods. At first, a linear mathematical model for motorcycle stability is developed from the equation of motion, which is derived from the various forces and moments acting on it. This model is used to determine open and closed-loop systems for the motorcycle and their regions of stability. These stability regions have been validated from the preliminary experiments, which provided confidence for further study. At the next stage, detailed experiments have been conducted. A statistical method has been used to analyze the experimental data. The maximum correlation coefficient (MCC) and lead time between input and output parameters are calculated and compared to find the useful output parameters for the motorcycle stability at low speeds. A linear multiple regression analysis (MRA) between these identified parameters and the input parameters is performed to find useful input parameter. A steering estimation model is developed using the MRA from these parameters. A Simulink control algorithm is developed using this model and validated by the simulation studies with a multi-body dynamics (MBD) model of the motorcycle in VI-motorcycle. Following conclusions are drawn from the study:

1. The theoretical method of analysis can be used to find the regions for the low-speed stability of a motorcycle as the experimental results validated it. The roll angle gain and lead time calculated from the experiments were within their stability regions derived from the theory.

2. The roll angle and roll rate are the significant parameters to be assessed in balancing the motorcycle at low speeds. The maximum correlation coefficients between these parameters and the steering angle were strong, and their lead time values were also within the human limit for using them, determined from the experiments.

3. The steering angle is the suitable input parameter for low-speed stability than the steering torque. The regression correlation for estimating the steering angle was significantly stronger than that of the steering torque, using the roll angle and the roll rate as independent parameters.

4. The co-simulation results validate that the experimental method of analysis used for determining the gain values for the controller balances the motorcycles at extremely low speeds.

5. The co-simulation results for directional stability show that the control algorithm developed in this research is robust as the motorcycle was stable with additional steering torque disturbances.

5.2 Future scope

In future, the control algorithm developed in this research is to be validated by experiments on a real prototype. This controller and motorcycle prototype system should also be able to achieve the roll stability at low-speeds and not interfere with the rider's inputs. It can further be studied and improved to achieve the directional control as the motorcycle was stable for open-loop cornering simulations in this research. Although, the past research studies showed that the steering inputs are significant at low speeds and the rider's body inputs do not contribute to the stability. An accurate rider model with a sufficient degree of freedom is to determined. It is required to assess the influence of riders' body motion on their riding feel. A control algorithm with a necessary rider model will perform better with different riders. Also, the theoretical model is to be improved by including other forces and parameters such as trail effect, structural stiffness, overturning moments, tire thickness and pitch motion of the motorcycle.

Bibliography

[1] "Population reference bureau." Available online: http://www.prb.org/pdf14/2014-world-population-data-sheeteng.pdf

[2] "Highway Statistics Series." Available online: https://www.fhwa.dot.gov/policyinformation/quickfinddata/qfvehicles.cfm.

[3] "World Vehicle Population Tops 1 Billion Units." Available online: http://wardsauto.com/news-analysis/world-vehicle-population-tops-1-billion-units.

[4] "Two-wheeler sales in India." Available online: https://www.statista.com/statistics/318023/two-wheeler-sales-in-india/.

[5] 'Automobile Domestic Sales Trends." Available online: http://www.siamindia.com/statistics.aspx?mpgid=8&pgidtrail=14.

[6] K. Mahmud, K. Gope and S.M.R. Chowdhury (2012). Possible Causes Solutions of Traffic Jam and Their Impact on the Economy of Dhaka City. *Journal of Management and Sustainability*, Vol. 2:2, ISSN 1925-4725, E-ISSN 1925-4733.

[7] Popov, A.A.; Rowell, S. and Meijaard, J.P. (2010). A review on motorcycle and rider modelling for steering control. *Veh. Syst. Dyn.*, vol. 48, pp. 775–792.

[8] Hikichi, T. and Tezuka, Y. (1995). Study on Improving the Motorcycle High Speed Stability Using a Rear Wheel Self-Steering System. *SAE Technical Paper*, 950198, doi:10.4271/950198.

[9] Huston, R.L.; Schartman, L.S. and Connelly, J. (2013). High-Speed Motorcycle Dynamics: Quick Turns While Going Straight and Around Curves. *Int. Journal of Engineering Research and Applications,* www.ijera.com, ISSN: 2248-9622, Vol. 3, Issue 6, pp.1281-1285.

[10] Cossalter, V. (2007). Motorcycle Dynamics, 2nd ed.; Lulu.com: Morrisville, NC, USA.

[11] Bartolozzi, R.; Frendo, F.; Guiggiani, M. and Di Tanna, O. (2009). Comparison Between Experimental and Numerical Handling Tests for a Three Wheeled Motorcycle, *SAE Int. J. Engines*, 1(1):1389-1395, doi: 10.4271/2008-32-0061.

[12] "Honda Neowing Concept," Available online: http://hondaautoreviews.com/ 2016-honda-neowing-concept/.

[13] "Isetta History," Available online: http://www.isettabob.com/History/

[14] Singhania, S.; Kageyama, I. and Karanam, V.M. (2019). Study on Low-Speed Stability of a Motorcycle. *Appl. Sci.*, vol. 9, 2278.

[15] "History of motorcycles." Available online: http://www.bicyclehistory.net/ bicycle-inventor/john-kemp-starley/

[16] Whipple, F.J.W. (1899). The stability of the motion of a bicycle. *Quarterly Journal of Pure and Applied Mathematics*, Vol 30, pp. 312–348.

[17] Sharp, R.S. (1971). The stability and control of motorcycles. *J. Mech. Eng. Sci.*, vol. 13, pp. 316–329.

[18] Eaton D.J. (1973). An experimental study of the motorcycle roll stabilization task. *Conference on Manual Control, Ninth Annual Proceedings*, Cambridge, Massachusetts Institute of Technology, pp. 232-243.

[19] Weir, D.H. (1972). Motorcycle Handling Dynamics and Rider Control and the effect of Design Configuration on Response and Performance. *PhD thesis*, University of California at Los Angeles.

[20] Astrom, K.J.; Klein, R.E. and Lennartsson, A. (2005). Bicycle dynamics and control: Adapted bicycles for education and research. *IEEE Control Syst.*, vol. 25, pp. 26–47, doi:10.1109/MCS.2005.1499389.

[21] Yokomori, M.; Higuchi, K. and Ooya, T. (1992). Rider's Operation of a Motorcycle Running Straight at Low Speed. *JSME Int. J.*, vol. 35, pp. 553–559.

[22] Zhang, Y.; Li, J.; Yi, J. and Song, D. (2011). Balance control and analysis of stationary riderless motorcycles. *In Proceedings of the 2011 IEEE International Conference on Robotics and Automation*, Shanghai, China, pp. 3018–3023, doi:10.1109/ICRA.2011.5979841.

[23] Jones D.E.H. (1970). The stability of the bicycle. *Phys. Today*, vol. 23, pp. 34–40.

[24] Doyle, A.J.R. (1988). The essential human contribution to bicycle riding. *Training, Human Decision Making and Control*, pp. 351 370.

[25] Kooijman, J.D.G.; Meijaard, J.P.; Papadopoulos, J.M.; Ruina, A. and Schwab A.L. (2005). A Bicycle Can Be Self-Stable Without Gyroscopic or Caster Effects. *Sci. Mag.*, 332, pp. 339–342.

[26] Sharp, R.S. and Watanabe, Y. (2013). Chatter vibrations of high-performance motorcycles. *Veh. Syst. Dyn.*, vol. 51, pp. 393–404, doi:10.1080/00423114.2012.727440.

[27] Massaro, M.; Lot, R.; Cossalter, V.; Brendelson, J. and Sadauckas, J. (2012). Numerical and experimental investigation of passive rider effects on motorcycle weave. *Veh. Syst. Dyn.*, 50 (Suppl. 1), pp. 215–227, doi:10.1080/00423114.2012.679284.

[28] Sakai, H. (2018). Theoretical and Fundamental Consideration to Accord Between Self-Steer Speed and Rolling in Maneuverability of Motorcycles. *SAE Technical Paper: Warrendale*, No. 2018-32-0049, PA, USA, doi:10.4271/2018-32-0049.

[29] Schwab A.L. and Meijaard J.P. (2013). A review on bicycle dynamics and rider control, *Vehicle System Dynamics*, 51:7, pp. 1059-1090, DOI: 10.1080/00423114.2013.793365.

[30] Karanam, V.M. (2012). Studies in the Dynamics of Two and Three Wheeled Vehicles, *Doctoral dissertation 2012*, Indian Institute of Science, India.

[31] Talaia, P.;Moreno, D.;Hajzman, M. and Hyncik, L. (2008). A 3D model of a human for powered two-wheeler vehicles. *In Procedings of the International Conference on Noise Vibration Engineering,* pp. 2229–2238, Leuven.

[32] Doria, A.; Tognazzo, M. and Cossalter, V. (2013). The response of the rider's body to roll oscillations of two wheeled vehicles; experimental tests and biomechanical models, *Proceedings of the Institution of Mechanical Engineers, Part D: Journal of Automobile Engineering*, 227(4), pp. 561–576.

[33] Schwab, A.L.; Kooijman, J.D.G. and Meijaard, J.P. (2008). Some recent developments in bicycle dynamics and control. *In Proceedings of the Fourth European Conference on Structural Control (4ECSC)*, St. Petersburg, Russia.

[34] Kooijman, J.D.G.; Moore J.K. and Schwab A.L. (2009). Some Observations on Human Control of a Bicycle. *In Proceedings of the ASME 2009 International Design Engineering Technical Conferences Computers and Information in Engineering Conference*, DETC 2009-86959, San Diego, CA.

[35] Kooijman, J.D.G.; Schwab, A.L. and Meijaard, J.P. (2008). Experimental validation of a model of an uncontrolled bicycle. *Multibody System Dynamics*, 19:115 132.

[36] Cain S.M.; Ashton-Miller J.A. and Perkins N.C. (2016). On the Skill of Balancing While Riding a Bicycle. *PLoS ONE*, 11(2): e0149340, doi:10.1371/journal.pone.0149340.

[37] Prem, H. and Good, M.C. (1984). Motorcycle rider skills assessment. *Technical Report CR 34*, University of Melbourn, Parkville, Victoria, Australia, 3052.

[38] Rice, R.S. and Kunkel, D. (1976). Accident avoidance capabilities of motorcycles - lane change maneuver simulation and full-scale tests. *Technical Report ZN-5899 V-1*, Calspan Corporation.

[39] Zhou, K.; Doyle, J. and Glover, K. (1996). Robust and Optimal Control. *Prentice-Hall.*

[40] Katayama, T.; Aoki, A.; and Nishimi, T. (1988). Control behaviour of motorcycle riders. *Vehicle System Dynamics*, vol. 17, pp. 211 – 229.

[41] Aoki, A. (1979). Experimental study on motorcycle steering performance. *SAE Technical Report*, 790265.

[42] Rice, R.S. (1978). Rider Skill Influences on Motorcycle Maneuvering. *SAE Transactions*, vol. 87, pp. 1419–1430. JSTOR, www.jstor.org/stable/44611112.

[43] Ruijs, P. and Pacejka, H. (1985). Recent research in lateral dynamics of motorcycles. *In Proceedings of 9th IAVSD Symposium on The Dynamics Of Vehicles on roads and on tracks*, Sweden, volume supplement to Vehicle System Dynamics, Vol. 15, pp. 467–480.

[44] Huang, C.; Tung, Y. and Yeh, T. (2017). Balancing control of a robot bicycle with uncertain center of gravity. *In Proceedings of the IEEE International Conference on Ro-botics and Automation (ICRA)*, Singapore, pp. 5858–5863, doi:10.1109/ICRA.2017.7989689.

[45] Vatanashevanopakorn, S. and Parnichkun, M. (2011). Steering control based balancing of a bicycle robot. *In Proceedings of the 2011 IEEE International Conference on Robotics and Biomimetics*, Karon Beach, Phuket, Thailand, pp. 2169–2174, doi:10.1109/ROBIO.2011.6181613.

[46] Tanaka, Y. and Murakami, T. (2004). Self sustaining bicycle robot with steering controller. *In Proceedings of the AMC '04 8th IEEE International Workshop on Advanced Motion Control*, Kawasaki, Japan, pp. 193–197, doi:10.1109/AMC.2004.1297665.

[47] Lenkeit, J.F. (1995). A servo rider for the automatic and remote path control of a motorcycle. *SAE Technical Report*, 950199.

[48] Miyagishi, S.; Kageyama, I.; Takama, K.; Baba, M. and Uchiyama, H. (2003). Study on construction of a rider robot for two-wheeled vehicle. *JSAE Rev.*, vol. 24, pp. 321–326, doi:10.1016/S0389-4304(03)00045-6.

[49] Takenouchi, S.; Sekine, T. and Okano, M. (2002). Study on condition of stability of motorcycle at low speed. *In Proceedings of the Small Engine Technology Conference Exposition*, Kyoto, Japan, No. 2002-32-1797; SAE Technical Paper: Warrendale, PA, USA.

[50] Schlipsing, M.; Salmen, J.; Lattke, B.; Schrter, K.G. and Winner, H. (2012). Roll angle estimation for motorcycles: Comparing video and inertial sensor approaches. *In Proceedings of the IEEE Intelligent Vehicles Symposium*, Alcala de Henares, Spain, pp. 500–505, doi:10.1109/IVS.2012.6232200.

[51] Schwab, A.L. and Appleman, N. (2013). Dynamics and Control of a Steer-by-Wire Bicycle, *Proceedings, Bicycle and Motorcycle Dynamics*, Symposium on the Dynamics and Control of Single Track Vehicles, Narashino, Japan.

[52] Nenner, U.; Linker, R. and Gutman, P. (2010). Robust feedback stabilization of an unmanned motorcycle. *Control Engineering Practice*, 18.8, pp. 970-978.

[53] Beznos, A.V.; Formal'sky, A.M.; Gurfinkel, E.V.; Jicharev, D.N.; Lensky, A.V.; Savitsky, K.V.; Tchesalin, L.S. (1988). Control of autonomous motion of two-wheel bicycle with gyroscopic stabilisation. *In Proceedings of the 1998 IEEE International Conference on Robotics and Automation*, Leuven, Belgium, Vol. 3, pp. 2670–2675, doi:10.1109/ROBOT.1998.680749.

[54] Lot, R. and Fleming, J. (2018). Gyroscopic stabilisers for powered two-wheeled vehicles. *Veh. Syst. Dyn.*, doi:10.1080/00423114.2018.1506588.

[55] Karnopp, D. (2002), Tilt control for gyro-stabilized two-wheeled vehicles. *Veh. Syst. Dyn.*, vol. 37, pp. 145–156.

[56] Yang, C. and Murakami, T. (2016). Full-speed range self-balancing electric motorcycles without the handlebar. *IEEE Trans. Ind. Electron.*, vol. 63, pp. 1911–1922.

[57] Yi, J.; Song, D.; Levandowski, A. and Jayasuriya, S. (2006). Trajectory tracking and balance stabilization control of autonomous motorcycles. *In ICRA*, pp. 2583-2589. ISBN 0-7803-9505-0.

[58] Kimura, T.; Ando, Y. and Tsujii, E. (2014). Development of new concept two-wheel steering system for motorcycles. *SAE Int. J. Passeng. Cars Electron. Electr. Syst.*, vol. 7, pp. 36–40, doi:10.4271/2013-32-9106.

[59] Keo, L.; Yoshino, K.; Kawaguchi, M. and Yamakita, M. (2011). Experimental results for stabilizing of a bicycle with a flywheel balancer. *In Proceedings of the 2011 IEEE International Conference on Robotics and Automation*, Shanghai, China, pp. 6150–6155, doi:10.1109/ICRA.2011.5979991.

[60] Keo, L. and Yamakita M. (2011). Control of an Autonomous Electric Bicycle with both Steering and Balancer Controls, *Advanced Robotics*, 25:1-2, 1-22, DOI: 10.1163/016918610X538462.

[61] Kageyama, I. and Owada, Y. (1996). An Analysis of a Riding Control Algorithm for Two Wheeled Vehicles with a Neural Network Modeling. *Vehicle System Dynamics*, Vol. 25, Iss. sup1.

[62] "KISTLER Torque Sensor". Available online: https://www.kistler.com/en/product/type-90x9/, (accessed on 27 April 2019).

[63] "Steering Potentiometer". Available online: http://2d-datarecording.com/en/produkte/hardware/sensoren/sensoren-winkel/51020304050-magnetisch/, (accessed on 27 April 2019).

[64] "Inertia Navigation System". Available online: https://www.sbg-systems.com/products/ellipse-2-series/ellipse2-n-miniature-ins-gnss, (accessed on 27 April 2019).

[65] "GPS antennas". Available online: https://www.vboxautomotive.co.uk/index.php/en/products/accessories/antennas, (accessed on 27 April 2019).

[66] "Data Logger". Available online: http://www.racelogic.co.uk/downloads/vbox/Datasheets/DataLoggers/RLVB3iData.pdf. (accessed on 27 April 2019).

[67] Karanam, V.M. and Chatterjee A. (2009). Some procedural details of analysis using ADAMS-Motorcycle, http://eprints.iisc.ernet.in/17639/.

[68] Mangaraju, K.; Govardan, D.; Chavan, C. and Babu, R. (2008). Optimization of Damping Characteristics for Two Wheelers, *SAE Technical Paper*, 2008-32-0068, https://doi.org/10.4271/2008-32-0068.

[69] Mangaraju, K.; Ghosh, S.; Anand, R. and Babu, R. (2007). Vehicle Handling Comparison of Motorcycles and Bebek Vehicles. *SAE Technical Paper*, 2007-32-0109.

[70] Available in website, Adams Matlab Co-simulation help, http://www.mscsoftware.com/eventsassets/Webcasts/2016SystemDynamics/Adams-Matlab-Co-simulation-for-Vehicle-ABS-Systems.html.

A1 Spring and dampers

The Figures A1a and A1b show the spring and damper properties respectively for the front and rear suspension systems for the motorcycle.
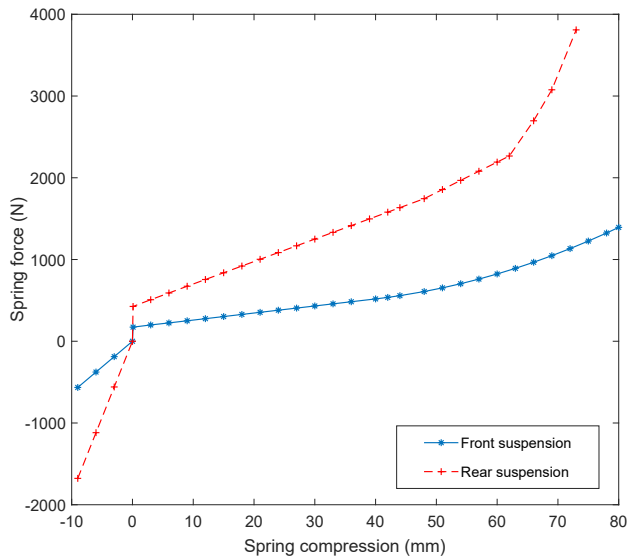
(a) Spring properties of the suspension systems
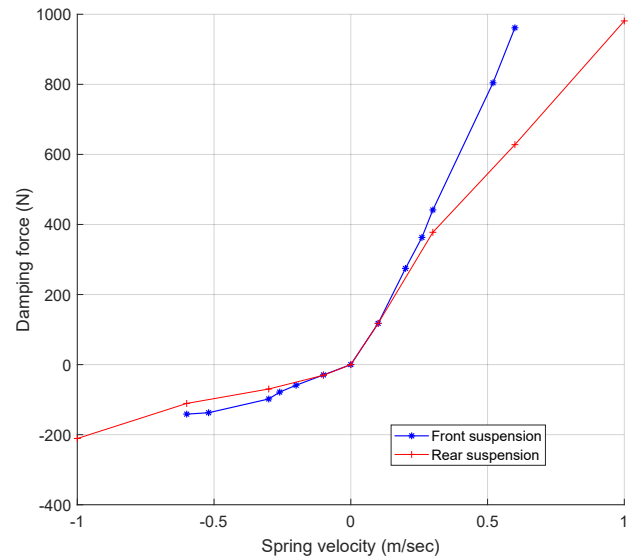
(b) Damper properties of the suspension systems

Figure A1: Spring and damper properties of the front and rear suspension systems of the motorcycle

A2 Mass-inertia details of the motorcycle

The mass-inertia details of the subsystems of the motorcycle in MBD simulation is shown in Table A1.

Table A1: Mass, center of gravity and inertia properties of various subsystems of the motorcycle. The center of gravity and moment-of-inertia matrices are defined with respect to a maker on the vehicle in ISO coordinate systems.

Subsystem	Mass (kg)	Center of gravity (m) & reference coordinates	Inertia (kg-m^2) $[I_{xx}\ I_{xy}\ I_{xz},$ $I_{yx}\ I_{yy}\ I_{yz},$ $I_{zx}\ I_{zy}\ I_{zz}]$
Front suspension assembly (w/o front wheel assembly)	10.79	(-0.044, -0.003, -0.2) wrt. fork top point and z-axis aligned to steering axis	[2.41 -0.03 0.08, -0.03 2.16 0.07, 0.08 0.07 0.38]
Front wheel assembly	6.91	(0, -0.002, 0) wrt. front wheel center point	[0.07 0 0, 0 0.12 0, 0 0 0.07]
Rear wheel assembly	6.22	(0, 0.005, 0) wrt. rear wheel center point	[0.06 0 0, 0 0.11 0, 0 0 0.07]
Engine assembly	33.81	(-0.24, -0.01, 0.06) wrt. rear wheel center point	[0.72 0.04 -0.38, 0.04 3.20 -0.03, -0.38 -0.03 3.3]
Rear suspension assembly	1.77	(-0.05, -0.086, 0.222) wrt. rear wheel center point	[0.24 0.02 -0.05, 0.02 0.22 -0.08, -0.05 -0.08 0.04]
Frame assembly	37.59	(-0.485, -0.023, 0.254) wrt. rear wheel center point	[5.01 0.42 -6.21, 0.42 25.10 -0.31, -6.21 -0.31 20.67]
Rider	65	(-0.371, 0, 0.653) wrt. rear wheel center point	[33.35 0.01 -14.72, 0.01 42.62 0.02, -14.72 0.02 11.63]

A3   Tire properties in MBD simulation

Front and rear tire properties of the motorcycle in MBD model is shown in Table A2.

Table A2: Front and rear tires properties of the motorcycle used in the MBD model. All other coefficients such as longitudinal, lateral, overturning, scaling, rolling and aligning are same between the tires.

Properties	Front tire	Rear tire	Units
Unloaded radius of the tire	0.217	0.208	m
Width of the tire	0.09	0.09	m
Radius of the front wheel rim	0.127	0.127	m
Width of the rim	0.055	0.055	m
Crown radius	0.052	0.050	m

A4   Tire property file for MBD simulation

The tire property file for the front tire of the motorcycle model in MBD simulation is as follows:

```
[MDI_HEADER]
FILE_TYPE               ='tir'
FILE_VERSION            =3.0
FILE_FORMAT             ='ASCII'
 : TIRE_VERSION :     PAC Motorcycle
 : COMMENT :          Tire                    120/70R12
 : COMMENT :          Manufacturer
 : COMMENT :          Nom. section with  (m)  0.12
 : COMMENT :          Nom. aspect ratio  (-)  70
 : COMMENT :          Infl. pressure     (Pa) 200000
 : COMMENT :          Rim radius         (m)  0.152
 : COMMENT :          Measurement ID
 : COMMENT :          Test speed        (m/s) 16.6
 : COMMENT :          Road surface
 : COMMENT :          Road condition          Dry
 : FILE_FORMAT :      ASCII
 : Copyright MSC.Software, 2005


USE_MODE specifies the type of calculation performed:
     0: Fz only, no Magic Formula evaluation
     1: Fx,My only
     2: Fy,Mx,Mz only
     3: Fx,Fy,Mx,My,Mz uncombined force/moment calculation
     4: Fx,Fy,Mx,My,Mz combined force/moment calculation
   +10: including relaxation behaviour
   *-1: mirroring of tyre characteristics

   example: USE_MODE = -12 implies:
     -calculation of Fy,Mx,Mz only
     -including relaxation effects
     -mirrored tyre characteristics


$-----------------------------------------------------------units
[UNITS]
LENGTH                  ='meter'
FORCE                   ='newton'
```

```
ANGLE                   ='radians'
MASS                    ='kg'
TIME                    ='second'
$-----------------------------------------------------------model
[MODEL]
PROPERTY_FILE_FORMAT    ='USER'
FUNCTION_NAME           ='vitools::vi_tire'
MODEL_TYPE              ='PAC_MC'
$LONSLIP_MODE           =1                  $enable modified transient resp. for locking
USE_MODE                = 4                 $Tyre use switch (IUSED)
VXLOW                   = 1
LONGVL                  = 16.6              $Longitudinal speed during measurements
TYRESIDE                = 'SYMMETRIC'       $Mounted side of tyre at vehicle/test bench
$-------------------------------------------------------dimensions
[DIMENSION]
UNLOADED_RADIUS         = 0.208             $Free tyre radius
WIDTH                   = 0.09              $Nominal section width of the tyre
RIM_RADIUS              = 0.127             $Nominal rim radius
RIM_WIDTH               = 0.05461
$-------------------------------------------section_profile_table
[SECTION_PROFILE_TABLE]
{     x          y      }
0.0000 0.0000
0.0025 0.0001
0.0050 0.0003
0.0075 0.0006
0.0100 0.0010
0.0125 0.0016
0.0150 0.0023
0.0175 0.0032
0.0200 0.0042
0.0225 0.0053
0.0250 0.0067
0.0275 0.0082
0.0300 0.0100
0.0325 0.0120
0.0350 0.0143
0.0375 0.0169
0.0400 0.0200
0.0425 0.0237
0.0450 0.0282
0.0475 0.0344
$----------------------------------------------------------parameter
[VERTICAL]
VERTICAL_STIFFNESS      = 1.7e+005          $Tyre vertical stiffness
VERTICAL_DAMPING        = 50                $Tyre vertical damping
BREFF                   = 8.4               $Low load stiffness eff. rolling radius
DREFF                   = 0.27              $Peak value of eff. rolling radius
FREFF                   = 0.07              $High load stiffness eff. rolling radius
FNOMIN                  = 1000              $Nominal wheel load
$---------------------------------------------------long_slip_range
[LONG_SLIP_RANGE]
KPUMIN                  = -1.5              $Minimum valid wheel slip
KPUMAX                  = 1.5               $Maximum valid wheel slip
$---------------------------------------------------slip_angle_range
[SLIP_ANGLE_RANGE]
ALPMIN                  = -1.5708           $Minimum valid slip angle
ALPMAX                  = 1.5708            $Maximum valid slip angle
$-----------------------------------------------inclination_slip_range
[INCLINATION_ANGLE_RANGE]
CAMMIN                  = -1.1996           $Minimum valid camber angle
CAMMAX                  = 1.1996            $Maximum valid camber angle
$-----------------------------------------------vertical_force_range
[VERTICAL_FORCE_RANGE]
FZMIN                   = 25                $Minimum allowed wheel load
FZMAX                   = 3000              $Maximum allowed wheel load
$----------------------------------------------------------scaling
[SCALING_COEFFICIENTS]
LFZO                    = 1                 $Scale factor of nominal load
LCX                     = 1                 $Scale factor of Fx shape factor
LMUX                    = 1                 $Scale factor of Fx peak friction coefficient
```

```
LEX                   = 1                 $Scale factor of Fx curvature factor
LKX                   = 1                 $Scale factor of Fx slip stiffness
LVX                   = 1                 $Scale factor of Fx vertical shift
LGAX                  = 1                 $Scale factor of camber for Fx
LCY                   = 1                 $Scale factor of Fy shape factor
LMUY                  = 1                 $Scale factor of Fy peak friction coefficient
LEY                   = 1                 $Scale factor of Fy curvature factor
LKY                   = 0.5               $Scale factor of Fy cornering stiffness
LCC                   = 1                 $Scale factor of camber shape factor
LKC                   = 1                 $Scale factor of camber stiffness (K-factor)
LEC                   = 1                 $Scale factor of camber curvature factor
LHY                   = 1                 $Scale factor of Fy horizontal shift
LGAY                  = 0.5               $Scale factor of camber force stiffness
LTR                   = 1                 $Scale factor of Peak of pneumatic trail
LRES                  = 1                 $Scale factor of Peak of residual torque
LGAZ                  = 1                 $Scale factor of camber torque stiffness
LXAL                  = 1                 $Scale factor of alpha influence on Fx
LYKA                  = 1                 $Scale factor of kappa influence on Fy
LVYKA                 = 1                 $Scale factor of kappa induced Fy
LS                    = 1                 $Scale factor of Moment arm of Fx
LSGKP                 = 1                 $Scale factor of Relaxation length of Fx
LSGAL                 = 1                 $Scale factor of Relaxation length of Fy
LGYR                  = 1                 $Scale factor of gyroscopic torque
LMX                   = 1                 $Scale factor of overturning couple
LVMX                  = 1                 $Scale factor of Mx vertical shift
LMY                   = 1                 $Scale factor of rolling resistance torque
$---------------------------------------------------longitudinal
[LONGITUDINAL_COEFFICIENTS]
PCX1                  = 1.7576            $Shape factor Cfx for longitudinal force
PDX1                  = 1.32              $Longitudinal friction Mux at Fznom
PDX2                  = -0.11             $Variation of friction Mux with load
PDX3                  = 0                 $Variation of friction Mux with camber
PEX1                  = 0.12915           $Longitudinal curvature Efx at Fznom
PEX2                  = 0.11232           $Variation of curvature Efx with load
PEX3                  = -0.0050538        $Variation of curvature Efx with load squared
PEX4                  = -3.7973e-005      $Factor in curvature Efx while driving
PKX1                  = 13.038            $Longitudinal slip stiffness Kfx/Fz at Fznom
PKX2                  = -0.050469         $Variation of slip stiffness Kfx/Fz with load
PKX3                  = 0.083032          $Exponent in slip stiffness Kfx/Fz with load
PVX1                  = -9.1193e-006      $Vertical shift Svx/Fz at Fznom
PVX2                  = -4.6005e-007      $Variation of shift Svx/Fz with load
RBX1                  = 7.862             $Slope factor for combined slip Fx reduction
RBX2                  = -8.6605           $Variation of slope Fx reduction with kappa
RBX3                  = -0.34399          $Influence of camber on stiffness for Fx combined
RCX1                  = 1.0137            $Shape factor for combined slip Fx reduction
REX1                  = -0.31972          $Curvature factor of combined Fx
REX2                  = 0.0040221         $Curvature factor of combined Fx with load
RHX1                  = -0.030359         $Shift factor for combined slip Fx reduction
PTX1                  = 0                 $Relaxation length SigKap0/Fz at Fznom
PTX2                  = 0                 $Variation of SigKap0/Fz with load
PTX3                  = 0                 $Variation of SigKap0/Fz with exponent of load
$---------------------------------------------------overturning
[OVERTURNING_COEFFICIENTS]
QSX1                  = 0.0030512         $Lateral force induced overturning moment
QSX2                  = 0.12521           $Camber induced overturning moment
QSX3                  = 0.057724          $Fy induced overturning moment
$---------------------------------------------------lateral
[LATERAL_COEFFICIENTS]
PCY1                  = 0.92316           $Shape factor Cfy for lateral forces
PCY2                  = 1.4731            $Shape factor Cfc for camber forces
PDY1                  = 1.169             $Lateral friction Muy
PDY2                  = -0.025201         $Exponent lateral friction Muy
PDY3                  = -0.62876          $Variation of friction Muy with squared camber
PEY1                  = -0.77295          $Lateral curvature Efy at Fznom
PEY2                  = 4.0791            $Variation of curvature Efy with camber squared
PEY3                  = 0.0026018         $Asymmetric curvature Efy at Fznom
PEY4                  = 3.1006            $Asymmetric curvature Efy with camber
PEY5                  = 32.105            $Camber curvature Efc
PKY1                  = -109.8            $Maximum value of stiffness Kfy/Fznom
PKY2                  = 2.3605            $Curvature of stiffness Kfy
PKY3                  = 14.106            $Peak stiffness factor
```

```
PKY4                = 41.325          $Peak stiffness variation with camber squared
PKY5                = -0.52605        $Lateral stiffness depedency with camber squared
PKY6                = -0.5793         $Camber stiffness factor Kfc
PKY7                = -0.11317        $Vertical load dependency of camber stiffn. Kfc
PHY1                = 5.4396e-006     $Horizontal shift Shy at Fznom
RBY1                = 6.9776          $Slope factor for combined Fy reduction
RBY2                = 7.1672          $Variation of slope Fy reduction with alpha
RBY3                = -0.077046       $Shift term for alpha in slope Fy reduction
RBY4                = 4.1445          $Influence of camber on stiffness of Fy combined
RCY1                = 1.0618          $Shape factor for combined Fy reduction
REY1                = 0.039115        $Curvature factor of combined Fy
REY2                = -0.003319       $Curvature factor of combined Fy with load
RHY1                = -2.5727e-006    $Shift factor for combined Fy reduction
RHY2                = 1.3536e-007     $Shift factor for combined Fy reduction with load
RVY1                = -2.6875e-005    $Kappa induced side force Svyk/Muy*Fz at Fznom
RVY2                = 3.8531e-006     $Variation of Svyk/Muy*Fz with load
RVY3                = -0.005499       $Variation of Svyk/Muy*Fz with camber
RVY4                = -403.28         $Variation of Svyk/Muy*Fz with alpha
RVY5                = 1.9             $Variation of Svyk/Muy*Fz with kappa
RVY6                = 0               $Variation of Svyk/Muy*Fz with atan(kappa)
PTY1                = 0               $Peak value of relaxation length Sig_alpha
PTY2                = 0               $Shape factor for Sig_alpha
PTY3                = 0               $Value of Fz/Fznom where Sig_alpha is maximum
$-------------------------------------------------rolling resistance
[ROLLING_COEFFICIENTS]
QSY1                = 0.01            $Rolling resistance torque coefficient
QSY2                = 0               $Rolling resistance torque depending on Fx
QSY3                = 0               $Rolling resistance torque depending on speed
QSY4                = 0               $Rolling resistance torque depending on speed^4
$----------------------------------------------------------aligning
[ALIGNING_COEFFICIENTS]
QBZ1                = 15.157          $Trail slope factor for trail Bpt at Fznom
QBZ2                = -0.37275        $Variation of slope Bpt with load
QBZ3                = -1.825          $Variation of slope Bpt with load squared
QBZ4                = 0               $Variation of slope Bpt with camber
QBZ5                = 0.6644          $Variation of slope Bpt with absolute camber
QBZ9                = 8.4302          $Slope factor Br of residual torque Mzr
QCZ1                = 1.7111          $Shape factor Cpt for pneumatic trail
QDZ1                = 0.064523        $Peak trail Dpt = Dpt*(Fz/Fznom*R0)
QDZ2                = -0.01919        $Variation of peak Dpt with load
QDZ3                = 0.47014         $Variation of peak Dpt with camber
QDZ4                = 0.49471         $Variation of peak Dpt with camber squared
QDZ6                = 0.0033745       $Peak residual torque Dmr = Dmr/(Fz*R0)
QDZ7                = -0.0072206      $Variation of peak factor Dmr with load
QDZ8                = -0.066486       $Variation of peak factor Dmr with camber
QDZ9                = -0.078795       $Variation of peak factor Dmr with camber and load
QDZ10               = -0.031778       $Variation of peak factor Dmr with camber squared
QDZ11               = 0.053746        $Variation of Dmr with camber squared and load
QEZ1                = -0.0024207      $Trail curvature Ept at Fznom
QEZ2                = 0.0048859       $Variation of curvature Ept with load
QEZ3                = 0               $Variation of curvature Ept with load squared
QEZ4                = 0               $Variation of curvature Ept with sign of Alpha-t
QEZ5                = 0               $Variation of Ept with camber and sign Alpha-t
QHZ1                = 0               $Trail horizontal shift Sht at Fznom
QHZ2                = 0               $Variation of shift Sht with load
QHZ3                = 0               $Variation of shift Sht with camber
QHZ4                = 0               $Variation of shift Sht with camber and load
SSZ1                = 0               $Nominal value of s/R0: effect of Fx on Mz
SSZ2                = 0.022067        $Variation of distance s/R0 with Fy/Fznom
SSZ3                = 0.14968         $Variation of distance s/R0 with camber
SSZ4                = 0.049557        $Variation of distance s/R0 with load and camber
QTZ1                = 0               $Gyroscopic torque constant
MBELT               = 2               $Belt mass of the wheel -kg-
```

A5 Riders details

Table A3 shows the details of different riders selected for the experiments.

Table A3: Details of different riders selected for the experiments.

Riders	Age (yr.)	Weight (kg)	Height (mm)	Gender	Experience (yr.)	(km)	Distance km/yr.	Category
Rider-1	25	75	170	Male	0.5	3000	6000	Beginner
Rider-2	32	68	163	Male	8.0	4800	600	Beginner
Rider-3	29	67	170	Male	12.0	87600	7300	Expert
Rider-4	27	70	158	Female	2.0	7300	3650	Beginner
Rider-5	28	84	178	Male	8.0	43800	5475	Intermediate
Rider-6	24	57	163	Female	1.0	520	520	Beginner
Rider-7	27	50	158	Female	7.0	25550	3650	Intermediate
Rider-8	54	79	170	Male	3.0	24300	8100	Intermediate
Rider-9	52	85	178	Male	33.0	361350	10950	Expert
Rider-10	57	58	163	Male	30.0	21840	728	Beginner
Rider-11	22	63	165	Female	1.5	4050	2700	Beginner
Rider-12	25	65	178	Male	8.0	29200	3650	Intermediate
Rider-13	25	63	175	Male	0.5	1800	3600	Beginner
Rider-14	42	56	158	Male	20.0	55200	2760	Intermediate
Rider-15	28	85	176	Male	7.0	102200	14600	Expert
Rider-16	25	73	179	Male	7.0	63875	9125	Intermediate
Rider-17	22	65	165	Female	1.0	3650	3650	Beginner
Rider-18	46	75	174	Male	20.0	12000	600	Beginner
Rider-19	33	65	173	Female	6.0	72	12	Beginner
Rider-20	31	67	170	Male	10.0	9100	910	Beginner
Rider-21	31	74	178	Male	6.0	26280	4380	Intermediate
Rider-22	26	56	170	Male	7.0	25550	3650	Intermediate